L.B.Krivdin
Russ. Chem. Rev., 2020, **89** (10) 1040 – 1073

https://doi.org/10.1070/RCR4948

Computational aspects of ^{19}F NMR

Leonid B. Krivdin [a, b]

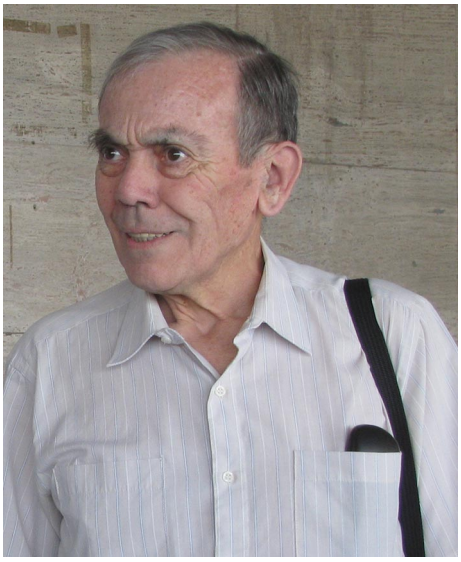
[a] *A.E.Favorsky Irkutsk Institute of Chemistry, Siberian Branch of the Russian Academy of Sciences, ul. Favorskogo 1, 664033 Irkutsk, Russian Federation*
[b] *Angarsk State Technical University, ul. Tchaikovskogo 60, 665835 Angarsk, Irkutsk Region, Russian Federation*

This review covers most recent advances in computation of ^{19}F NMR chemical shifts and spin – spin coupling constants involving ^{19}F nucleus calculated at different levels of theory. It deals mainly with electronic and stereochemical effects influencing these parameters, with a special emphasis on practical applications of such calculations. For ^{19}F NMR chemical shifts, a good deal of attention is focused on less common solid state studies, in addition to much more popular liquid state data. For spin – spin coupling constants, the main interest is concentrated on the most popular ^{19}F – ^{1}H, ^{19}F – ^{13}C and ^{19}F – ^{19}F couplings providing marked stereochemical behaviour.
The bibliography includes 149 references.

Contents

1. Introduction 1041
2. Computation of ^{19}F NMR chemical shifts 1042
3. Calculation of spin – spin coupling constants involving ^{19}F nucleus 1050
   3.1. ^{19}F – ^{1}H spin – spin coupling constants 1050
   3.2. ^{19}F – ^{13}C spin – spin coupling constants 1053
   3.3. ^{19}F – ^{19}F spin – spin coupling constants 1058
   3.4. Other coupling constants involving ^{19}F nucleus 1065
4. Conclusion 1071

In memory of Professor Rubén Horacio Contreras, to commemorate his achievements in the field of theoretical and computational ^{19}F NMR.



Professor Emeritus Rubén Horacio Contreras
(1938 – 2014)

This review is written in memory of the late Professor Rubén Horacio Contreras, a well-known specialist in theoretical and computational ^{19}F NMR, who worked for many decades at the University of Buenos Aires, Argentina. Professor Contreras was born in 1938 in Berazategui, the Province of Buenos Aires, and after graduating from the University of Buenos Aires was doing NMR-oriented research for three years at the University of Uppsala (Sweden) and the University of Manitoba (Canada). Almost all of his life he worked at the Department of Physics of the Faculty of Exact and Natural Sciences at the University of Buenos Aires carrying out scientific research in the field of experimental, together with theoretical and computational NMR, mostly that in the field of ^{19}F NMR. As an example, a number of his publications (many of which are cited in this review), dealing with computational aspects of ^{19}F NMR chemical shifts and different spin – spin coupling constants involving fluorine became classical examples of how computational ^{19}F NMR could provide an insight into various intra- and intermolecular interactions involving fluorine. In 2004 Rubén Contreras was elected Professor Emeritus of the University of Buenos Aires. Among a couple of dozens of his PhD students, now working in different parts of the world, mostly in the United States, South America and Europe, there are many

Leonid Krivdin graduated from M.V.Lomonosov Moscow State University in 1977, received his PhD in 1982 from the Irkutsk State University, which was followed by a post-doctoral fellowship at Flinders University of South Australia in the group of Professor Ernst Della (1990 – 1991). He received his DSc in 1989 and Full Professor in 1993.
ORCID: http://orcid.org/0000-0003-2941-1084
E-mail: krivdin_office@irioch.irk.ru
His research interests focus on computation of NMR parameters being substantiated with some 400 research publications including 15 reviews and book chapters. Under his scientific supervision, 12 PhD dissertations were defended in the interim of 1989 until present. He is currently a Head of the NMR Laboratory the A.E.Favorsky Irkutsk Institute of Chemistry and a Chair of Chemistry at the Angarsk State Technical University.

Received 12 February 2020
© 2020 Uspekhi Khimii, ZIOC RAS, Russian Academy of Sciences and IOP Publishing Limited

prominent scientists and famous public figures very well known worldwide.

Coming to more personal reminiscences, I remember that we have started our scientific collaboration with Rubén in the field of computational NMR as early as in the middle of the 1980s, which was about 35 years ago. How fast the time is passing by! There was no electronic means of communication those days, so that we were exchanging with our ordinary post letters (the so-called «snail mail», almost not used in our time for scientific correspondence), and it was about a couple of months for a letter to get through from Irkutsk to Buenos Aires and the same period of time to get back. Anyway, in spite of those obvious difficulties, we have managed to publish in the interim of 1985 – 1995 several joint research papers involving those in J. Mol. Struct. THEOCHEM, J. Magn. Reson., Austr. J. Chem. and RSC Dalton Trans.

In 1990 I went to the Flinders University of South Australia for a sabbatical for a whole year (which was not in common those days in our country), where we have established a regular e-mail correspondence with Rubén. It was a new opportunity for both of us of having rapid personal communication, when our letters (e-mail messages) were getting through in-between Australia and Argentina almost instantly (within two seconds) instead of two months, the time which had earlier been taken them to be delivered via an ordinary mail. Much later, in 2010 and after that in 2012, I visited Rubén in person at his 'native nest' — the Faculty of Exact and Natural Sciences of the University of Buenos Aires, where he cordially accepted me both times as a visiting professor. My personal impressions were that he was a nice, amiable and very modest person, being at this an outstanding scientist of our time. Rest in peace, Rubén!

P.S. The above photo was taken in 2012 at Jorge Newbery airport, Buenos Aires, where Rubén was seeing me off on my departure to Ushuaia, the most southern continental point of Argentina (and South America as well).

1. Introduction

The fundamentals of computational NMR are generally discussed in the Encyclopedia of Molecular Electromagnetism by Stephan Sauer [1] and in a number of general reviews covering different computational aspects of chemical shifts and spin – spin coupling constants.[2 – 19] More specialized reviews concentrate on practical aspects of the computation of particular NMR parameters, including those of proton,[20 – 22] carbon,[23 – 25] nitrogen,[26] silicon [27] and phosphorous [28, 29] NMR spectra. Present review deals with the computation of ^{19}F NMR chemical shifts and spin – spin coupling constants involving fluorine in a wide series of organofluorine compounds in an isotropic phase as well as in solid state. However, computational ^{19}F NMR stands a bit apart from a vivid progress in theoretical calculations of the above-mentioned isotopes in view of a very specific nature of an extremely electronegative fluorine having as many as three lone electron pairs. Indeed, 'accurate determination of molecular magnetic properties of fluoro-substituted systems has remained a long-standing challenge for computational methods... Similar difficulties are encountered for ^{19}F NMR parameters: the range of ^{19}F chemical shifts and sensitivity to subtle differences in local and electronic environments imposes a considerable demand on the computational description of these parameters'.[30] However, in spite of the mentioned problems, computational ^{19}F NMR is rapidly developing, so that it deserves a thorough attention in view of a growing interest in the computation of NMR properties of other nuclei.

The first part of the present review deals with the calculation of ^{19}F NMR chemical shifts in particular classes of organofluorine compounds, while the second part focuses on the computational aspects of the most popular spin – spin coupling constants, ^{19}F – ^{1}H, ^{19}F – ^{13}C and ^{19}F – ^{19}F, together with some more exotic types of couplings involving fluorine. In contrast to the earlier computational studies of spin – spin coupling constants involving fluorine,[31 – 36] modern calculations of ^{19}F NMR chemical shifts are performed, apart from the numerous DFT schemes, mostly at non-empirical levels like MP2, CCSD and CCSD(T), while calculations of spin – spin coupling constants involving fluorine are carried out at the SOPPA(MP2), SOPPA(CC2) and SOPPA(CCSD) levels. Herewith, I will not give numerous references on these methods and most efficient basis sets, which can be found in our previous reviews.[20 – 29] Moreover, calculations of spin – spin coupling constants involving fluorine are generally more difficult than those for the other nuclei, so that higher levels of theory for such calculations are apparently required. For spin – spin coupling constants involving fluorine, this is likely due to the relative importance of the non-contact contributions which may be rather essential for fluorine in particular molecular systems and may even dominate the Fermi contact term, which provides a certain 'skeleton in a cupboard' and implies that such calculations should be performed with much caution.

At present, the chemistry of organofluorine compounds is a leading and rapidly developing area of organic chemistry providing the most 'promising growth areas and challenges'.[37] In line with a general progress in this area, the present review concentrates on the computational aspects of ^{19}F NMR being oriented mainly on NMR spectroscopists and on a broad audience of researches, working with organofluorine compounds and utilizing modern computational methods for the calculation and interpretation of their ^{19}F NMR spectra.

Glossary of abbreviations:

CBS — complete basis set,

CC3 — coupled cluster singles, doubles and triples model,

CCSD — coupled cluster single and double excitation model,

CCSD(T) — coupled cluster single and double excitation model with perturbative triples corrections,

CMO — canonical molecular orbital,

CP MAS — cross-polarization magic angle spinning,

CPU — central processing unit,

DFT — density functional theory,

DSO — diamagnetic spin – orbit (contribution),

FC — Fermi contact (contribution),

GGA — generalized gradient approximation,

GIPAW — Gauge including projected augmented wave,

EOM-CCSD — equations-of-motion coupled cluster single and double excitation model,

HF — Hartree – Fock,

HOMO — highest occupied molecular orbital,

HRPA — higher random phase approximation,

HRPA(D) — higher random phase approximation (doubles),

IEF-PCM — integral equation formalism polarizable continuum model,

LDBS — locally dense basis set,

LMO — localized molecular orbital,
LP — lone pair,
LUMO — lowest unoccupied molecular orbital,
MAE — mean absolute error,
MAS — magic angle spinning,
MO — molecular orbital,
MP2 — second-order Møller – Plesset perturbation theory,
PBE — Perdew – Burke – Ernzerhof (functional),
PCM — polarizable continuum model,
PSO — paramagnetic spin – orbit (contribution),
RHF — restricted Hartree – Fock,
RMS — root mean squares,
RPA — random phase approximation,
RPA(D) — random phase approximation (doubles),
SD — spin dipolar (contribution),
SO — spin – orbit,
SOPPA — second-order polarization propagator approach,
SOPPA(MP2) — second-order polarization propagator approach in combination with Møller – Plesset perturbation theory,
SOPPA(CC2) — second-order polarization propagator approach in combination with second-order approximate Coupled Cluster model,
SOPPA(CCSD) — second-order polarization propagator approach in combination with coupled cluster single and double excitation model,
TO — total (sum of all coupling contributions),
ZORA — zeroth order regular approximation,
ZPVC — zero-point vibrational correction,
J — spin – spin coupling constant,
σ — shielding constant,
φ — dihedral angle.

2. Computation of ^{19}F NMR chemical shifts

Generally, I will not go deeper in time than the last decade of this century. Numerous earlier calculations of ^{19}F NMR chemical shifts [38–41] were performed mostly at the DFT level, in particular using the most known popular functionals (such as B3LYP or PBE) and classical Pople's basis sets like 6-31++G(d,p) or 6-311++G(2d,2p). A typical example of such studies is presented in the early paper by Fukaya and Ono [42] who evaluated ^{19}F NMR chemical shifts in a wide variety of perfluoro derivatives of more than 50 types of compounds, where authors used the B3LYP functional with a variety of Pople's basis sets.

Coming back to the present time, let us begin this Section with the discussion of three simple inorganic molecules. Very recently, Field-Theodore *et al.*[30] performed state-of-the-art calculations of ^{19}F NMR shielding constants in a series of three trifluorides, NF_3, PF_3 and AsF_3, providing a good theoretical benchmark for the calculation of the dynamic electron correlation effects on NMR shielding constants. Chemical shieldings of NF_3, PF_3 and AsF_3 were calculated at a simple Hartree – Fock and all-electron CCSD, CCSD(T) and CCSDT levels of theory together with Dunning's core aug-cc-pCVXZ (X = D, T, Q, 5, 6) basis sets at the CCSD(T)/aug-cc-pCVTZ optimized geometries. Relativistic effects were evaluated at the DFT level as the difference between the values of chemical shielding obtained with a fully relativistic four-component Hamiltonian and its non-relativistic counterpart. The adequate treatment of electron correlation effects, ensuring gauge-origin independence overcoming basis set incompleteness, together with taking into account zero-point vibrational effects and relativistic corrections at the most complete four-component level, was employed. Chosen systems offered a rigorous test of current computational methods including those taking into account dynamic electron correlation effects. The latter were expected to be very important for these electron-rich systems, especially due to the presence of electronegative fluorine atoms that have three lone electron pairs each.

As for the rovibrational corrections, it was found that for all the three compounds, vibrational and temperature effects were negative in sign. The vibrational averaging effect was much larger than the temperature effect, with the temperature corrections being generally an order of magnitude smaller than the corresponding vibrational corrections. For the NF_3 molecule, the rovibrational correction to the isotropic fluorine shielding was found to be extremely large, being almost 20 ppm in magnitude. On the other hand, relativistic corrections to fluorine chemical shielding (σ_{equil}) in all the three compounds were found to be rather small and positive being in the range of 2 – 4 ppm. The results on calculated isotropic shielding constants including contribution of vibrational (σ_{vib}), temperature (σ_{temp}) and relativistic (σ_{rel}) effects are compiled in Table 1.

Table 1. Calculated ^{19}F NMR isotropic shielding constants (ppm). Compiled from Field-Theodore *et al.*[30]

Compound	σ_{equil}	σ_{vib}	σ_{temp}	σ_{rel}	σ_{total}
NF_3	67.14	−19.36	−1.76	3.62	49.64
PF_3	231.48	−3.73	−0.75	3.54	230.54
AsF_3	245.71	−3.80	−1.31	1.80	242.40

Another example of early theoretical studies of the ^{19}F NMR chemical shifts in simple inorganic molecules is presented in a paper by Jaszuński.[43] In that paper, the state-of-the-art calculations of fluorine shielding constants were performed for a series of three simple molecules, ClF_3, PF_3 and PF_5, at the SCF, CCSD and CCSD(T) levels of theory using relatively large cc-pCVTZ basis sets, as compared to experiment (Table 2). The most essential tendency following from those data was an apparent decrease of calculated ^{19}F NMR shielding constants towards their experimental values with the completeness of the degree of electron correlation being taking into account at different levels of theory.

Ten years ago Shaghaghi *et al.*[44] calculated ^{19}F NMR chemical shifts of a number of the most representative and most simple fluorine-containing inorganic and organic compounds at the DFT (B3LYP functional), HF and MP2 levels in gas-phase. The authors employed a variety of Pople's

Table 2. ^{19}F NMR shielding constants (ppm) calculated at different levels of theory *vs.* experiment. Compiled from Jaszuński.[43]

Compound	Nucleus	SCF	CCSD	CCSD(T)	Experiment
ClF_3	F_e	217.99	216.08	210.61	201.7
	F_a	145.27	107.61	90.55	75.7
PF_3	F	260.34	245.70	239.23	222.7
PF_5	F_e	292.88	283.13	294.64	
	F_a	279.83	271.88	288.94	
	F (averaged)	287.66	278.63		266

a — axial, *e* — equatorial.

basis sets, those from the most simple 6-31G (having no polarization and/or diffuse functions) to 6-31 + G(df,p) basis set, augmented with both polarization (df) and diffuse (p) functions. The wave functions for calculating gas phase ^{19}F NMR chemical shifts were optimally selected using the factorial design. The effects of electron correlation together with inclusion of diffuse and polarization functions on calculated ^{19}F NMR chemical shifts in this series of compounds showed that electron correlation and polarization functions most significantly affected computational results. Based on the results, compiled in Table 3, the B3LYP/6-31 + G(df,p) method had been advertised as the most efficient tool at the DFT level for the computation of ^{19}F NMR chemical shifts of simple fluorine-containing inorganic and organic molecules. Those results looked very promising for this set of compounds with the exception of two most difficult cases (strong electron correlation, relativistic effects, *etc*.) — PF_3 and SF_6, providing deviations of the computed values of 5 – 6 ppm against experiment.

A couple of years later the same principal authors [45, 46] performed an extensive calculation of ^{19}F NMR chemical shifts in a number of small fluorine-containing molecules (mainly, fluorine derivatives of methane and ethane) at the DFT, as compared to the Hartree – Fock (HF) and the second-order Møller – Plesset perturbation theory (MP2) levels. It was found that the MP2 method gave essentially better results, as compared to DFT and HF. Calculated ^{19}F NMR chemical shifts showed satisfactory agreement with experiment for all basis sets (in this study, only Pople's basis sets were considered), especially for those including polarization functions. Indeed, polarization functions expectedly demonstrated a significant improving effect on the correlation coefficient between calculated and experimental shifts, as could be judged from the data presented in Table 4.

Table 3. ^{19}F NMR chemical shifts of the representative fluorine-containing molecules (ppm) calculated at different levels of theory *vs.* experiment. Compiled from Shaghaghi *et al.*[44]

Compound	Method	Calculation	Experiment
BF_3	HF/6-311G(df,p)	36.49	36.02
CF_4	HF/6-311 + G(df,p)	103.87	104.21
CF_3Cl	B3LYP/6-311G(df,p)	139.07	138.77
CH_3F	HF/6-311G(df,p)	−107.96	−107.71
CF_3Br	HF/6-31G	149.67	149.31
CF_2Cl_2	MP2/6-31G	160.72	160.53
CF_3H	HF/6-31G	88.40	89.06
CF_2ClH	MP2/6-31G	95.93	95.88
CF_3CH_3	B3LYP/6-311G	104.66	104.49
CF_3CF_2Cl	MP2/6-31G	80.29	81.25
CF_3CF_3	MP2/6-311G	78.63	80.2
PF_3	B3LYP/6-31 + G(df,p)	140.87	134.83
POF_3	HF/6-31G(df,p)	74.98	74.94
COF_2	B3LYP/6-31G(d,p)	141.83	141.5
SF_6	MP2/6-311G(d,p)	228.83	223.57

Another interesting finding of this study [45] is that diffuse functions are the most effective factor to minimize the difference between calculated and experimental values. Not surprisingly, taking into account electron correlation (at the MP2 and DFT levels) essentially improved those calculations, especially in the case when large basis sets were applied. A rather strange unexpectedly good behaviour of the very small 6-31G basis set was found, but not discussed (RMS error for this basis set was only 3.53 ppm as compared to 20 – 30 ppm for much larger basis sets, see Table 4), which is usually ascribed in the literature to the so-called 'fortuitous cancellation of errors'.

Almost a decade ago Saielli, Bini and Bagno [47, 48] performed a systematic computational study of ^{19}F NMR chemical shifts in a vast amount of simple fluorine-containing inorganic molecules involving a well-known family of uranium(VI) chlorofluorides, UF_nCl_{6-n}, providing all possible ligand and stereochemical combinations (UF_6, UF_5Cl, *cis*-UF_4Cl_2, *trans*-UF_4Cl_2, *mer*-UF_3Cl_3, *fac*-UF_3Cl_3, *cis*-UF_2Cl_4, *trans*-UF_2Cl_4 and $UFCl_5$). Here, the notation '*fac*' stands for the complexes in which three identical ligands occupy one face of an octahedron, so that the isomer is called 'facial'. In this isomer, any two identical ligands are adjacent or occupy a '*cis*' position to each other. If these three ligands and the metal ion are in one plane, the isomer is called 'meridional', which is denoted as '*mer*'.

In the cited study, authors used the Generalized Gradient Approximation (GGA) DFT functionals BP86 and BLYP and the hybrid PBE0 functional employed within a zero-order regular approximation (ZORA) in the case of a heavy environment. The triple-zeta, doubly polarized Slater's basis set TZ2P was used on the rest of atoms. Calculated ^{19}F NMR chemical shifts were referenced to $CFCl_3$ (σ_{ref} = 133, 120 and 182 for BP86, BLYP and PBE0 functionals, respectively) and represented the sum of the diamagnetic, paramagnetic and spin – orbit terms. Calculated ^{19}F NMR chemical shifts of several dozens of compounds, including those with F bonded to B, C, N, O, P, Si,

Table 4. Statistical parameters of the correlations of ^{19}F NMR chemical shifts calculated at the HF, B3LYP and MP2 levels against experiment for a series of fluorinated ethanes. Compiled from Ebrahimi and Tafazzoli.[45]

Statistical parameter	Method	Basis set							
		6-31G	6-311G	6-31 + G	6-311 + G	6-31G(d,p)	6-311G(d,p)	6-31 + G(d,p)	6-311 + G(d,p)
Slope	HF	1.281	1.177	1.215	1.133	1.263	1.168	1.169	1.095
	B3LYP	1.13	1.01	1.07	0.98	1.13	1.01	1.00	0.97
	MP2	1.169	1.068	1.169	1.070	1.121	1.013	1.100	1.006
Intercept	HF	−2.99	−7.73	5.41	2.00	3.79	−3.94	10.85	7.86
	B3LYP	−47.63	−43.09	−31.72	−30.44	−33.05	−30.74	−20.10	−18.84
	MP2	−6.39	12.43	21.11	25.27	21.85	19.47	33.02	30.02
RMS	HF	15.49	5.84	18.78	11.34	19.82	8.29	20.97	14.20
	B3LYP	29.23	35.31	15.63	23.27	20.82	29.33	11.11	18.30
	MP2	3.53	13.39	25.09	24.26	28.70	19.90	33.31	28.27
Correlation coefficient	HF	0.9662	0.9685	0.9645	0.9807	0.98.64	0.9883	0.9845	9887
	B3LYP	0.9629	0.9612	0.9585	0.9727	0.9801	0.9834	0.9801	0.9847
	MP2	0.9876	0.9871	0.9806	0.9757	0.9893	0.9860	0.9818	0.9829

S, Cl, Se, Ge, As, Xe, W, U, spanned in the range of almost 1300 ppm varying from the most shielded (ClF, $\delta = -448$ ppm) to the most deshielded (FOOF, $\delta = 825$ ppm) species. It was found that the BP86 functional performed fairly well in predicting ^{19}F NMR spectra, with a Mean Absolute Error (MAE) of 33 ppm for the range of about 1300 ppm.

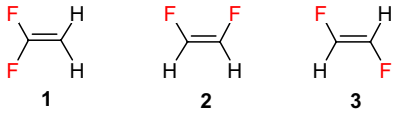
However, no any trend was apparent in the relatively small range for uranium chlorofluorides, as could be judged from the data presented in Table 5. Indeed, the range of calculated ^{19}F NMR chemical shifts was essentially correct (*ca.* 760 ppm) with the employed BP86 and PBE0 functionals, but much lower (*ca.* 530 ppm) with the much less known SAOP functional,[49] the latter critically underestimating experimental values. Unfortunately, the overall correlation with experiment was apparently weak, which meant that none of theoretical levels adopted in that study was sufficiently accurate to make quantitative predictions of ^{19}F NMR chemical shifts of uranium complexes.

Table 5. Calculated and experimental ^{19}F NMR chemical shifts (ppm) of uranium chlorofluorides. Compiled from Saielli *et al.*[47]

Compound	Spin system	SAOP	BP86	PBE0	Experiment
UF_6	A_6	603.0	831.7	771.5	764.0
UF_5Cl	A_4X (A_4)	571.5	812.2	773.2	781.5
	A_4X (X)	555.3	781.9	768.1	762.0
cis-UF_4Cl_2	A_2X_2 (A_2)	555.5	799.8	775.3	785.8
	A_2X_2 (X_2)	536.9	765.8	768.4	760.0
trans-UF_4Cl_2	A_4	560.4	800.6	782.0	755.5
mer-UF_3Cl_3	A_2X (A_2)	548.4	791.0	782.2	782.6
	A_2X (X)	527.0	755.8	775.8	753.0
fac-UF_3Cl_3	A_3	526.0	754.6	770.5	786.4
cis-UF_2Cl_4	A_2	520.4	762.8	778.1	781.0
trans-UF_2Cl_4	A_2	543.8	784.8	789.3	746.1
$UFCl_5$	A	516.8	743.9	787.1	774.3

Passing to organic molecules containing fluorine substituents, it should be recalled that the most simple example of *gem*-, *cis*- and *trans*-difluoroethylenes **1** – **3** was systematically investigated by Nozirov *et al.*,[50] who perfomed the DFT together with the wave function HF, MP2, CCSD and CCSD(T) calculations of their ^{19}F NMR chemical shifts.

Structures 1 – 3

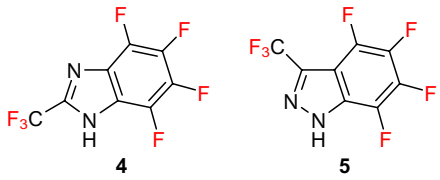


Not unexpectedly, Becke's 'half and half' (BHandH) density functional predicted more accurate ^{19}F NMR isotropic shieldings, as compared to the most common B3LYP method. A surprisingly good performance of the Hartree – Fock calculations in predicting the nuclear shieldings in these molecules was also observed. Inclusion of a zero-point vibrational correction markedly improved agreement between the performed calculations and experiment for nuclear shieldings calculated with HF, MP2, CCSD and CCSD(T) methods but generally worsened the DFT results.

In more detail, those results[50] indicated that fluorine shieldings were very sensitive to the ZPVC and temperature corrections. Thus, the initial data (those without the title correction) predicted fluorine shieldings significantly underestimated by the VSXC and BHandH functionals (−21 and −13 ppm, respectively) and overestimated by the HF calculations by about 23 ppm. Besides, the MP2 method predictions were even better than those of the coupled cluster theory (7 *vs* 9 – 10 ppm). However, in this case one could suspect that the reason of this result was that the MP2 results were obtained with a significantly better quality basis set than in the CCSD and CCSD(T) calculations. The inclusion of the vibrational and temperature corrections calculated at the MP2 level significantly improved the HF, MP2, CCSD and CCSD(T) results. The use of those corrections calculated at the HF level increased observed deviations by only about 1 ppm. However, the DFT shieldings evaluated with the ZPV corrections were significantly worse (showing the deviations of as much as −20 to −29 ppm). Those results demonstrated general difficulties of DFT in predicting the ^{19}F NMR nuclear shielding constants and, on the other hand, showed a surprisingly good performance of the HF method.

Most recently, Alkorta and co-workers[51 – 58] performed a number of the Gauge Including Projected Augmented Wave (GIPAW)[59] calculations of the solid-state ^{19}F NMR chemical shifts for a series of representative organofluorine compounds. In the most recent paper from that series,[51] the GIPAW calculations of the ^{19}F CP MAS shielding constants of the polymorphic crystal structures of several fluorinated benzazoles (exemplified with the structures of the perfluorinated derivatives of 1*H*-benzimidazole **4** and 1*H*-indazole **5**) were performed. The latter were compared with the liquid-phase B3LYP)/6-311++G(d,p) results obtained within the Polarizable Continuum Model (PCM) for dimethyl sulfoxide used as a solvent. This method was tested and approved earlier for the related species by the same principal authors.[53, 54, 60 – 62]

Structures 4, 5



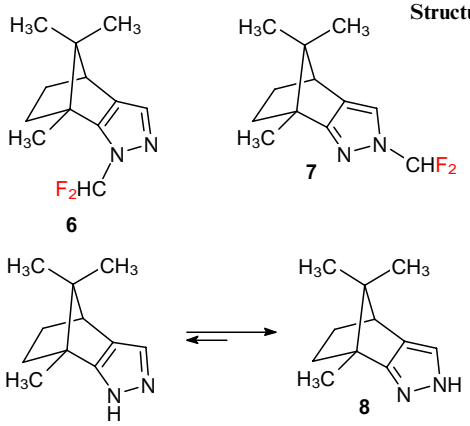
The equation (1) to transform absolute fluorine shielding constants calculated at the B3LYP/6−311++G(d,p) level in gas phase into ^{19}F NMR chemical shifts was used, as suggested in the earlier publications of this research team.[63, 64]

$$\delta(^{19}\mathrm{F}) = 175.7 - 0.963\,\sigma(^{19}\mathrm{F}) \qquad (1)$$

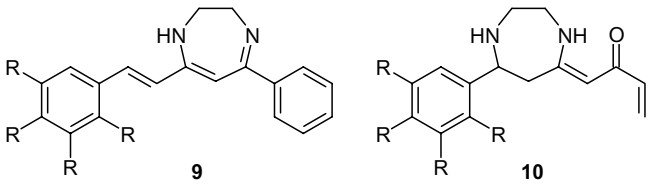
Statistical comparison between both methods revealed that the B3LYP)/6−311++G(d,p) method was more accurate in the calculation of ^{19}F NMR chemical shifts, as compared to the GIPAW results. More work was declared to be necessary to ascertain if the GIPAW calculations were justified, depending on the kind of molecules to be studied. However, it was also stated that in any case, the GIPAW calculations would be very helpful to predict and assign the ^{19}F NMR signals of the CP MAS spectra of polymorphic crystal structures of fluorinated azoles and related nitrogen-containing compounds.

García-Pérez *et. al.*[52] reported the anisochrony of the fluorine atoms of the CHF_2 group in compounds **6** and **7**, which are the two derivatives of (4*S*,7*R*)-7,8,8-trimethyl-

Structures 6 – 8



Structures 9, 10



R = H, OH, OCH_3, F R = H, OH, OCH_3, F

4,5,6,7-tetrahydro-4,7-methanoindazole existing almost entirely in the tautomeric 2*H*-form **8**,[65 – 68] which is also known as (4*S*,7*R*)-camphopyrazole. Calculations of ^{19}F NMRF chemical shifts were performed at the B3LYP/6-311 + + G(d,f) level in good agreement with experiment, as illustrated in Table 6 compiled from the former publication [52] ($CHCl_3$ was used as a solvent both in the calculations and experiment; additionally, computational gas phase data were reported). As follows from those data, the anisochronic difference in the ^{19}F NMR chemical shifts of the CHF_2 group in these compounds, both in liquid and gas phases, was rather small, almost next to negligible.

Table 6. Calculated and experimental ^{19}F NMR chemical shifts of the anisochronic fluorines of the CHF_2 group in the derivatives of (4*S*,7*R*)-camphopyrazole in $CHCl_3$. Compiled from García-Pérez *et al.*[52]

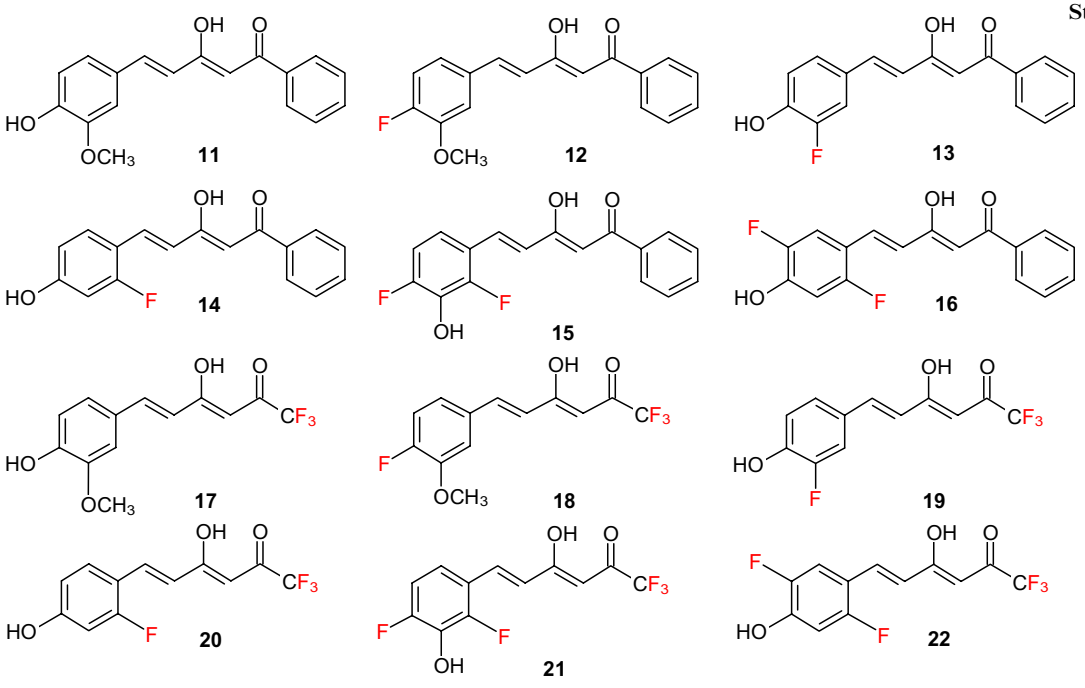
Compound	Anisochronic ^{19}F NMR chemical shifts (ppm)			
	B3LYP/6-311 + + G(d,f)		experiment	
6	−94.07 (−93.18)[a]	−90.23 (−89.73)	−91.64	−89.16
7	−94.21 (−92.83)	−90.68 (−88.66)	−92.05	−90.80

[a] Given in parentheses are the ^{19}F NMR chemical shifts calculated in gas phase.

In the preceding paper,[53] the derivatives of two different 1,4-diazepine series, **9** and **10**, with different substituents in the styrene and benzene moieties, R = H, OH, OCH_3, F, were studied in terms of their structures and tautomerism. In the cited study, the experimental liquid- and solid-state ^{19}F NMR data were supported by the calculations of fluorine chemical shifts at the B3LYP/6-311 + + G(d,p) level. It was established that series **9** (R = H, OH, OCH_3, F) existed predominantly as zwitterions, which is a rather unusual tautomeric structure for such systems. The seven-membered ring had a twisted conformation based on the ^{19}F NMR computational study performed at the B3LYP/6-311 + + G(d,p) level. On the other hand, series **10** (R = H, OH, OCH_3 and F) existed mainly in the form of tautomers with the intramolecular hydrogen bond involving the seven-membered ring in a chair conformation. For this series, theoretically calculated chemical shifts agreed well with experimental data and allowed the assignment of the ^{19}F MAS NMR signals of the disordered molecules present in the solid state of these compounds.

Two years earlier, the same principal authors [54] reported the ^{19}F NMR chemical shift tensors for the crystal and isolated configurations of eleven hemicurcuminoids **12** – **22**, the derivatives of parent compound **11**. For the solid state, the DFT gauge-including projector augmented wave

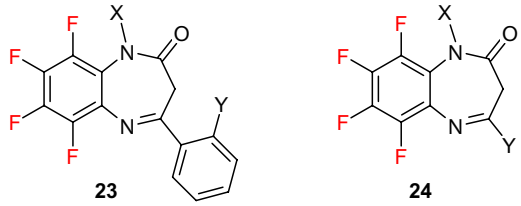
Structures 11 – 22



method GIPAW [59] with pseudopotentials to approximate the core electron wavefunction was employed to predict ^{19}F NMR chemical shift tensors using the PBE functional, both for crystal and isolated configurations. The fact is that two independent methods, one based on the geometries optimized in gas phase and the other one based on the experimental geometries of a crystal, led to the highly proportional absolute shielding constants. Therefore the solid-state chemical shifts can be unambiguously assigned based on the B3LYP/6-311++G(d,p) calculations including DMSO solvent effects evaluated at the PCM level. In this way, it was established that calculations of ^{19}F NMR chemical shifts in DMSO, used as a solvent, can properly reproduce the crystal field effects.

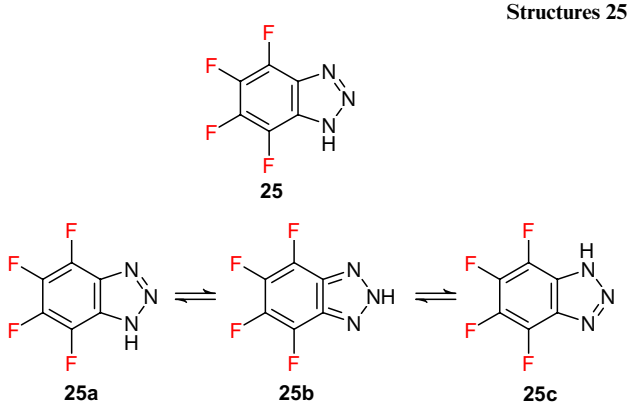
At the same period of time, a series of twelve 4-aryl-6,7,8,9-tetrafluoro-1,5-benzodiazepin-2-ones represented by structures **23** and **24** with different substituents X and Y have been synthesized and fully characterized by their ^{19}F NMR spectra in solution and in solid state.[55] Both for the tautomerism studies and for the conformational analysis, theoretical calculations of their ^{19}F NMR chemical shifts at the B3LYP/6-311++G(d,p) level were carried out. As a principle finding of the performed study, the enamine tautomers of fluorinated 4-aryl-1,5-benzodiazepinones have been identified in this series for the first time.

Structures 23, 24



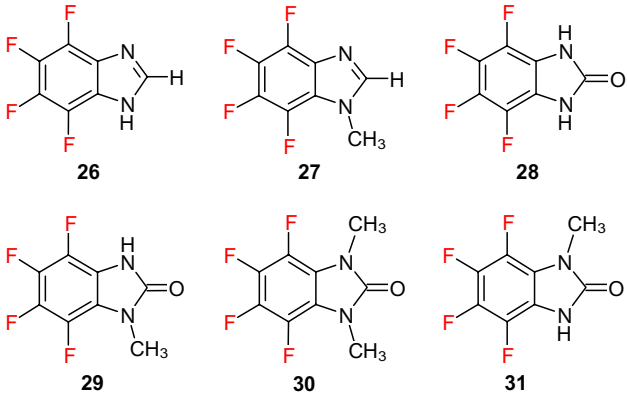
Also, Santa María *et al.*[56] studied the properties of unsubstituted 4,5,6,7-tetrafluoro-1*H*-benzotriazole (**25**) by means of experimental measurements supported by the B3LYP/6-311++G(d,p) calculations of its ^{19}F NMR chemical shifts in liquid phase and solid state. It was shown that compound **25** was present as a mixture of two tautomeric forms **25a** and **25c**, being in fast exchange in solution and providing no exchange in the solid state, where it formed a catemer. It was thus established that the presence of the symmetrical form **25b** in solution can safely be excluded based on the calculated ^{19}F NMR chemical shifts as compared to experiment.

Structures 25



A closely related study was performed in the same period of time by the same principal authors [57] on eight 4,5,6,7-tetrafluorobenzazoles **4**, **5** and **26**–**31** (three benzimidazoles, three benzimidazolinones and two indazoles) in liquid and solid phases. Calculated and experimental ^{19}F NMR chemical shifts were discussed taking into account solvent effects and, for the solid state, hydrogen bonds (solid state was simulated by the clusters of up to three molecules). The obtained results confirmed that B3LYP/6-311++G(d,p) calculations afford reliable ^{19}F NMR chemical shifts when combined with the robust regression equations relating fluorine shielding and chemical shift values, in parallel with the earlier publications by different authors.[42, 69, 70]

Structures 26 – 31



It was found [57] that taking into account solvent effects at the PCM level for different solvents (Fig. 1), noticeably improved gas phase results (Fig. 2) and, combined with small clusters (trimers), proved to be a good starting point for the calculation of the solid-state ^{19}F NMR chemical shifts, as illustrated in Fig. 3. This finding should be useful for the identification of organic compounds employing the ^{19}F NMR 'fingerprints', as was written by the authors. It is

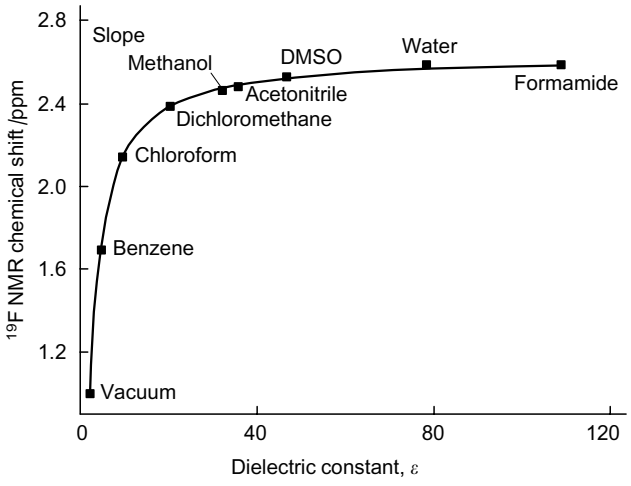


Figure 1. Solvent effects on the ^{19}F NMR chemical shifts of compound **4**, evaluated in terms of the PCM model as a function of the dielectric constant of a solvent. Reproduced with minor editing privilege from Alkorta *et al.*[57] with the permission of *John Wiley and Sons*.

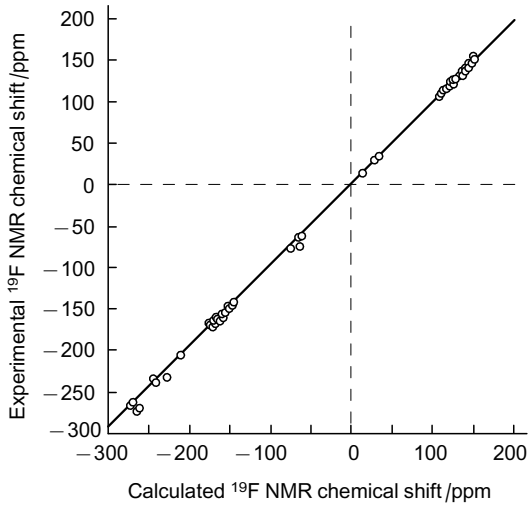
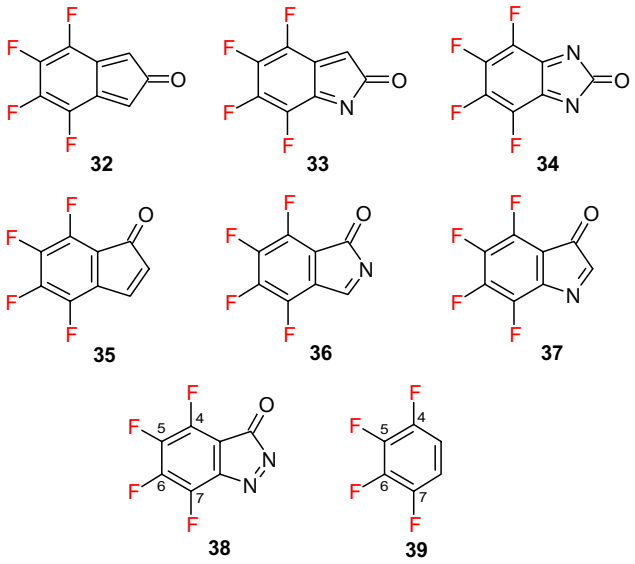


Figure 2. Correlation of experimental ^{19}F NMR chemical shifts of compounds **4**, **5**, **26** – **31** in DMSO against calculated values. Reproduced with minor editing privilege from Alkorta *et al.*[57] with the permission of *John Wiley and Sons*.

Structures 32 – 39



noteworthy and practically important that Fig. 1 allows prediction of ^{19}F NMR chemical shifts of 4,5,6,7-tetrafluorobenzazoles in any solvent known dielectric constant.

A year earlier, Poater *et al.*[58] studied the stability and aromaticity of the 4,5,6,7-tetrafluoro derivatives of 1- and 2-indenones and their aza derivatives **32** – **38** along with some related compounds by means of a quantum chemical analysis and DFT calculations of their ^{19}F NMR chemical shifts. Prior to that work, almost nothing was known about those compounds, apart from the fact that all of them were considered to be fairly unstable and highly reactive. The ^{19}F NMR chemical shifts were calculated in this series at the OPBE/TZ2P level of theory using the PBE/TZ2P optimized geometries. An acceptable performance of the calculations, carried out at the DFT level of theory using the OPBE functional, was verified by the comparison between calculated and experimental ^{19}F NMR chemical shifts of 1,2,3,4-tetrafluorobenzene (**39**), see Table 7.

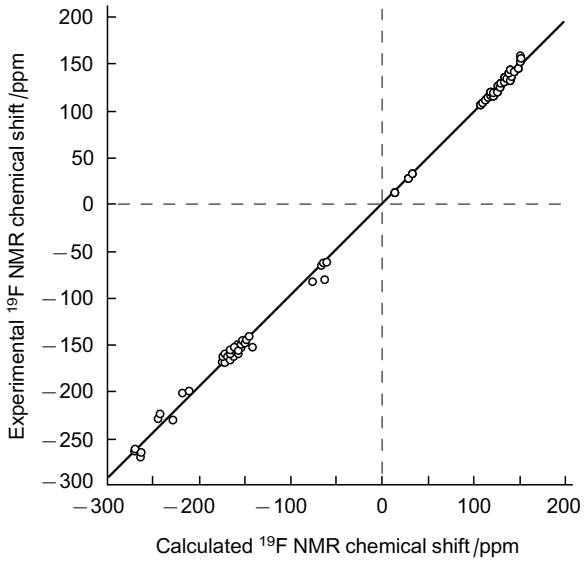


Figure 3. Correlation of the ^{19}F NMR chemical shifts of compounds **4**, **5**, **26** – **31** in solid state against calculated values in DMSO for the central monomer of the related trimers. Reproduced with minor editing privilege from Alkorta *et al.*[57] with the permission of *John Wiley and Sons*.

Several years earlier a very similar study was performed on pentafluoropyridine derivatives[71] providing an extensive and growing chemistry that arises from the nucleophilic aromatic substitution of ring fluorine in pentafluoropyridine (**40**) and resulting in the formation of a variety of novel pyridine systems **41** – **47** presented in Fig. 4. These systems lead to a number of mixed macrocycles, glycosyl donors and polycyclic scaffolds produced by the sequential regioselective displacement of fluorine atoms. Results of the ^{19}F NMR chemical shifts calculations in this series performed at the B3LYP/6-311G(d) level with the MP2 geometries are exemplified for compounds **48a** – **48e** in Table 8. It is seen that a rather satisfactory correlation between calculations and experiment was achieved even at this simple level.

A year later the same principal authors[72] performed similar studies (^{19}F NMR experiment supported by the relevant DFT calculations) for the identification of perfluoroquinoline and perfluoroisoquinoline derivatives, which were produced by their interaction with benzylamine,

Table 7. Calculated ^{19}F NMR chemical shifts (ppm) of the 4,5,6,7-tetrafluoro derivatives of 1- and 2-indenones using $CFCl_3$ as a reference. Compiled from Poater *et al.*[58]

Compound	F4	F5	F6	F7
32	−151.0	−152.3	−152.3	−151.0
33	−136.5	−155.7	−128.2	−150.8
34	−137.8	−130.2	−130.2	−137.8
35	−132.9	−151.6	−150.4	−147.9
36	−128.8	−143.9	−146.4	−141.8
37	−126.2	−153.1	−143.2	−144.9
38	−122.1	−143.6	−135.7	−140.6
39	−147.3	−163.6	−163.6	−147.3
	(−139.8)[a]	(−156.8)	(−156.8)	(−139.8)

[a] Given in parentheses are the experimental ^{19}F NMR chemical shifts.

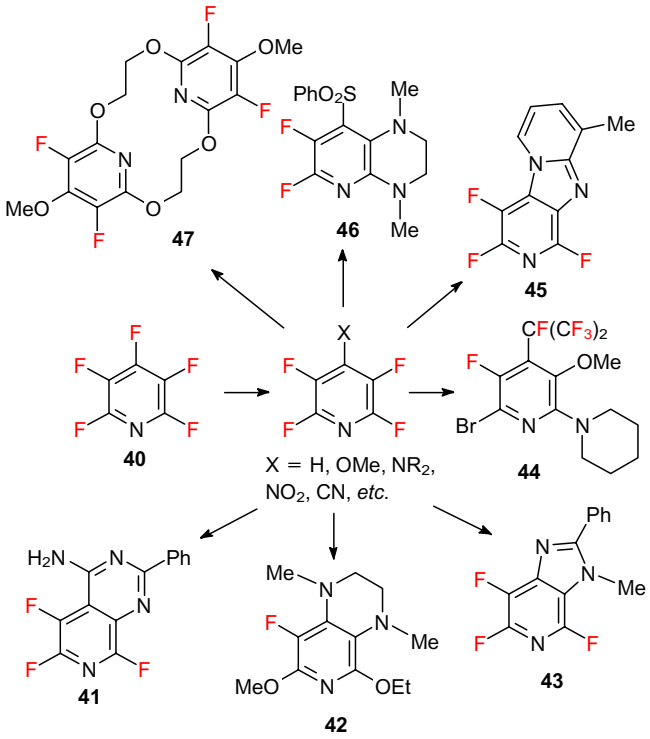
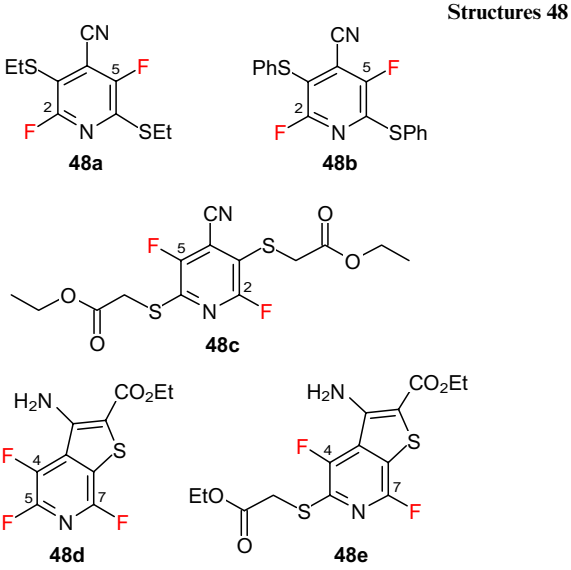


Figure 4. Multi-substituted systems from pentafluoropyridine (**40**). Adapted from Fox *et al.*[71]

Structures 48



as exemplified in Fig. 5 by the X-ray structure of *N*-benzyl-3,4,5,6,7,8-hexafluoroisoquinoline-1-amine (**49**).

All calculations were performed at the B3LYP/6-311G(d) level on the MP2/6-31G(d) geometries and demonstrated an excellent agreement with experiment, as illustrated for the parent perfluoroquinoline (**50**) and perfluoroisoquinoline (**51**) in Table 9.

In the second part of their comprehensive computational ^{19}F NMR survey (the first part dealing mostly with fluorine-containing inorganic compounds is discussed earlier, *vide supra*), Saielli *et al.*[73] performed a systematic study of the fluorine chemical shifts of a wide series of fluorine-

Table 8. Calculated ^{19}F NMR chemical shifts (ppm) of the representative derivatives of pentafluoropyridine, as compared to experiment. Compiled from Fox *et al.*[71]

Compound	Fluorine	Calculation	Experiment
48a	F2	−65.2	−64.9
48a	F5	−119.4	−119.0
48b	F2	−67.4	−62.6
48b	F5	−109.0	−118.0
48c	F2	−63.4	−64.4
48c	F5	−116.4	−118.9
48d	F7	−77.7	−71.7
48d	F5	−104.0	−100.5
48d	F4	−175.9	−158.1
48e	F7	−76.3	−71.4
48e	F4	−144.7	−137.3

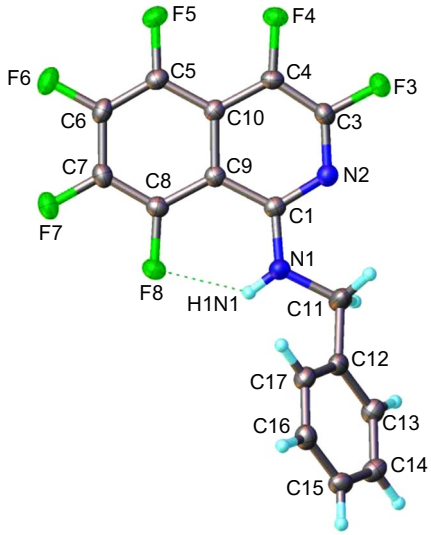
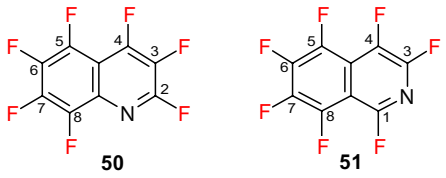


Figure 5. Molecular structure of *N*-benzyl-3,4,5,6,7,8-hexafluoroisoquinoline-1-amine (**49**). The C1–N1–C11–C12 torsion angle is 161.0(1)°. Reproduced from Fox *et al.*[72] with the permission of *Elsevier*.

Structures 50, 51



containing organic compounds involving those with the diverse functional groups. As in the first part of this survey, the authors adopted the GGA BLYP functional and a triple-zeta doubly polarized Slater's basis set TZ2P used within ZORA at the scalar level for the geometry optimization and at the spin–orbit level for the calculation of ^{19}F NMR chemical shifts.

Basically, a convincing correlation was reached between ^{19}F NMR chemical shifts calculated at this level of theory and experimental values in a wide series of the fluorine organic species ranging from simple monofluorinated alka-

Table 9. Calculated ^{19}F NMR chemical shifts (ppm) of perfluoroquinoline (**50**) and perfluoroisoquinoline (**51**), as compared to experiment. Compiled from Fox *et al.*[72]

Fluorine	Compound **50**		Compound **51**	
	calculation	experiment	calculation	experiment
F1			−63.0	−62.1
F2	−72.5	−72.9		
F3	−163.4	−161.3	−94.4	−96.8
F4	−124.0	−124.6	−156.0	−155.7
F5	−146.6	−146.5	−146.2	−145.9
F6	−155.5	−154.8	−147.1	−145.4
F7	−152.0	−151.0	−155.2	−153.1
F8	−148.2	−148.8	−138.7	−139.9

nes to aromatic fluorine compounds, polyfuorinated molecules and systems containing different heteroatoms, such as oxygen, nitrogen, silicon, chlorine and bromine, which is illustrated in Fig. 6. Calculated ^{19}F NMR chemical shifts spanned in a broad range of about 300 ppm, namely from the most shielded fluorine in Me_3SiCH_2F (−277 ppm) to the most deshielded one in CF_2I_2 (+18.6 ppm). The performance of the applied computational protocol was found to be quite satisfactory with the overall correlation overestimating ^{19}F NMR chemical shifts by about 15% and a mean absolute error of 35 ppm, *i.e.* 10% of the whole range.

As an example, the established computational protocol was tested for the identification of two fluorinated steroids, including the drug fluticasone propionate (**52**) and its derivative **53**, the latter bearing two diastereotopic fluorine atoms. The relevant data are given in Table 10 which provide a convincing agreement between the ^{19}F NMR chemical shifts of those challenging benchmark compounds calculated at the applied level of theory and experiment.

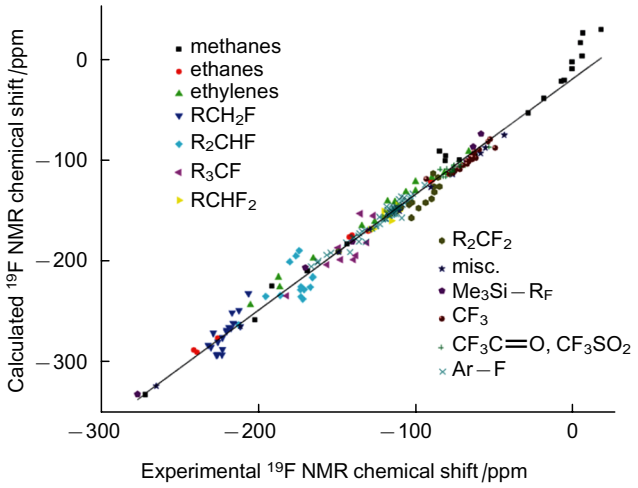


Figure 6. Correlation between calculated and experimental ^{19}F NMR chemical shifts. The compounds are categorized as methane, ethane and ethylene derivatives; primary (RCH_2F), secondary (R_2CHF) and tertiary (R_3CF) monofluorides; primary ($RCHF_2$) and secondary (R_2CF_2) geminal difluorides; trimethylsilyl fluorides (Me_3SiR_F); trifluoromethyl groups (CF_3); trifluoroacetyl and trifluoromethanesulfonyl derivatives ($CF_3C{=}O$, CF_3SO_2); aryl fluorides (ArF) and miscellaneous fluorine compounds (misc.). Reproduced with minor editing privilege from Saielli *et al.*[73] with the permission of *RSC Publishing*.

Structures 52, 53

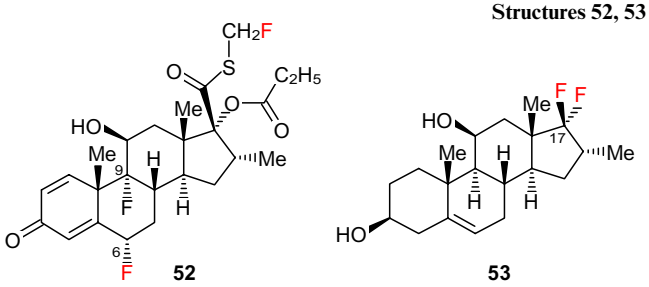


Table 10. Calculated ^{19}F NMR chemical shifts (ppm) of fluticasone propionate (**52**) and its derivative **53**, as compared to experiment. Compiled from Saielli *et al.*[73]

Compound **52**			Compound **53**		
fluorine	calculation [a]	experiment	fluorine	calculation [a]	experiment
F6α	−191.1	−186.7	F17α	−106.3	−100.8
F9α	−159.4	−164.6	F17β	−118.2	−113.6
SCH_2F	−192.7	−192.0			

[a] Chemical shifts estimated using the linear fitting parameters.

The proposed computational scheme was tested also for the prediction of ^{19}F NMR chemical shifts in the series of fluorinated taxol derivatives (exemplified here with structures **54**–**59**, see Table 11), for any of which experimental data were not available. Chemical shifts derived from the DFT calculations showed 'an appreciable distribution of values' which allowed an easy identification of the fluorinated taxols in mixture. The general conclusion was that 'DFT predictions allow to distinguish the slightly different chemical environments of fluorine in these compounds

Structures 54 – 59

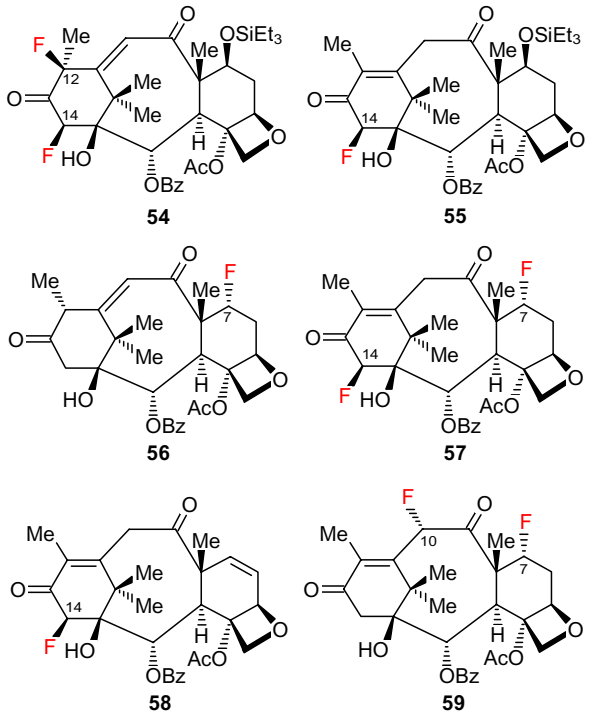


Table 11. Calculated ^{19}F NMR chemical shifts (δ_{calc}/ppm) of fluorinated taxol derivatives. Compiled from Saielli *et al.*[73]

Compound	Fluorine	δ_{calc} [a]	Compound	Fluorine	δ_{calc} [a]
54	F12	−126.6	**57**	F7	−164.5
	F14	−209.4		F14	−187.6
55	F14	−187.7	**58**	F14	−186.9
56	F7	−165.4	**59**	F7	−162.3
				F10	−171.2

[a] Chemical shifts estimated using the linear fitting parameters.

(or mixtures thereof), and can be envisioned as a valuable help in their structure determination'.[73]

3. Calculation of spin – spin coupling constants involving ^{19}F nucleus

Discussed in this Section are the computational aspects of different spin – spin coupling constants involving fluorine: most popular $^{19}F-^{1}H$, $^{19}F-^{13}C$ and $^{19}F-^{19}F$ couplings together with less common $^{19}F-^{15}N$, $^{19}F-^{31}P$ and $^{19}F-^{77}Se$ ones. Theoretical backgrounds of such calculations are almost entirely omitted since they are discussed in much detail elsewhere (see references given in the Introduction). The main goal of the present Section is primarily to give insight into practical application of such calculations performed at different levels of theory.

3.1. $^{19}F-^{1}H$ spin – spin coupling constants

A number of early papers [74–88] deal with the calculation of $^{19}F-^{1}H$ coupling constant in the most simple but most troublesome (in the meaning of computation of its NMR parameters) molecule containing both coupled nuclei — hydrogen fluoride, HF. As an example of such studies, Keal *et al.*[89] calculated this coupling at the DFT level with several functionals and reached the following results: 369.0 Hz (PBE), 439.3 Hz (B3LYP), 444.7 Hz (B97-2) and 458.0 Hz (B97-3), as compared to experimental value of 538.0 Hz. It was found that the errors of calculation correlated with the percentage of exact orbital exchange in the used functionals. Thus, the errors reduced from PBE (0% of exact exchange) to B3LYP (20%), to B97-2 (21%) and B97-3 (27%). However, those errors are too large to provide reasonable agreement between the calculated values and experiment.

Much later, Gryff-Keller and Szczeciński [90] optimized the HF molecular geometry using the BHandH/aug-pcJ-3 method and then evaluated $^{1}J_{F,H}$ coupling constant calculated for this molecule with the same functional and basis set, which provided the value of 543.3 Hz. Such an excellent coincidence with experiment (538.0 Hz) is probably due to the so-called 'cancellation of errors'. Even if it is so, the reasonable question raised by the of the cited publication was how frequently such error cancellations did occur for the calculated coupling constants $^{n}J_{F,X}$ and whether it should be ignored or taken into account.

Herewith, other relevant results for the HF molecule are not discussed and only the most convincing example of the early studies provided by the SOPPA-based calculations of $^{1}J_{F,H}$ in this intriguing molecule is considered.[74] Enevoldsen *et al.*[74] applied the most advanced SOPPA(MP2) and SOPPA(CCSD) methods in combination with cartesian and spherical basis sets, which are specified in the footnote to Table 12. In the latter (and hereinafter in the text), the following notations for the coupling contributions are used: DSO for Diamagnetic Spin – Orbit, PSO for Paramagnetic Spin – Orbit, SD for Spin Dipolar, FC for Fermi contact and TO for TOtal, *i.e.* the algebraic sum of all four coupling contributions. In the cited study, very large basis sets of Gaussian basis functions, optimized for the calculation of indirect nuclear spin – spin coupling constants, were used instead of the standard small basis sets traditionally used in such calculations. It was generally found that for the $^{1}J_{F,H}$ coupling constant, the SOPPA(CCSD) method performed noticeably better than SOPPA(MP2). The most amazing fact was a noticeable coincidence of the total theoretical values reached at in the performed calculations [74] with cartesian and spherical basis sets (525.40 and 529.43 Hz, respectively) with experiment (529 ± 23 Hz), as illustrated in Table 12.

Turning to fluorine-containing organic compounds, it should be recalled that Alkorta *et al.*[91,92] performed SOPPA(MP2) and EOM – CCSD calculations of all possible three-, four- and five-bond $^{19}F-^{1}H$ coupling constants in a series of twelve fluorobenzenes **39**, **60** – **70** using Ahlrichs' qzp basis set on carbons and fluorines and qz2p on protons.

Structures 60 – 70

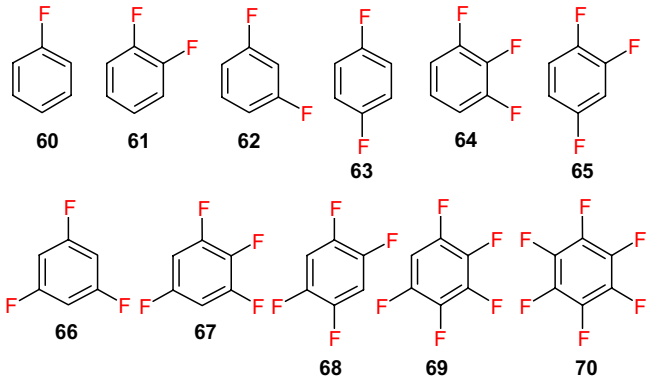


Table 12. Calculated $^{19}F-^{1}H$ spin – spin coupling constants (Hz) in the HF molecule *vs.* experiment. Compiled from Enevoldsen *et al.*[74]

Basis set	Method	DSO	PSO	SD	FC	TO	Experiment
I [a]	RPA	−0.06	199.41	−12.43	468.65	655.57	
	SOPPA(MP2)	0.02	195.88	−0.65	339.74	534.99	
	SOPPA(CCSD)	0.03	194.58	−1.12	331.91	525.40	529 ± 23
II [b]	RPA	−0.03	195.05	−11.73	483.62	666.91	
	SOPPA(MP2)	0.04	190.65	−0.56	349.40	539.52	
	SOPPA(CCSD)	0.05	189.82	−0.94	340.50	529.43	529 ± 23

[a] Cartesian Gaussian basis set 13*s*8*p*4*d*/8*s*3*p*1*d* contracted to 9*s*6*p*4*d*/6*s*3*p*1*d*. [b] Spherical Gaussian basis set 15*s*6*p*3*d*1*f*/10*s*3*p*1*d*.

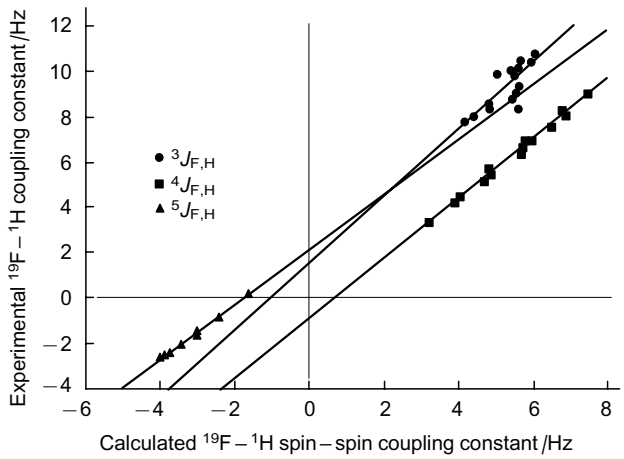


Figure 7. Correlation of experimental $^{n}J_{F,H}$ ($n = 3$, 4 and 5) coupling constants in the series of fluorobenzenes against those calculated at the SOPPA(MP2) level. Reproduced with minor editing privilege from Alkorta *et al.*[91] with the permission of *Elsevier*.

A rather good correlation between calculated and experimental couplings was observed, as illustrated in Fig. 7. However, the calculated values were systematically underestimated, which was most pronounced for vicinal couplings, $^{3}J_{F,H}$. As an example, it was found that $^{3}J_{F,H} = 5.42$ Hz (calc.) *vs* 8.82 Hz (exp.) in **60**; 5.47 Hz (calc.) *vs* 9.95 Hz (exp.) in **64**; and 5.64 Hz (calc.) *vs* 10.42 Hz (exp.) in **69**. On the other hand, negative long-range five-bond coupling constants were noticeably overestimated in magnitude, as can be followed in the series of the same three compounds: $^{5}J_{F,H} = -1.65$ Hz (calc.) *vs* 0.23 Hz (exp.) in **60**; -3.40 Hz (calc.) *vs* -2.07 Hz (exp.) in **64**; and -4.02 Hz (calc.) *vs* -2.65 Hz (exp.) in **69**.[92]

Very recently, Viesser *et al.*[93] examined the dependence of the $^{3}J_{F,H}$ coupling constant on the bond angle and spatial separation of coupled nuclei in the series of fluorocycloalkenes **71**–**74** at the DFT, SOPPA(CC2) and SOPPA(CCSD) levels. This series of compounds was selected in view of the fact that the F–C=C–H dihedral angle, describing the $^{19}F-{}^{1}H$ coupling pathway, is equal to zero, so that the bonding pattern, relevant for a through-space transmission, was formally the same in all compounds. All calculations were performed with Sauer's aug-cc-pVTZ-J basis set for atoms involved in this particular coupling, while the Dunning's aug-cc-pVTZ basis set was implied for the rest of atoms. The cc-pVTZ basis set was used for the non-coupled atoms of compound **71** due to the enormous computational costs in this case. Diffuse and polarization functions in the aug-cc-pVTZ basis sets, that are absent in the aug-cc-pVTZ-J, were added to the latter in order to keep the basis sets well balanced in the valence regions.

As can be seen in Table 13, the SD and DSO contributions to $^{19}F-{}^{1}H$ spin – spin coupling constants are small, as

Structures 71 – 74

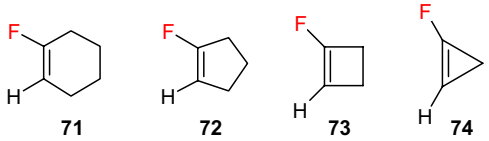


Table 13. $^{19}F-{}^{1}H$ spin – spin coupling constants (Hz), calculated at different levels of theory, *vs.* experiment. Compiled from Viesser *et al.*[93]

Compound	Method	DSO	PSO	SD	FC	TO	Experiment
71	PBE0	0.0	−3.5	−0.8	19.1	14.8	18.4
	CCSD	−0.1	−2.6	−0.8	15.7	12.2	
	CC2	−0.1	−2.5	−0.8	16.5	13.1	
72	PBE0	−0.5	−3.6	−0.3	4.4	0.0	0.0
	CCSD	−0.5	−2.5	−0.4	1.9	−1.5	
	CC2	−0.5	−2.5	−0.4	2.5	−0.9	
73	PBE0	−1.1	−4.9	−0.2	−3.8	−10.0	−8.8
	CCSD	−1.1	−3.6	−0.3	−5.9	−10.9	
	CC2	−1.1	−3.5	−0.3	−5.7	−10.6	
74	PBE0	−1.9	−3.2	0.9	−5.9	−10.1	
	CCSD	−1.9	−2.4	0.7	−6.2	−9.8	
	CC2	−2.0	−2.2	0.7	−6.3	−9.8	

compared to their total values for all compounds **71** to **74**, while the FC term decreases drastically from positive to negative, suggesting that different FC transmission mechanisms are coming into play for different compounds. The PSO contribution was found to be sizable, but it remained relatively constant across that set of molecules. Interesting to note that increased steric strain in compounds **73** and **74** resulted in a negative sign of their total $^{3}J_{F,H}$ coupling constants, determined by the negative Fermi contact contributions, which is rather unusual for the related systems. Another interesting observation, following from the data presented in Table 13, is that the spin dipolar contribution, being negative in compounds **71**–**73**, changes its sign to a positive one in the most strained 1-fluorocycloprop-1-ene (**74**).

Calculated correlation[93] between interatomic distances and the Fermi contact terms or the total $^{3}J_{F,H}$ coupling constant is shown in Fig. 8. It can be seen, that $^{3}J_{F,H}$ exponentially decreases with a F–H distance in the series of compounds **71**–**74**, suggesting the interplay between the nonbonding interactions and the through-space transmis-

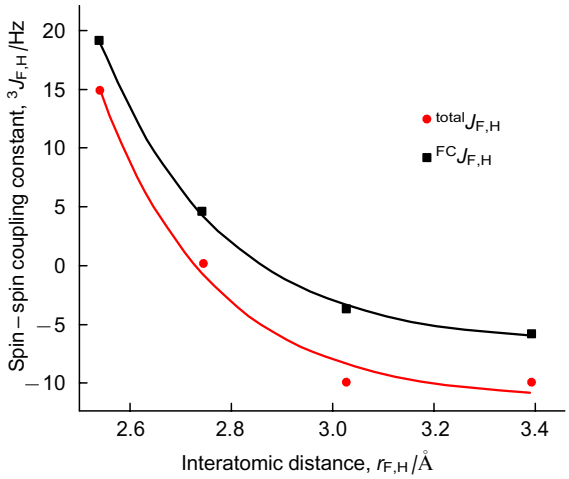


Figure 8. Dependences of the $^{3}J_{F,H}$ coupling constant and its Fermi contact contribution, calculated at the PBE0/TZ2P level, on the interatomic distance between coupled nuclei. Reproduced with minor editing privilege from Viesser *et al.*[93] with the permission of the *Royal Society of Chemistry*.

sion of this coupling constant. A similar trend was previously reported by Mallory *et al.*[94] for the $J_{F,F}$ coupling constants in difluoronaphthalene and difluorophenanthrene derivatives, where a nonbonding overlap interaction between fluorine lone pairs was found to be responsible for this spin – spin coupling transmission *via* a through-space mechanism. Based on those results, it was concluded that the through-space mechanism took place in compounds **71** and **72**, vanished in compound **73** and appeared in compound **74** in the 'rear lobe' region around carbons.[93] Similar observations were made earlier by Contreras *et al.*[95] and much earlier by San Fabián *et al.*[96,97] for the related systems.

On the other hand, $^3J_{F,H}$ and its Fermi contact contribution strongly decrease with the bond angle θ in this series of compounds because of the increasing distance between two coupled nuclei, as shown in Fig. 9. The range of θ from 60 to 120° corresponds to the bond angles found for that series of compounds. However, $^3J_{F,H}$ does not change its sign to negative in model fluoroethylene, as it takes place in compound **74**, but approaches zero for the largest θ, suggesting that the ring strain in the cyclic compounds may contribute to the change of this coupling constant.

Viesser *et al.* concluded[93] that the Fermi contact term of $^3J_{F,H}$ was strongly dependent on the corresponding bond angles and the distance between hydrogen and fluorine nuclei. Two main transmission mechanisms, the through-space and the hyperconjugative through-bond interactions, explained how nuclear hyperfine field-induced spin density was transferred in those coupling pathways. It was generally found that both transmission pathways of $^3J_{F,H}$ take place in the studied fluorocycloalkene compounds, but the through-space mechanism was dominant for compounds **71** and **74**, while the through-bond mechanism prevailed in compounds **72** and **73**. It was also suggested that the ring strain in **73** and **74** can be associated with the experimental negative sign of $^3J_{F,H}$ in those compounds.

More recently, the same principal authors[98] performed the PBE0/TZ2P calculations of $^3J_{F,H}$ and $^5J_{F,H}$ coupling constants in the molecule of the triazole antifungal fluori-

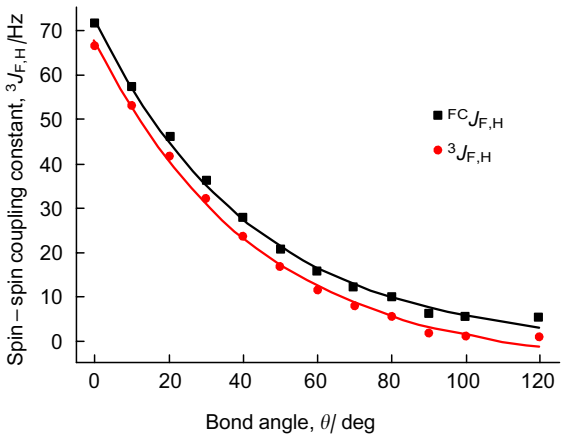
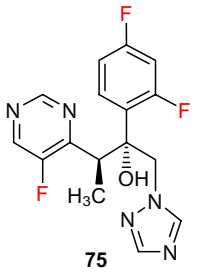


Figure 9. Bond angle dependences of the $^3J_{F,H}$ coupling constant and its Fermi contact contribution in fluoroethylene taken as a model system, calculated at the SOPPA(CCSD)/aug-cc-pVTZ-J level of theory. Reproduced with minor editing privilege from Viesser *et al.*[93] with the permission of the *Royal Society of Chemistry*.

Structure 75



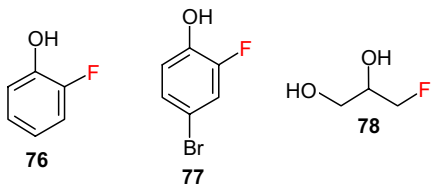
75

nated drug voriconazole (**75**). A decomposition analysis of $^nJ_{F,H}$ (n = 3, 5) in terms of the localized molecular orbital contributions allowed authors to determine that interactions involving nitrogen lone pairs are the main reason for the larger value of experimental $^5J_{F,H}$, as compared to $^3J_{F,H}$. Performed molecular orbital analysis indicated that delocalization of the nitrogen lone pairs had a positive contribution to $^5J_{F,H}$, while a negative one was found for $^3J_{F,H}$, which explained their experimental difference. This result is of particular importance in view of the fact that $^5J_{F,H}$ is a well-known probe for evaluating the glycosidic torsion dependence in 5-fluoropyrimidine-substituted RNA.[99]

In two related papers,[100,101] transmission mechanism of $^{19}F - ^1H$ coupling involving intramolecular hydrogen bonding was studied for two fluorophenols **76** and **77** together with 3-fluoro-1,2-propanediol (**78**). In the first paper,[100] it was found that for compounds **76** and **77** it was typical of a Fermi contact term to be transmitted mainly through the exchange interactions owing to the overlap of the proximate electron clouds. Therefore, it was suggested to identify such couplings as $^{nTS}J_{F,H}$, where n stands for the number of formal σ-bonds separating coupled nuclei (n = 4 in the reported case). These results provided an interesting rationalization for the different experimental trends known in the current literature for the long-range $J_{F,H}$ couplings. In the second paper,[101] the preferred orientation of the OH and F substituents in compound **78** was derived from the calculated $^{19}F - ^1H$ coupling constants, as compared to experiment. The established conformational preference of 'all-*gauche*' conformations, which was found to exist both in gas phase and in solution, was better described by the predominant hyperconjugative interactions over the Lewis-type interactions in **76** and **77**. On the other hand, the strong contribution from the antiperiplanar interactions involving σ_{CH} and σ_{CC} as the electron donors and σ^*_{CF} and σ^*_{CO} as the electron acceptors, rather than a hydrogen bond, was found to be responsible for the *gauche* effect in **78**.

A bit later, the same principal authors[102] examined transmission mechanisms of such unusual through-space coupling constants, $^{TS}J_{F,H}$, to rationalize them in terms of the molecular electronic structure using 2-fluorobenzaldehyde as a model compound. The calculations were per-

Structures 76 – 78



76 **77** **78**

formed at the SOPPA(CCSD) level with the EPR-III basis set.

Transmission mechanisms of the through-bond and through-space contributions of $J_{F,H}$ are not always clear, so that some effort to rationalize such cases was worthy of a more detailed investigation. As evidenced from the performed study,[102] the through-space transmission of $J_{F,H}$ is composed of three different types of intramolecular contributions, namely,

(a) those originating from the exchange interactions taking place in the region where electron clouds surrounding the fluorine and hydrogen atoms overlap;

(b) the direct charge-transfer interactions between either fluorine lone pairs or the σ_{C-F} occupied and, on the other hand, σ^*_{CH} vacant orbitals;

(c) long-range charge-transfer interactions through concatenated sequences of hyperconjugative interactions.

Canonical Molecular Orbital (CMO) analysis[102] showed that the through-space fluorine-hydrogen coupling transmission is mediated by the virtual transitions between occupied and vacant CMOs, unless the Fermi-contact interaction is mostly transmitted by the exchange interactions. In that case, only occupied CMOs contained simultaneously fluorine and coupled hydrogen, are effective, as shown in Fig. 10. This indicates that the main transmission mechanism of the Fermi-contact term of $^{TS}J_{F,H}$ is the exchange interaction in the region where the fluorine and chemically non-bonded hydrogen electron clouds overlap.

To study the behaviour of the $^{TS}J_{F,H}$ coupling constant in 2-fluorobenzaldehyde, Favoro *et al.*[102] performed BHandH/EPR-III calculations varying interatomic distances with 0.1 Å step, as shown in Fig. 11. It was essential that computed through-space contributions of coupling constants, $^{TS}J_{F,H}$, were transmitted through space between chemically non-bonded fluorine and hydrogen atoms. An important contribution to this Fermi-contact interaction was found to be transmitted by the LP(F) $\rightarrow \sigma^*_{CH}$ hyperconjugative interaction, which strongly depends on the overlap between the carbon – hydrogen bond and the fluorine lone pair. The basic result of the performed study[102] was that a particular caution should be taken when trying to use the through-space coupling constants, $^{TS}J_{F,H}$, as a probe to detect the spatial proximity between fluorine and hydrogen atoms.

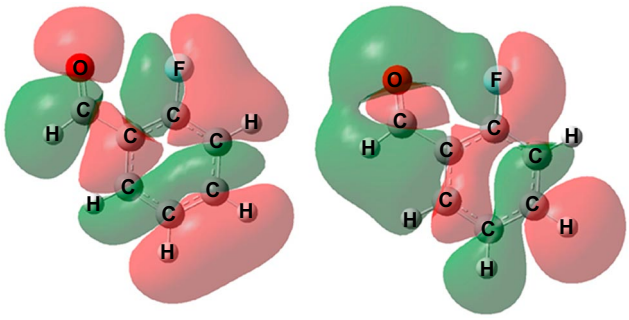


Figure 10. Canonical molecular orbitals of fluorobenzaldehyde including fluorine and coupled hydrogen, responsible for the through-space fluorine – hydrogen coupling. Reproduced with minor editing privilege from Favaro *et al.*[102] with the permission of the *American Chemical Society*.

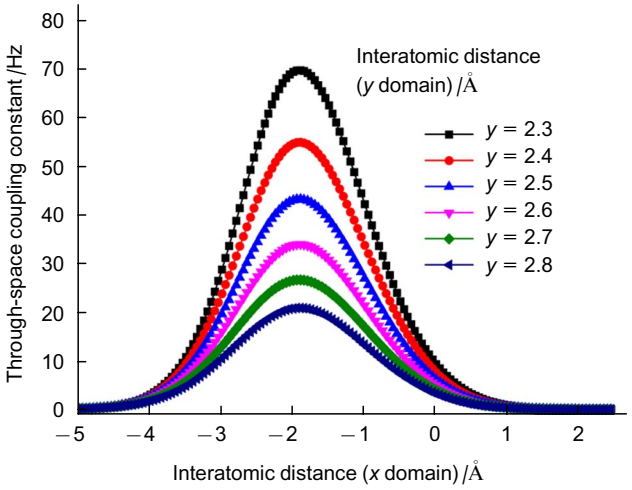


Figure 11. Variation of the Fermi-contact contribution of the through-space coupling constant, $^{TS}J_{F,H}$, in the $CH_4\cdots F-H$ model dimer as a function of interatomic distance (see the original publication for details). Reproduced with minor editing privilege from Favaro *et al.*[102] with the permission of the *American Chemical Society*.

3.2. $^{19}F - ^{13}C$ spin – spin coupling constants

Beginning the discussion of the computational aspects of $^{19}F - ^{13}C$ coupling constants, let us turn to difluoroethyne (also referred to as difluoroacetylene), F – C≡C – F, as one of the most simple but very intriguing molecules. It received a good deal of attention in relation of its one-bond and geminal fluorine-carbon couplings.[103 – 106]

As an example, in one of the most recent publications, Caputo *et al.*[106] performed a theoretical study of $F-C\equiv F:(H_2O)_n$ complexes with $n = 1$ and 2 by means of the most sophisticated computational methods. In particular, $^{19}F - ^{13}C$ coupling constants in the relevant complexes were calculated at the CCSD level using Sauer's core-property basis set aug-cc-pVTZ-J. A special attention was paid to the dependence of the one-bond and geminal fluorine – carbon intramolecular coupling constants in the F – C≡C – F molecule on the distance between the coupled nuclei and the presence or absence of water molecules in the computational space. These coupling constants were found to be exceptionally sensitive to the presence of water molecules, which can provide information on the bonding structure of the molecule. In particular, three kinds of interactions were observed in the localized complexes **79** – **84** of difluoroethyne with water (which are shown in Fig. 12), namely those including H···p interactions, H···F hydrogen bonds and O···F – C tetrel bonds. A very good agreement between $^1J_{F,C}$ calculated at this level (−288.99 Hz for complex **84**) and the experimental value of −287.3 Hz was reported by Bürger and Sommer.[107]

The absolute value of the $^1J_{F,C}$ coupling constant was shown[106] to decrease with increasing interatomic distance. This behaviour, however, cannot be attributed to a mere dependence of $^1J_{F,C}$ on the F – C≡C – F geometry. The results for the $^1J_{F,C}$ couplings in isolated difluoroethyne, where the molecular geometry was fixed to the one present in the complexes, are due to the fact that in this case the coupling slightly increased in magnitude with the C – F distance. The differences between two $^1J_{F,C}$ couplings were the largest for complexes **81** and **82**. The case of intermo-

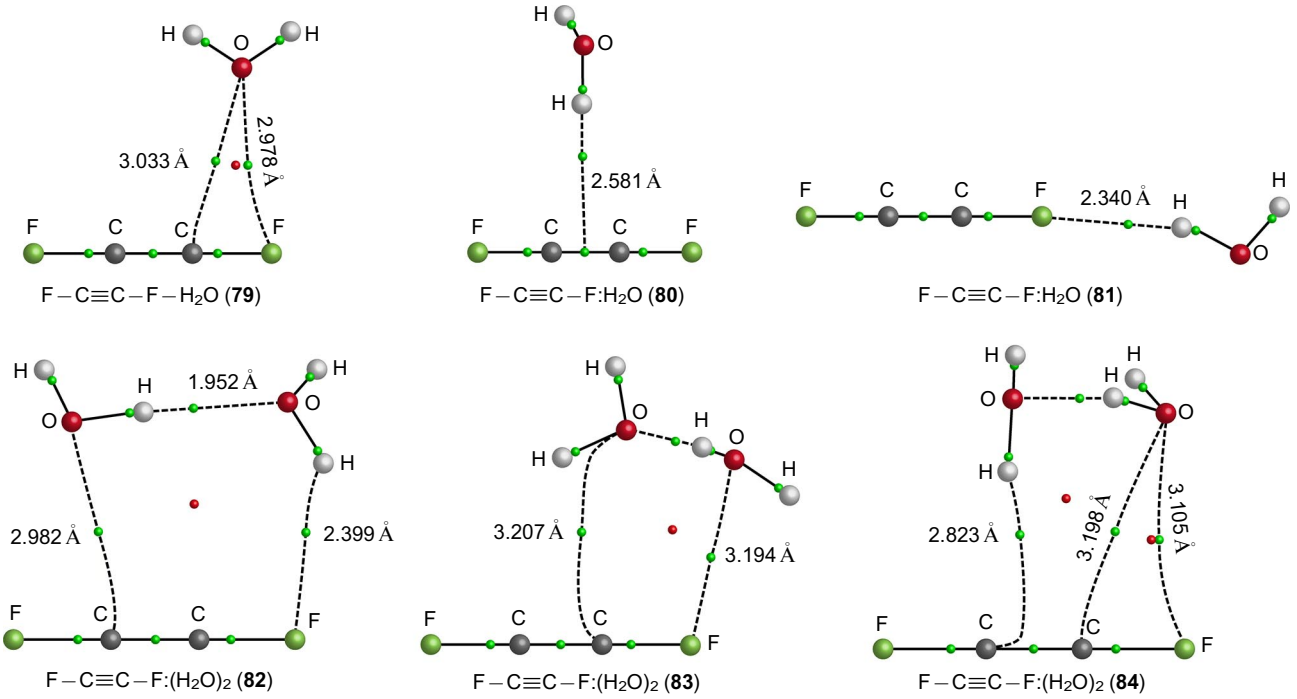


Figure 12. Molecular graphs of the minima found for the F – C≡C – F:H_2O (upper raw) and F – C≡C – F:$(H_2O)_2$ (bottom raw) complexes. The small dots on dashed and solid lines (shown in green) indicate the location of the bond critical points, while the small dots not superimposed on lines (given in red) indicate the location of the ring critical points. Reproduced with minor editing privilege from Caputo *et al.*[106] with the permission of *Taylor & Francis*.

lecular complex **81** was particularly 'conspicuous' (as was written in the original publication [106]) with a large difference between the computed $^1J_{F,C}$ coupling and the value predicted by theoretical trend. This could be due to the fact that complex **81** was the only structure with the F···H hydrogen bonding in the direction of the fluorine lone pair, which was also reflected in the shortest intermolecular bonds among all complexes **79** – **84**.

For the geminal $^2J_{F,C}$ coupling, no distinct dependence on the corresponding interatomic distance d_{C-F} was observed. In fact, basically the same values were obtained for two couplings in complexes **79**, **83** and **84**, in spite of the markedly different C – F bond lengths in those three compounds. The lack of a systematic relation between $^2J_{F,C}$ and d_{C-F} interatomic distance was underlined by the authors when comparing the results for complexes **81** and **82**. Indeed, the larger of the two $^2J_{F,C}$ couplings corresponded to the shorter C≡C – F distance in complex **81** and, on the contrary, to the larger C≡C – F distance in complex **82**.

Also, a paper by Gryff-Keller and Szczeciński [90] should be recalled where the $^nJ_{F,C}$ (together with some other fluorine-containing coupling constants) were calculated at the DFT level in a series of four fluoromethanes, five fluoroethanes, two fluorocyclopropanes and eleven fluoro compounds containing five- and six-membered rings, which is exemplified for the fluoromethanes and fluoroethanes in Table 14. All calculations were performed using three hybrid functionals, B3LYP, PBE0 and BHandH, in combination with three basis sets, Pople's 6-311 + + G(2d,p) and 6-311 + + G(3df,3pd) together with Jensen's quadruple zeta aug-pcJ-3. It is clearly seen that only the BHandH functional ensures calculating the proper values of the one-bond fluorine-carbon spin – spin coupling constants, which was surprisingly not so for the most popular PBE0 functional used in those calculations.

Table 14. $^{19}F - ^{13}C$ spin – spin coupling constants (Hz) of fluoromethanes and fluoroethanes calculated at the DFT level using different functionals with Jensen's aug-pcJ-3 basis set. Compiled from Gryff-Keller and Szczeciński.[90]

Compound	Coupling constant	B3LYP	PBE0	BHandH	Experiment
CH_3F	$^1J_{F,C}$	−226.2	−226.8	−193.9	−163.0
CH_2F_2	$^1J_{F,C}$	−311.3	−302.1	−251.6	−234.6
CHF_3	$^1J_{F,C}$	−363.2	−346.5	−277.4	−272.3
CF_4	$^1J_{F,C}$	−363.5	−341.0	−250.7	−259.4
CH_2FCH_3	$^1J_{F,C}$	−201.3	−216.8	−174.5	−160.6
	$^2J_{F,C}$	15.8	20.4	19.6	20.7
CHF_2CH_3	$^1J_{F,C}$	−288.1	−294.5	−233.4	−233.5
	$^2J_{F,C}$	17.4	22.3	21.4	22.5
CF_3CH_3	$^1J_{F,C}$	−343.2	−337.9	−259.5	−273.0
	$^2J_{F,C}$	27.8	32.8	32.1	31.5

As was stated by the authors,[90] 'further improvement of the agreement between the theoretical calculations and experiment should be achieved, first of all, by the inclusion of the effects of molecular vibrations, molecular collisions and a more elaborate description of impact of other medium effects, into the theoretical model'. However, in our opinion, a priority should be given first to the non-empirical calculations, as compared to any of the DFT approaches, and only after that other accuracy factors, like medium effects and vibrational corrections, should be taken into account.

As an example of the early non-empirical calculations of $^nJ_{F,C}$ coupling constants, Alkorta *et al.*[91,92] performed SOPPA(MP2) and EOM-CCSD studies of geminal, vicinal

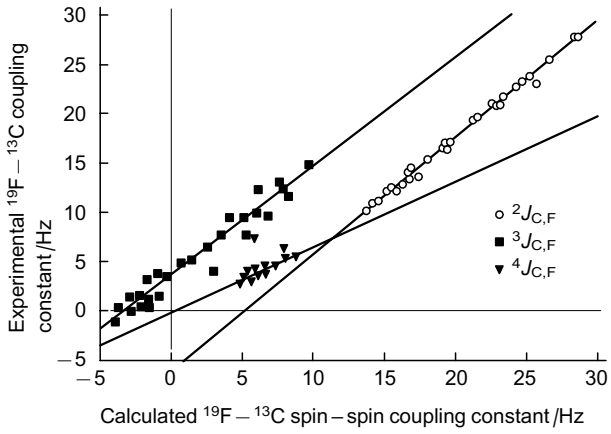


Figure 13. Correlation of the experimental $^nJ_{F,C}$ (n = 2, 3 and 4) coupling constants in the series of fluorobenzenes against those calculated at the SOPPA(MP2) level. Reproduced with minor editing privilege from Alkorta *et al.*[91] with the permission of *Elsevier*.

and longer-range four-bond $^{19}F-{}^{13}C$ couplings in fluorobenzenes. A fairly good agreement with experiment was eached, as compared to other types of the fluorine coupling constants ($^nJ_{F,H}$ and $^nJ_{F,F}$ with n = 3, 4 and 5), also calculated in this series (see Fig. 13).

An interesting insight into the molecular electronic structure in the series of ten fluorobenzenes **60**, **85**–**93** together with the antibiotic ezetimibe (**94**), used as a drug to reduce the cholesterol blood level by decreasing cholesterol absorption in human intestine, was provided by Vilcachagua *et al.*[108] based on the substituent effects on $^1J_{F,C}$. Calculations of the title coupling constants were performed at the SOPPA(CCSD) level in comparison with the DFT results obtained with Becke's BHandH and BHandHLYP functionals using the EPR-III basis set with the B3LYP/aug-cc-pVTZ equilibrium geometries.

The spin–spin coupling constants $^1J_{F,C}$ in the series of **60**, **85**–**93** calculated at the SOPPA(CCSD) level together

Structures 85–94

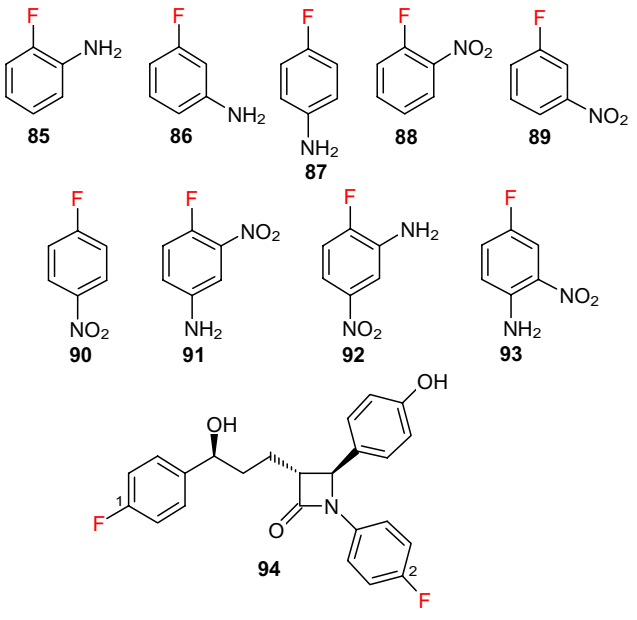


Table 15. One-bond spin–spin coupling constants $^1J_{F,C}$ (Hz) in the series of **60**, **85**–**93** calculated at the SOPPA(CCSD) level, as compared to experiment. Compiled from Vilcachagua *et al.*[108]

Compound	DSO	PSO	SD	FC	TO	Experiment
60	0.8	0.0	7.0	−264.2	−256.4	−245.5
85	0.9	10.7	8.6	−258.1	−237.9	−238.4
86	0.9	−4.3	6.2	−252.9	−250.1	−246.2
87	0.9	9.7	8.4	−261.7	−242.7	−235.7
88	1.0	−14.2	2.8	−276.5	−286.9	−264.8
89	0.9	−3.2	5.9	−266.2	−262.7	−251.2
90	0.9	−9.3	4.7	−268.2	−272.0	−257.9
91	0.0	−3.1	3.8	−275.6	−274.9	−255.3
92	0.9	1.6	5.8	−266.9	−258.6	−250.1
93	0.9	8.3	7.8	−261.6	−244.6	−239.2

with their experimental values (measured and reported in the same publication) are presented in Table 15. It is seen that a satisfactory agreement between calculations and experiment (in average, *ca.* 10 ppm) was achieved with the only marked deviation (almost 20 ppm) for compound **88** which is probably due to the strong steric interactions known as '*ortho*-effect', not taken into account in full in the performed calculations. The observed deviations were rationalized in terms of the conjugative interaction between the lone pairs of fluorine and the aromatic π-system.

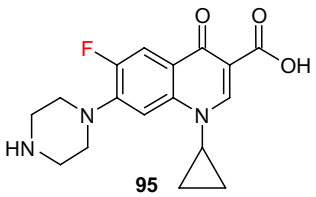
As an example bearing more practical interest, two different $^1J_{F,C}$ coupling constants of ezetimibe (**94**) were calculated[108] at the DFT level using the BHandH functional, as shown in Table 16 (due to the large molecular size, it was not possible to perform such calculations at the SOPPA(CCSD) level). Taking $^1J_{F,C}$ of fluorobenzene as a reference, a slightly negative increase in $^1J_{F,C1}$ and a positive increase in $^1J_{F,C2}$ were observed. However, it was noted that the Fermi contact contribution of the former coupling in compound **94** differed by only 0.1 Hz from that in a parent fluorobenzene (**60**). On the other hand, for the latter, it was the FC and the PSO terms which defined that trend. Those two observations suggested that a similar analysis performed for the fluorobenzene derivatives can be used for the ezetimibe molecule as well.

Table 16. One-bond spin–spin coupling constants $^1J_{FC}$ (Hz) of fluorobenzene (**60**) and ezetimibe (**94**) calculated at the BHandH/EPR-III level, as compared to experiment. Compiled from Vilcachagua *et al.*[108]

Compoun	Coupling constant	DSO	PSO	SD	FC	TO	Experiment
60	$^1J_{F,C1}$	0.9	−4.7	5.1	−269.8	−268.4	−245.5
94	$^1J_{F,C1}$	0.9	−6.0	4.5	−269.9	−270.4	−246.1
	$^1J_{F,C2}$	0.9	−1.5	5.1	−258.4	−264.0	−243.9

Much more recently Koch *et al.*[109] calculated a number of $^{19}F-{}^{13}C$ coupling constants in the molecule of ciprofloxacin (**95**), the widely known fluoroquinolone antibiotic. Recently, a series of ciprofloxacin derivatives with novel benzamidomethyl substituents were synthesized,[110] which showed much higher lipophilicity than the parent ciprofloxacin. Calculations for this promising drug were performed in the cited paper[109] with different DFT methods and a variety of basis sets. In general, calculations of different $^{19}F-{}^{13}C$ coupling constants ($^nJ_{F,C}$, n = 1–4) with the

Structure 95



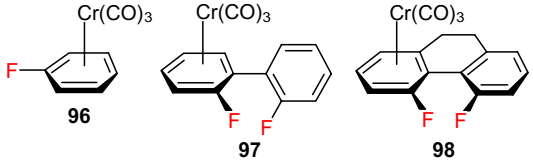
95

BHandH functional and 6-311++G(d,p), EPRII and EPRIII basis sets demonstrated the best reproducibility of their experimental values. Interesting to note that Dunning's aug-pVDZ and Jensen's pcJ-1, pcJ-2 and aug-pcJ-1 basis sets provided much less reliable results. It was also found that taking into account solvent effects did not show any improvement of the computational results in most cases.

The general findings of the performed study [109] were as follows: for the one-bond couplings, $^{1}J_{F,C}$, the best overall agreement between the calculated and experimental values has been achieved with BHandH/6-311++G(d,p) calculations. The best overall agreement between the the experimental and calculated data for $^{2}J_{F,C}$ has also been achieved with the BHandH functional and the 6-311++G(d,p) basis set, followed by the results of B3LYP calculations with the EPRII, pcJ-2 and EPRIII basis sets. The values of the geminal coupling constants, $^{2}J_{F,C}$, involving substituted and unsubstituted coupling carbon in ciprofloxacin, presented a difference of about 10 Hz, which was almost similar to the corresponding experimental values. For vicinal coupling constants, $^{3}J_{F,C}$, an expected Karplus-type relationship with the corresponding dihedral angle was found. Also, the correlation of calculated $^{3}J_{F,C}$ with π-bond orders and bond lengths of the central carbon-carbon bond in the F–C–C–C moiety was reported. The long-range $^{4}J_{F,C}$ coupling constant was significant, if it was in a coplanar 'W' structural orientation. These couplings were relatively large and rather well reproduced at the DFT level. Taking into account the solvent effect did not improve the results in general. In addition, it was found that all applied methods surprisingly failed to reproduce experimental $^{4}J_{F,C}$ involving quaternary carbons.

Gryff-Keller and Szczeciński [111, 112] performed a number of DFT calculations of fluorine–carbon coupling constants in the series of tricarbonylchromium complexes exemplified with structures **96**–**98** using the B3LYP and/or BHandH functionals in combination with Pople's 6-311++G(2d,p) basis set. As was stated in the original publications, interest to those compounds stemmed from the fact that formation of tricarbonylchromium complexes with aromatic compounds substantially modified the electronic structure of the arene unit and essentially changes its chemical behaviour. The electron-withdrawing effect of the $Cr(CO)_3$ moiety enables efficient nucleophilic attack on arene resulting in the dearomatization of the latter, activates halogen substituents for the cross-coupling reactions and finally stabil-

Structures 96–98



96 **97** **98**

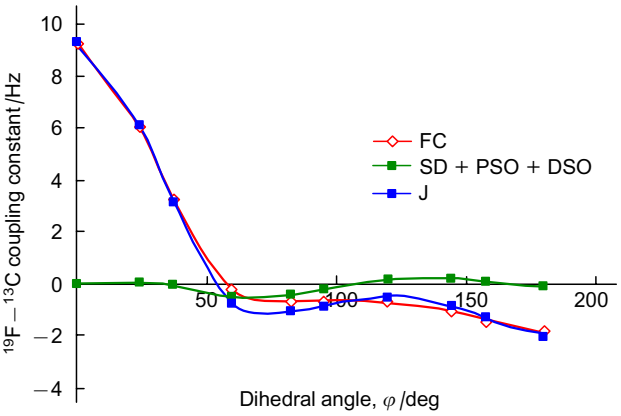


Figure 14. Dihedral angle dependence of spin–spin coupling constant between fluorine and carbonyl carbon and its coupling contributions calculated for (η⁶-fluorobenzene)tricarbonylchromium (**96**) using the BHandH/6-311++G(2d,p) method. Reproduced with minor editing privilege from Gryff-Keller and Szczeciński [111] with the permission of the *Royal Society of Chemistry*.

izes negative charges in the benzylic positions. Moreover, aromatic compounds form chiral complexes, which can be used as intermediates, auxiliary compounds or catalysts in asymmetric synthesis.

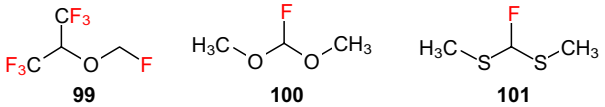
One of the main conclusions of the performed calculations of fluorine–carbon coupling constants in this series was that the 'fluorine–aliphatic carbon' and 'fluorine–carbonyl carbon' couplings were dominated by the *through-space* coupling mechanism. This was especially so for the $^{n}J_{F,C}$ coupling constants involving carbonyl carbon directly bonded to chromium.

Another noteworthy and mostly expected observation reached at in the first publication [111] of this research was that the formally vicinal coupling constant between fluorine and carbonyl carbon provided a classical Karplus-type dependence, as was calculated for (η⁶-fluorobenzene)tricarbonylchromium (**96**) and shown in Fig. 14. This dependence was almost totally due to a predominant Fermi contact contribution, while the three non-contact terms (DSO, PSO and SD) were almost constant in the whole range of φ, showing an imperceptible minimum at $\varphi \approx 60^{\circ}$.

In several related publications by Freitas and coworkers,[113–116] fluorine–carbon coupling constants, $J_{F,C}$, were theoretically investigated in terms of the stereoelectronic interactions including hyperconjugation, anomeric effect, and steric and electrostatic interactions together with different conformational effects. The general result was the discovery of the so-called 'reverse fluorine Perlin-like effect', as exemplified in sevoflurane (**99**), fluoro(dimethoxy)methane (**100**) and fluoro(bismethylsulfanyl)methane (**101**). Undoubtedly, this effect could be useful in the stereochemical studies of diverse organofluorine compounds.

In particular, it was found [114] that hyperconjugation, widely invoked to explain anomeric and Perlin effects, was

Structures 99–101



99 **100** **101**

not a determining factor influencing conformational behaviour of sevoflurane (**99**), which is illustrated in Fig. 15 in relation to the internal rotation around the C—O bond. Thus, hyperconjugation was shown to be much more significant in solution and particularly in polar solvents, as compared to that in a gas phase. Also, it appeared that the larger the molecular dipole, dominated by the interaction between oxygen lone pairs and the polar F—C bond, the lesser the corresponding $^1J_{F,C}$ coupling constant. Similar findings were reported also for 1,2-difluoroethane,[113] the compound, where variation of $^1J_{F,C}$ was independent of hyperconjugation.

Two years later, Silla and Freitas[115] calculated the dihedral angle dependences of $^1J_{F,C}$ in fluoro(dimethoxy)-methane (**100**) and fluorobis(methylsulfanyl)methane (**101**) shown in Fig. 16. The reverse fluorine Perlin-like effect in the values of $^1J_{F,C}$ was observed in those two compounds that can be useful for investigation of the stereochemistry and molecular properties of related species.

It is well known that 1,3-dioxane (**102**) exhibits Perlin effect while 1,3-dithiane (**103**) demonstrates the reverse Perlin effect. On the contrary, both their fluorinated analogues, 2-fluoro-1,3-dioxane (**104**) and 2-fluoro-1,3-dithiane (**105**), were found to show the reverse fluorine Perlin-like effect.[116] This finding was attributed to an interplay between the hyperconjugative, steric and electrostatic interactions. Further on, the role of the C—X and n_X orbitals in the transmission of the Fermi contact term for the $^1J_{F,C}$ coupling constant has been analyzed on the basis of canonical molecular orbitals.[116] A reverse Perlin-like effect was also observed in the values of the $^1J_{F,C}$ coupling constant of α- and β-D-glucopyranosyl fluoride tetraacetates (accordingly, **106** and **107**), both in nonpolar and polar solution, and was shown to be governed by the dipolar interactions rather than by hyperconjugation. Herewith, it should be noted that the reverse fluorine Perlin-like effect does not have a general relationship with a classically known anomeric effect.

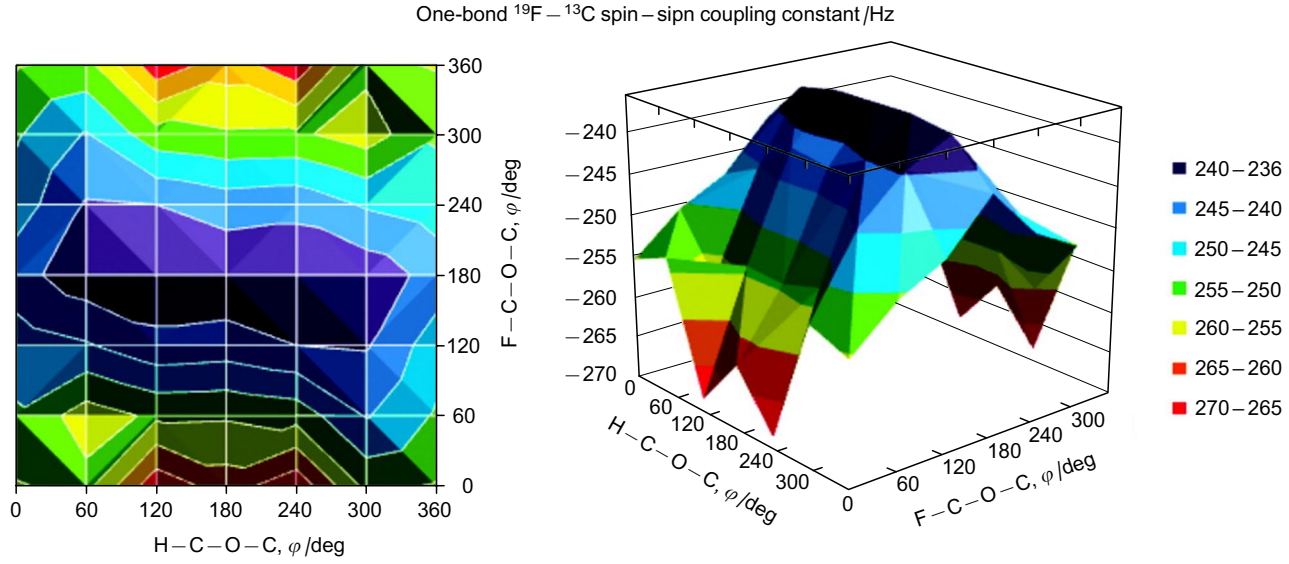


Figure 15. Two-dimensional dihedral angle dependence of $^1J_{F,C}$ in sevoflurane (**99**). Reproduced with minor editing privilege from Freitas *et al.*[114] with the permission of the *American Chemical Society*.

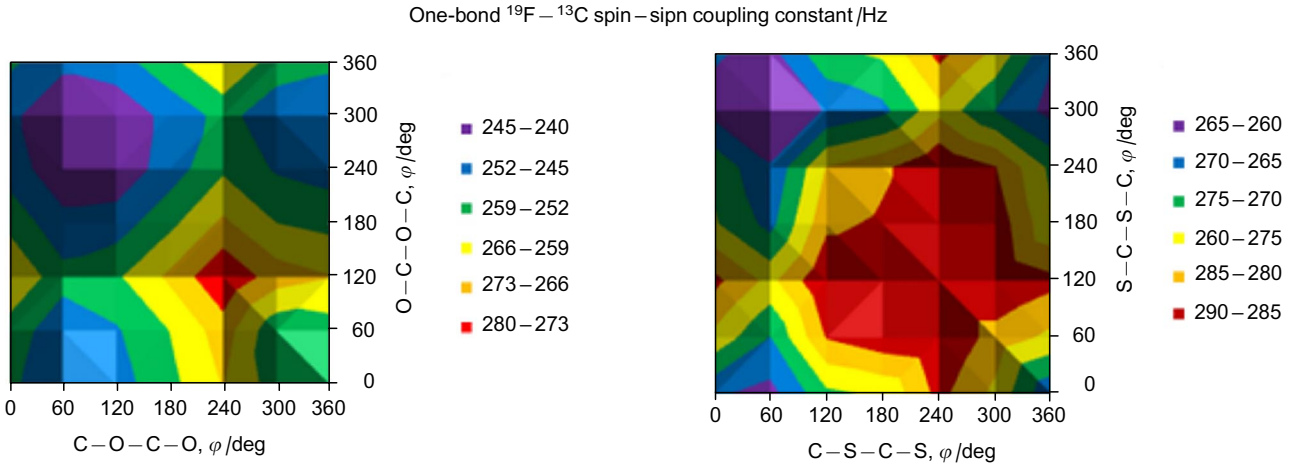
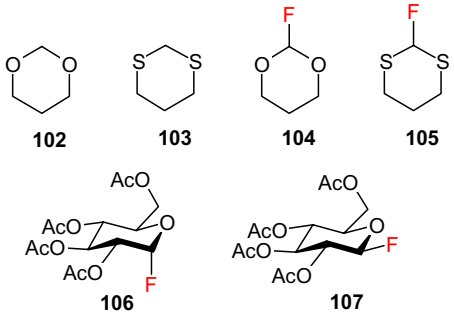


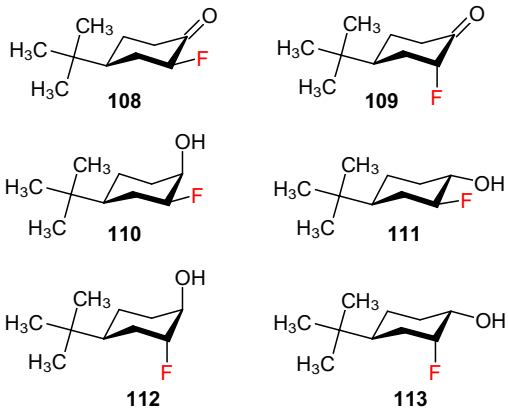
Figure 16. Two-dimensional dihedral angle dependence of $^1J_{F,C}$ in fluoro(dimethoxy)methane (**100**) and fluorobis(methylsulfanyl)methane (**101**). Reproduced with minor editing privilege from Silla and Freitas[115] with the permission of *Elsevier*.

Structures 102 – 107



In parallel with the studies,[113–116] Anizelli *et al.*[117] investigated the effect of electronic interactions on $^{n}J_{F,C}$ (n = 1 and 2) in *cis*- and *trans*-4-*tert*-butyl-2-fluorocyclohexanones and their alcohol derivatives **108** – **113**. Those coupling constants were calculated at both density functional B3LYP/EPR-III and polarization propagator SOPPA(CCSD)/EPR-III levels and compared with their experimental values measured in the same paper.

Structures 108 – 113



Experimental trends in the total calculated coupling constants were, in general, surprisingly slightly better reproduced within the DFT framework rather than at the SOPPA(CCSD) level. To illustrate a very interesting example reported in the cited communication shown in Fig. 17 are the two occupied canonical molecular orbitals participating in the Fermi contact transmission of $^{2}J_{F,C}$ in compounds **108** and **109**, which were found to be notably different (accordingly, 13.5 and 21.0 Hz).

In general, qualitative analysis performed by Anizelli *et al.*[117] had provided an insight into the transmission mechanisms of the Fermi contact and paramagnetic spin – orbit terms of the one-bond and geminal fluorine – carbon coupling constants. Of particular interest was the analysis of the effect of 'proximate' interactions (as named in the original publication) on their paramagnetic spin – orbit interactions. The obtained results suggested that attractive interactions involving fluorine lone pairs increased their *s*-character, while the repulsive interactions worked in the opposite direction.

3.3. ^{19}F – ^{19}F spin – spin coupling constants

In this Section let us start with the discussion of the SOPPA(MP2), SOPPA(CCSD), CCSD and CC3 calculations of the unique vicinal fluorine-fluorine coupling constant in one of the most simple fluorine-containing organic molecules — that of difluoroethyne, F – C≡C – F, performed by Faber and Sauer.[118] The uniqueness of this coupling lies in the linearity of its coupling path characterized by the unusual 180° bond angles at both carbons. In spite of the seeming simplicity of this molecule, its $^{3}J_{F,F}$ coupling proved to be very difficult to calculate accurately, even at the most sophisticated levels of theory. In the performed study, the authors had systematically investigated the dependence of this coupling constant on the choice of the one-electron basis set, the choice of the correlated wave function method and the inclusion of the zero-point vibrational and temperature corrections. All terms of this coupling constant were evaluated at the most advanced levels of theory, SOPPA(MP2), SOPPA(CCSD) and CCSD, while for the most correlated paramagnetic spin – orbit contribution the related calculations were performed also at a very accurate Coupled Cluster singles, doubles and triples (CC3) level.

It was found that in order to get results, which would be well converged with respect to the basis set, one needs to use specially optimized basis sets of at least quadruple zeta quality with diffuse functions, as specified in Table 17. Furthermore, the PSO term was found to be not yet converged even at the CCSD level, as followed from the comparison with the performed CC3 calculations. Finally, it was shown that vibrational effects were also very important. Only by using a converged basis set and including both vibrational and higher order correlation effects, the authors managed to obtain a reasonably good agreement between the calculated $^{3}J_{F,F}$ in difluoroethyne and its experimental value.

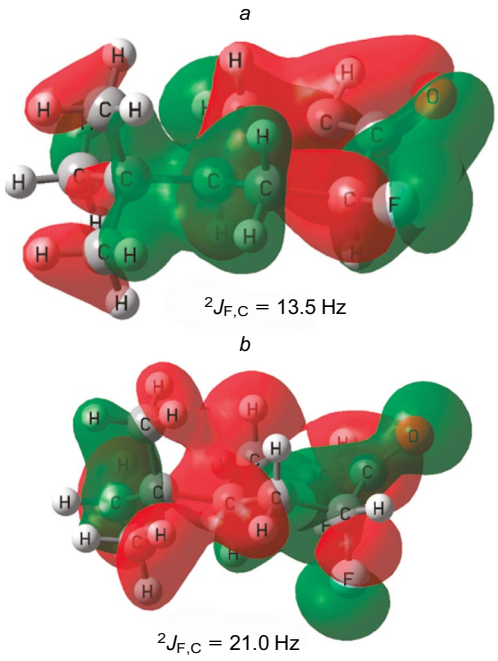


Figure 17. Contour plots of the occupied canonical molecular orbitals participating in the Fermi contact transmission of $^{2}J_{F,C}$ in *cis*- and *trans*-4-*tert*-butyl-2-fluorocyclohexanones, **108** (*a*) and **109** (*b*). Reproduced with minor editing privilege from Anizelli *et al.*[117] with the permission of the *American Chemical Society*.

Table 17. Vicinal $^{19}F-^{19}F$ spin–spin coupling constant of difluoroethyne (Hz), calculated at the CCSD level of theory at the CCSD(T)/cc-pCVQZ geometry, *vs.* experiment. Compiled from Faber and Sauer.[118]

Basis set	DSO	PSO	SD	FC	TO
ccJ-pVDZ	−1.81	−30.34	40.07	11.55	19.46
ccJ-pVTZ	−1.85	−31.30	36.31	8.97	12.14
ccJ-pVQZ	−1.85	−30.96	35.03	8.02	10.24
ccJ-pV5Z	−1.85	−32.29	33.60	7.10	6.56
ccJ-pVDZ-unc	−1.83	−34.22	38.33	12.40	14.68
ccJ-pVTZ-unc	−1.84	−32.86	36.00	9.04	10.35
ccJ-pVQZ-unc	−1.85	−31.49	34.85	7.99	9.50
qzp	−1.80	−36.33	32.52	10.98	5.37
aug-ccJ-pVDZ	−1.81	−31.60	33.08	7.24	6.90
aug-ccJ-pVTZ	−1.85	−32.80	33.30	7.10	5.76
aug-ccJ-pVQZ	−1.85	−32.83	33.20	7.01	5.52
aug-ccJ-pV5Z	−1.85	−32.91	33.12	6.90	5.26
CBS limit	−1.85	−32.91	33.09	6.87	5.20
Experiment					2.1

In the early study by Jaszuński,[43] the mechanisms and stereochemical dependences of $^2J_{F,F}$ coupling constants in the series of three simple inorganic molecules, ClF_3, PF_3 and PF_5, were studied at approximately the same high level of theory. It is noteworthy that for such electron-rich molecules, including a number of fluorine lone pairs, the dynamic correlation effects are extremely significant, so that the accuracy of the computed fluorine–fluorine couplings drastically depended on the correct description of electron correlation. This implied the usage of the coupled clusters methods, such as CCSD, CCSD(T), and even CCSDT which were the only ones that described systematically strong electron correlation effects. In the above-mentioned paper,[43] calculation of fluorine–fluorine coupling constants was performed at the CCSD level, and final results of this study are collected in Table 18, compiled from that publication. A general drawn by Jaszuński was that the non-contact paramagnetic spin–orbit (PSO) and spin dipolar (SD) terms of geminal fluorine–fluorine couplings generally dominate over the Fermi contact (FC) contribution.

Table 18. Geminal $^{19}F-^{19}F$ spin–spin coupling constants (Hz), calculated at the CCSD level *vs.* experiment. Compiled from Jaszuński.[43]

Compound	Coupling constant	DSO	PSO	SD	FC	TO	Experiment
ClF_3	$^2J_{ea}$	0.0	127.0	213.5	35.8	376.2	403
	$^2J_{aa}$	−3.4	−104.8	123.8	28.9	44.6	
PF_3	$^2J_{F,F}$	−0.8	−40.0	46.3	−5.1	0.4	
PF_5	$^2J_{ee}$	−1.9	−23.6	9.9	−20.6	−36.2	
	$^2J_{ea}$	0.3	−184.9	21.4	47.1	−116.1	
	$^2J_{aa}$	−3.9	6.3	−0.1	−6.2	−3.9	

In a series of the earlier cited papers, Sauer and coworkers [103–106] applied specialized core-property basis sets aug-cc-pVTZ-J and (aug)-ccJ-pVXZ (X = D, T, Q, 5) at the SOPPA(MP2), SOPPA (CCSD), CCSD, CC3 and even CCSDT levels to the study of $^3J_{F,F}$ coupling constant in difluoroethyne. They found that vibrational effects in the value of $^3J_{F,F}$ were of the same order of magnitude as the equilibrium geometry value of this coupling constant and that triples corrections to the one- and three-bond couplings calculated at the CC3 level were in the order of 4–6 Hz. Herewith, when using the aug-ccJ-pVTZ basis set, the basis set error still remained, compared to the basis set limit of 2–3 Hz. The currently most accurately calculated values of $^3J_{F,F}$ coupling constant in difluoroethyne in that series of papers was thus 2.56 Hz (as compared to experimental value of 2.1 Hz).[107]

Ducati *et al.*[119] reported the unexpected geometrical effects on paramagnetic spin–orbit and spin dipolar isotropic contributions to the $^2J_{F,F}$ coupling constant in difluoromethane. The second-rank tensors of those contributions were shown to be strongly dependent on the relative orientation of the C–F bonds and corresponding tensor eigenvectors. In this way, a pure geometrical effect was detected and described in terms of the isotropically averaged values of the PSO and SD second-rank tensors. It was also found that isotropically averaged paramagnetic spin–orbit term noticeably increased while the Fermi contact contribution markedly decreased with the increasing of the angle between the C–F bonds and the eigenvectors of the corresponding second-rank tensors, as can be seen in Fig. 18 retrieved from the cited publication.

Passing to organofluorine molecules, it should be recalled that Nozirov *et al.*[50] performed a systematic study of $^nJ_{F,F}$ (n = 2, 3) in a classical series of *gem*-, *cis* and *trans*-difluoroethylenes **1**–**3** at different levels of theory [DFT, HF, MP2, CCSD and CCSD(T)]. It was shown that both DFT (exemplified with the BHandH functional) and CCSD methods predicted geminal and vicinal fluorine–fluorine couplings significantly more accurately (approximately, as much as 3 times) in *cis*- and *trans*-difluoroethylenes than in *gem*-difluoroethylene (**2** and **3**, respectively, *vs* **1**), as shown in Fig. 19.

A general conclusion arrived at in the performed study [50] was that 'the most reliable' BHandH density functional completely failed to predict $^2J_{F,F}$ and underestimated their experimental and CCSD/pcJ-2 values by about 40 Hz. Moreover, the $^3J_{F,F}$ in *cis* and *trans*-1,2-difluoroethylenes were also unreliably evaluated at this level of theory deviating from experiment by about 12 and −12 Hz, respectively. The current performance of the BHandH functional in predicting $^2J_{F,F}$ in 1,1-difluoroethylene was about three

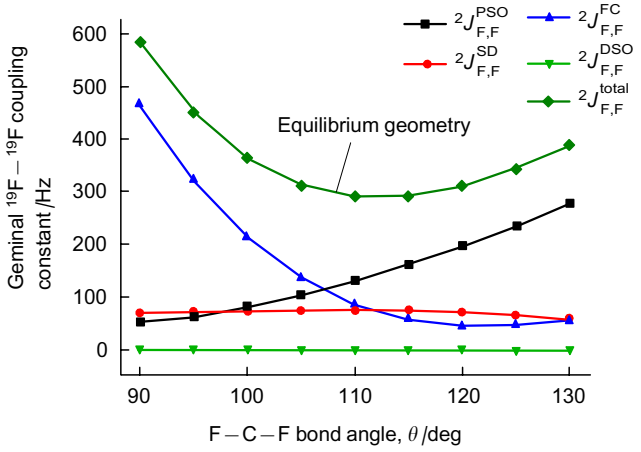


Figure 18. The FC, PSO, SD and DSO contributions to the $^2J_{F,F}$ coupling constant in difluoromethane *vs* the F–C–F bond angle calculated at the SOPPA(CCSD)/EPR-III level. Reproduced with minor editing privilege from Ducati *et al.*[119] with the permission of the *American Chemical Society*.

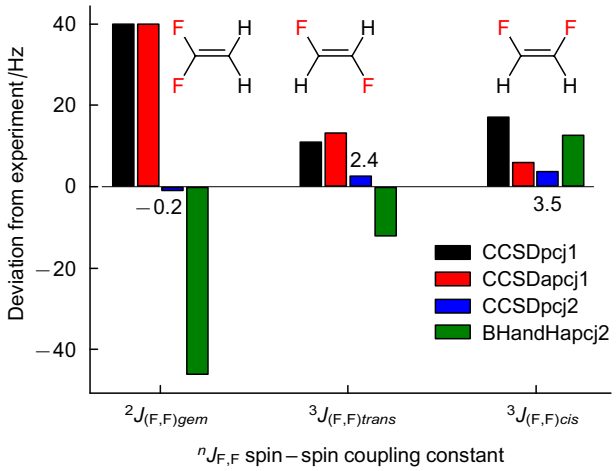


Figure 19. Deviation of the total $^nJ_{F,F}$ coupling constant in three difluoroethylene isomers calculated by the BHandH and CCSD methods with the selected basis sets. Given numerical deviations are those for the CCSD/pcJ-2 results. Reproduced with minor editing privilege from Nozirov *et al.*[50] with the permission of *AIP Publishing*.

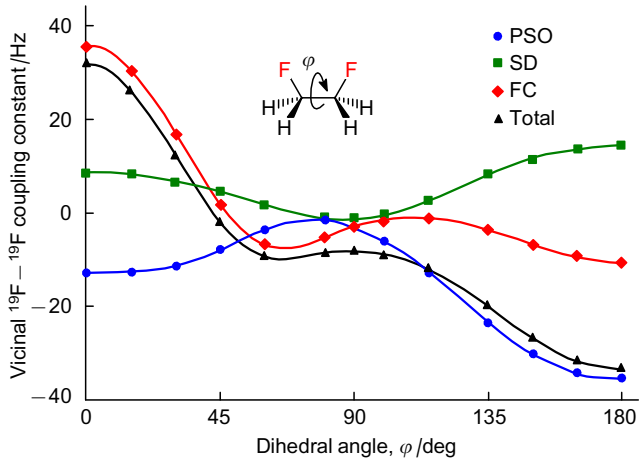


Figure 20. Dihedral angle dependences of the DSO, PSO, SD and FC contributions to the $^3J_{F,F}$ coupling constant of 1,2-difluoroethane evaluated at the SOPPA(CCSD) level of approximation. Reproduced with minor editing privilege from Provasi and Sauer [121] with the permission of the *American Chemical Society*.

times better than the B3LYP result (corresponding deviations were −46 and −115 Hz, respectively). However, it was possible to distinguish *gem*-, *cis*- and *trans*-1,2-difluoroethylenes by checking their $^2J_{F,F}$ and $^3J_{F,F}$ coupling constants calculated at the BHandH/aug-pcJ-2 level of theory. Performed study pointed out the need for a designing a novel density functional(s) capable to correctly calculate fluorine – fluorine coupling constants (as was stated by the authors). However, the author of the present review doesn't agree with that conclusion based on his own experience in using many dozens of functionals providing unpredictable behaviour in many particular cases.

Very recently it was shown at the SOPPA(MP2) level (as discussed and reviewed by Aucar *et al.*[120]) that the largest contribution to the FC mechanism of the vicinal fluorine – fluorine coupling constant, $^3J_{F,F}$, in 1,2-difluoroethene originated in both fluorine *s*-type molecular orbitals and its *s*-type lone pairs. All of those contributions were found to be negative, while those ones arising from the occupied σ_{CF} orbitals were markedly positive. In the case of the SD mechanism, contributions from the *s*-type molecular orbitals were not observed, and the main contributions to that coupling constant were found to be originated mainly in the *p*-type lone pairs and the σ_{CF} orbitals. For the PSO mechanism, the largest contributions were found to be also from the fluorine *p*-type lone pairs and σ_{CF} orbitals. The π-type contribution to $^3J_{F,F}$, arising from the intervening C=C bond, was by far the largest one. Such transmission of the FC and SD mechanisms generally explained why there was a long-distant transmission of the $^3J_{F,F}$ coupling in the unsaturated compounds.

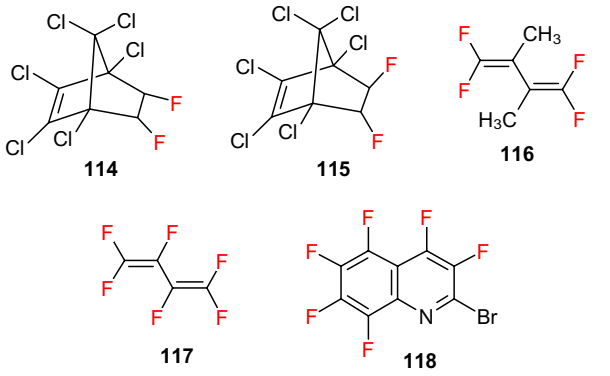
The related saturated 1,2-difluoroethane molecule was thoroughly investigated much earlier by Provasi and Sauer,[121] who studied the dihedral angle dependence of its $^3J_{F,F}$ at the RPA, SOPPA(MP2) and SOPPA(CCSD) levels using the locally dense basis set scheme, based on Sauer's aug-cc-pVTZ-J for fluorines and carbons and Dunning's cc-pVTZ for hydrogens. Theoretical results were compared with those measured experimentally. It was found that inclusion of electron correlation in the calculation of $^3J_{F,F}$ reduced the absolute value of the latter. This was mainly due to the changes in the Fermi contact contribution, which even changed its sign for the dihedral angles around the *trans*-conformation has. It was the sign change that was found to be responsible for the breakdown of the Karplus-like dependence, as illustrated in Fig. 20.

The obtained dihedral angle curves for $^3J_{F,F}$ were fitted to the Fourier cosine series, and it was found that the shape of the resulting Karplus curves depends on the method chosen for the geometry optimization with the changes being the largest ones for the *cis*-conformation.[121] With the exception of dihedral angles close to the *gauche* orientation, it was mostly the FC term which was influenced by the changes in the geometry. Electron correlation effects were shown to be mostly reflected in the FC contribution. However, those changes were essentially larger for the 'near-*trans*' conformations than for the 'near-*cis*' or 'near-*gauche*' ones. Thus, for the near-*trans* conformations even the sign of the FC term was changed by the effect of electron correlation. On the other hand, the SD contribution was affected almost equally for all dihedral angles, while the DSO and PSO terms were almost not affected by the electron correlation at all. Hence, the 'capricious' (as termed in the original publication [121]) shape of the $^3J_{F,F}$ Karplus curve in 1,2-difluoroethane was attributed to the electron correlation effects in the FC contribution. For the dihedral angles in the range from *cis* to *gauche* conformation, the total vicinal coupling constant, $^3J_{F,F}$, was shown to be dominated by the FC contribution, whereas around the *trans*-conformation it was mostly determined by the PSO term.

García de la Vega and San Fabián [122] conducted a comprehensive investigation of the performance of different exchange and correlation DFT functionals in the calculation of fluorine – fluorine coupling constants, $^nJ_{F,F}$, with n ranging from 1 to as much as 7. This study was accomplished on a series of about two dozens of organofluorine compounds with known experimental $^{19}F - {}^{19}F$ coupling constants, exemplified with structures **40**, **114** – **118**.

A number of different exchange (SLYP, BLYP, PW91LYP, G96LYP, PBELYP, mPWLYP, PBEhLYP,

Structures 114 – 118



OLYP, BRxLYP, PKZBLYP and TPSSLYP) and correlation (PBEVWN, PBEVWN5, PBEPL, PBEP86, PBEVP86, PBEW91, PBEPBE, PBEB95, PBELYP, PBEKCIS, PBEPKZB and PBETPSS) functionals were tested in a representative set of organofluorine compounds, as shown in Fig. 21. The one-bond, geminal, vicinal and longer-range (up to seven separating bonds) fluorine – fluorine coupling constants were calculated taking into account all four coupling contributions (Fermi contact, spin – dipolar, paramagnetic and diamagnetic spin – orbit). Results of the performed study demonstrated that DFT methods gave appropriate values for $^{n}J_{F,F}$ (n = 4 to 7), while calculated geminal and vicinal fluorine – fluorine couplings (n = 2 and 3) demonstrated large deviations from their experimental values. Unlike most of spin – spin coupling constants, fluorine – fluorine couplings showed that the Fermi contact term was not dominant in most cases, particularly in polyfluorinated organic molecules.

In particular, it was found [122] that most of the exchange functionals displayed similar behaviour with insignificant

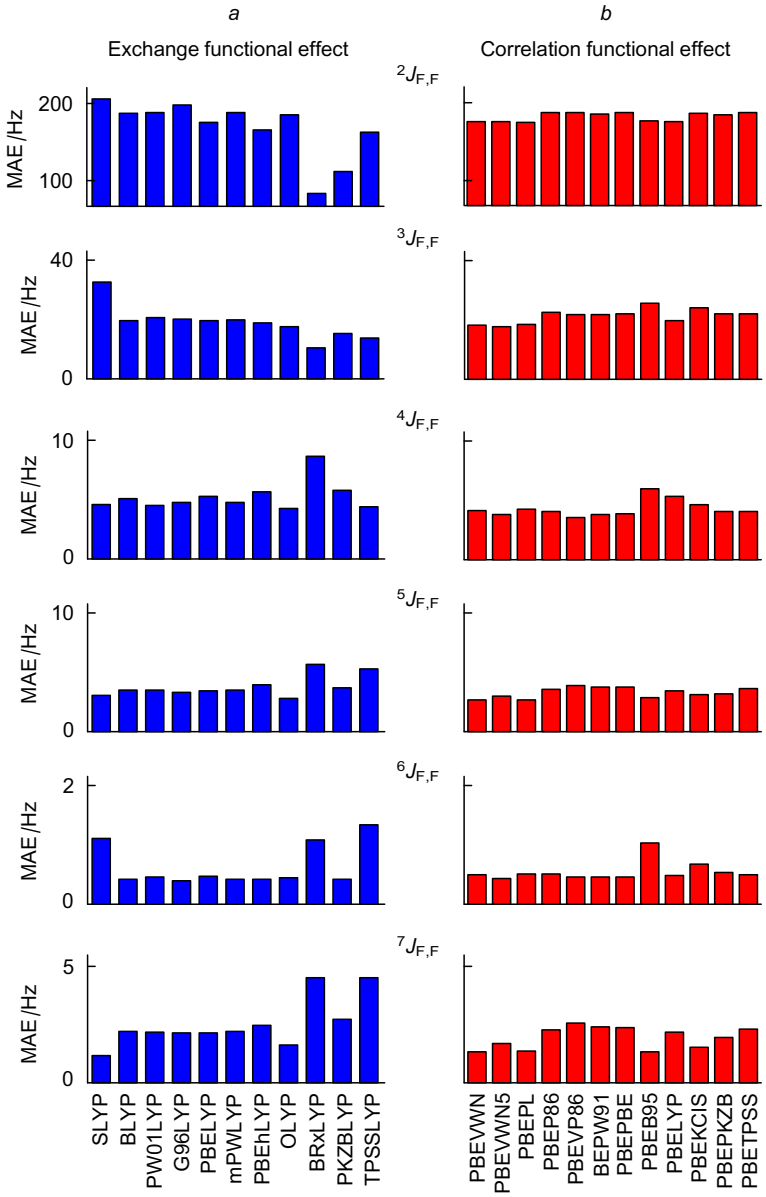


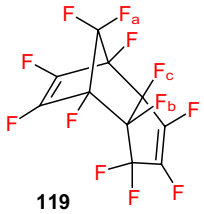
Figure 21. Dependence of the mean absolute error (MAE) on the exchange (*a*) and correlation (*b*) functionals given in their original designation. Reproduced with minor editing privilege from García de la Vega and San Fabián[122] with the permission of *Taylor and Francis*.

variations in the MAE values. However, SLYP, BRxLYP and TPSSLYP showed some discrepancies with the rest of the exchange functionals tested. As an example, the SLYP functional yielded larger MAE values for $^{2}J_{F,F}$, $^{3}J_{F,F}$ and $^{6}J_{F,F}$, while it provided the best value for the $^{7}J_{F,F}$ coupling constant.

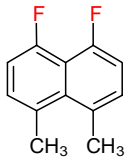
García de la Vega and San Fabían[122] also combined twelve *correlation* functionals with the PBE exchange functional. The MAE values obtained with that set of functionals presented rather small variations. The larger values of MAE were obtained with the B95 correlation functional for the $^{3}J_{F,F}$, $^{4}J_{F,F}$ and $^{6}J_{F,F}$ coupling constants. It was noticed that the percentage of the Hartree – Fock exchange included in the particular functional was quite important. The functionals S55VWN5, S47LYP and S41 with a Hartree – Fock exchange percentage, ranging in the interim of 41 to 55%, were found to be between the ten best functionals for geminal and vicinal fluorine – fluorine couplings.

In the early paper by Peralta *et al.*,[123] the stereochemical behaviour of the long-range $^{4}J_{F,F}$ was examined theoretically at the B3LYP/6-311G(d,p) level using compounds **119** and **120**, and the efficiency of the through-space coupling mechanism was evaluated based on the performed calculations. Based on the computational results for $^{4}J_{F,F}$ in compound **119**, the authors concluded that the negative term of this coupling constant was composed of both through-space and through-bond contributions, the former originating in the direct superposition of two C – F bonds. Not surprisingly, the absolute value of this term for $^{4}J_{Fa,Fb}$, 16 – 20 Hz, was considerably larger than that for $^{4}J_{Fa,Fc}$, 3 – 5 Hz. To rationalize this marked difference, the interatomic distances for $F_a - F_b$ (2.56 Å) and $F_a - F_c$ (2.92 Å) were taken into account. A reasonable assumption was made that the origin of this effect was the through-space interaction between the fluorine atoms under consideration. On the other hand, for the $^{4}J_{F,F}$ coupling constants in compound **120**, the negative through-bond and through-space terms of $^{4}J_{F,F}$ were larger for the shorter distance, which was explained by the authors by the efficiency of the through-bond contribution.

Structures 119, 120



119



120

The early studies of vicinal fluorine – fluorine couplings were thoroughly reviewed in 2005 by Sanchez *et al.*[124] It was pointed out that the locally dense basis sets were developed for the correlated *ab initio* calculations of vicinal fluorine – fluorine couplings in several representative saturated and unsaturated fluorinated hydrocarbons. In those studies, the choice of the basis set for each atom depended on its location with respect to the coupled fluorine atoms and on the *cis*/*trans* or *synperiplanar*/*antiperiplanar* configuration/conformation of the molecule, reflected in the corresponding stereochemistry of the coupling path. One *had* to use more extended basis sets for carbon atoms in the bonding pathway connecting coupled fluorine atoms compared to those suitable for carbon atoms outside this path. For the hydrogen atoms directly connected to the coupling pathway in molecules with *trans* or *antiperiplanar* conformations and for all hydrogen atoms not directly connected to the coupling pathway, one could employ a minimal basis set. With employing this type of locally dense basis set, the number of necessary basis functions could be safely reduced by about 30% without losing more than about 1 Hz in accuracy. The analysis of all four contributions to the vicinal fluorine – fluorine coupling constants showed that the non-contact orbital paramagnetic term was the most important contribution. At that, the Fermi contact term dominated only in the *synperiplanar* conformations.

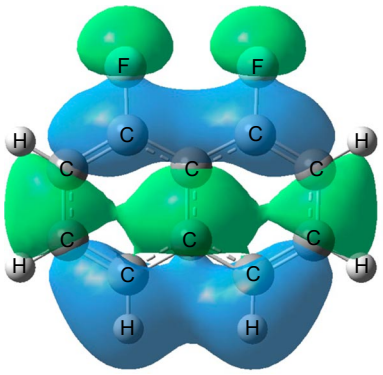


Figure 22. Principal canonical molecular orbital of 1,8-difluoronaphthalene, contributing to the Fermi contact contribution of $^{4}J_{F,F}$ spin – spin coupling constant. Reproduced from Contreras *et al.*[125] with the permission of the *American Chemical Society*.

In the earlier paper by Contreras *et al.*,[125] the $^{4}J_{F,F}$ of the reference set of compounds were studied in terms of the through-space transmission mechanism, involving occupied canonical molecular orbitals exemplified in Fig. 22 for 1,8-difluoronaphthalene. In compounds of that type some interesting aspects of the transmission mechanisms for the PSO and FC contributions to $^{4}J_{F,F}$ spin – spin coupling constants were rationalized in terms of the proximate through-space fluorine – fluorine interactions.

Coming back to the paper by Jaszuński *et al.*,[131] the hybrid functionals and in particular the functionals with the highest amount of Hartree – Fock exchange, namely, PBE0, CAM-B3LYPx, BHandH and CAM-B3LYP, performed best of all for the through-space $^{n}J_{F,F}$ couplings. Not surprisingly, the most popular B3LYP functional gave the worse results, as compared to other hybrid functionals. On the other hand, for the set of 26 through-bond different coupling constants studied in that work, the PBE0, B3LYP and B97-D functionals gave on average the best agreement with available experimental data, implying that there was no correlation of their performance with the amount of the Hartree – Fock exchange in the particular functional.

Alkorta and coauthors[91,92] performed SOPPA and EOM-CCSD calculations with Ahlrichs' qzp and qz2p basis sets of three-, four- and five-bond fluorine – fluorine couplings in the series of twelve representative fluorobenzenes. A rather good correlation between calculated and experimental values was generally reached, as can be seen in Fig. 23. However, several examples were found, where SOPPA(MP2) calculations were unable to reproduce experimental results, mostly those dealing with the calculation of $^{3}J_{F,F}$ couplings.

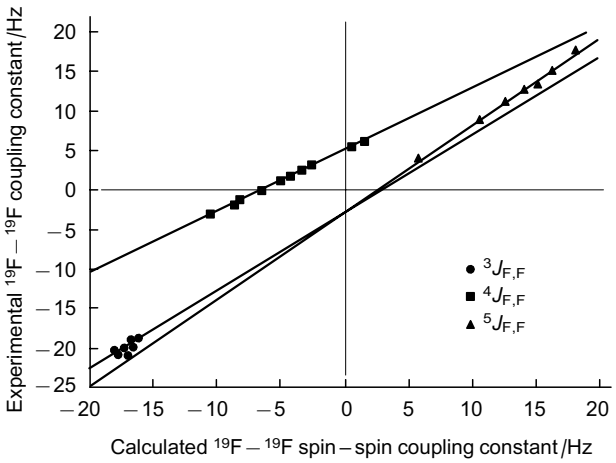
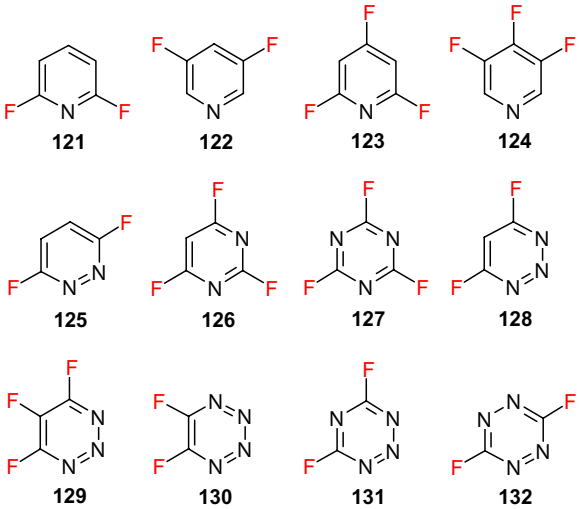


Figure 23. Correlation of experimental $^{n}J_{F,F}$ ($n = 3$, 4 and 5) coupling constants against those calculated at the SOPPA(MP2) level in the series of fluorobenzenes. Reproduced with minor editing privilege from Alkorta *et al.*[91] with the permission of *Elsevier*.

In continuation of their earlier studies,[92,126–129] Del Bene and coauthors[130] conducted extensive EOM-CCSD calculations of three-, four- and five-bond long-range $^{19}F-{}^{19}F$ coupling constants, $^{n}J_{F,F}$ ($n = 3$, 4 and 5), for a series of about thirty fluoroazines, exemplified with structures **121**–**132**. Generally, the computed absolute values of $^{n}J_{F,F}$ appeared to be slightly underestimated, as compared to experiment, but they were mostly in a rather good agreement with experiment.

Structures 121 – 132

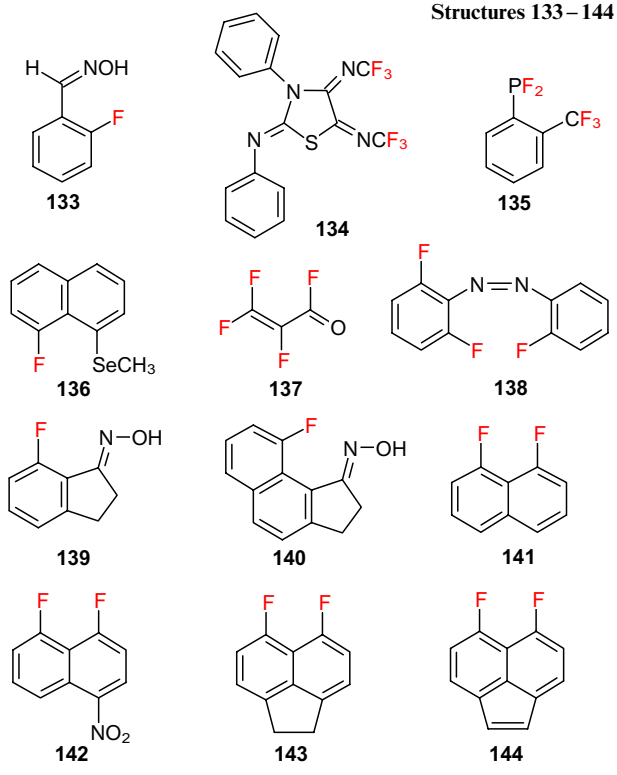


It was found that the values of $^{3}J_{F,F}$ were relatively large and negative, ranging from −17 to −24 Hz. On the other hand, all $^{5}J_{F,F}$ were relatively large and positive, falling into range of 15 – 34 Hz. On the other hand, $^{4}J_{F,F}$ were found to be either positive or negative and either large or small varying from −13 to +30 Hz. The values of those coupling constants depended on the nature of the atom that connected the two C – F bonds together, with the number and position of the nitrogen atom in the ring. As an example, $^{4}J_{F,F}$ were negative if the intervening atom, that is bonded to the two C – F bonds, was nitrogen and there was no more than one additional nitrogen atom in the ring. The largest positive values of $^{4}J_{F,F}$ (26 – 30 Hz) were found when the intervening atom was carbon of either a C – H or C – F bond while a nitrogen atom was adjacent to each of the C – F bonds. The remaining three four-bond coupling constants involved spin – spin coupling across an intervening carbon atom and were always positive, ranging from 1 to 4 Hz.

It is noteworthy that in the series of molecules included in the study,[130] only 6 of 28 values of calculated $^{n}J_{F,F}$ have been measured experimentally, so that reported values of those couplings essentially contributed to the bank of available $^{n}J_{F,F}$ data. In addition, the patterns that described the changes of $^{n}J_{F,F}$ occurring in those molecules provided a basis for predicting their values in larger related systems in the absence of experimental data.

In a very recent paper by Jaszuński *et al.*,[131] nine different exchange-correlation functionals, four of the GGA type, namely KT2, PBE, BP86 and the dispersion-corrected B97-D, as well as five hybrid functionals, namely BHandH, B3LYP, two versions of CAM-B3LYP and PBE0, were used for the calculation of $^{n}J_{F,F}$ in a series of twelve reference compounds **133**–**144**. For the first four molecules, **133**–**136**, experimental values of those couplings were available, while for the rest of molecules, **137**–**144**, no experimental data were ever reported, and those compounds were chosen for the investigation of the through-space transmission through the corresponding coupling paths. For several of the studied compounds, SOPPA(MP2) together with SOPPA(CCSD) calculations were performed for the comparison with the DFT results. The general conclusion of the performed study was that the PBE0 functional was the most robust among those studied. Hybrid functionals and, in particular, functionals with the largest amount of Hartree – Fock exchange, such as PBE0, CAM-B3LYPx, BHandH, and CAM-B3LYP, performed

Structures 133 – 144



best for through-space coupling interactions. In the case of through-space coupling constants, the most commonly used B3LYP functional provided worse results as compared to the other hybrid functionals. On the other hand, the PBE0, B3LYP and, to a minor degree, B97-D functionals showed on average the best agreement with the experimental results, which is evidence that there was no correlation with the amount of the Hartree – Fock exchange in the functional.

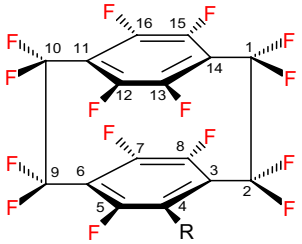
Ghiviriga *et al.*[132] investigated transmission mechanisms of the Fermi contact term of the four- and five-bond $^{19}F-^{19}F$ couplings together with conformational preferences of eight monosubstituted perfluoroparacyclophanes **145** – **152** which was indicative of a skewed geometry of these compounds in which the upper deck moves towards or away from the substituent, depending on the substituent electron-donor character and molecular size. It is well known that aromatic rings of perfluoroparacyclophanes are extremely reactive with respect to the nucleophilic substitution,[133] which was well elucidated by detailed experimental ^{19}F NMR multipulse experiments.[134] With the oxygen-based nucleophiles, such as hydroxide, alkoxide and aryloxide, the monosubstituted products were found to be generally formed, in most cases along with the corresponding di- and polysubstituted products, depending on the condition of the reaction and the number of equivalents of the nucleophile added. In this respect, performed computational ^{19}F NMR investigation of $^{n}J_{F,F}$ (n = 4, 5) couplings of **145** – **152** opened a new guide to theoretical interpretation of the long-range fluorine – fluorine spin – spin coupling together with the reaction mechanisms and pathways of these exotic compounds.

In particular, it was found that the values of $^{4}J_{F,F}$ and $^{5}J_{F,F}$ in compounds **146** – **152** depended on the size of the substituent. For instance, the values of $^{4}J_{F,F}$ in **145** were found to be larger than in the same positions of **146** and **150** – **152**. This suggested the existence of the equilibrium between the normal and a twisted conformer, in which the C^9-C^{10} bridge had the 'towards' geometry, while the C^1-C^2 bridge possessed the 'away' one (notations 'towards' and 'away' for the spatial arrangments of the bridging moieties are taken from the original publication [132]). It was also found that $^{4}J_{F,F}$ depended strongly on the F – F distance between coupled nuclei.

Most recently, Fadeev and co-workers performed a number of SOPPA(CCSD) calculations with Sauer's aug-cc-pVTZ-J basis set of $^{19}F-^{19}F$ coupling constants in a series of fluorinated carbocations [135, 136] together with their neutral precursors.[137, 138] Those calculations were supported by the corresponding experimental measurements reported (and performed) in the title publications. The most comprehensive investigation was conducted on pentafluoroallyl, heptafluorobenzyl and heptafluoroindenyl cations, presented by structures **153** – **155**.

As one can see in Figs 24 and 25, $^{4}J_{F,F}$ provided the most characteristic Karplus-type dependence on the rotation around the carbon – carbon bonds with two maxima at

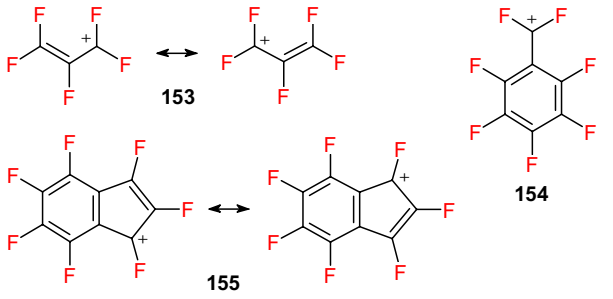
Structures 145 – 152



145 – 152

R = H (**145**), $CH(CO_2Me)_2$ (**146**), OH (**147**), OMe (**148**), NH_2 (**149**), NMe_2 (**150**), NEt_2 (**151**), $N(CH_2)_4$ (**152**)

Structures 153 – 155



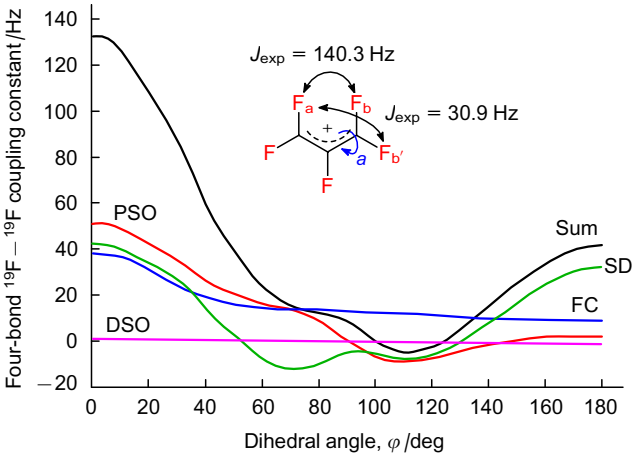


Figure 24. Dihedral angle dependence of $^{4}J_{F,F}$ in the pentafluoroallyl cation (**153**). Reproduced with minor editing privilege from Fadeev *et al.*[135] with the permission of *Elsevier*.

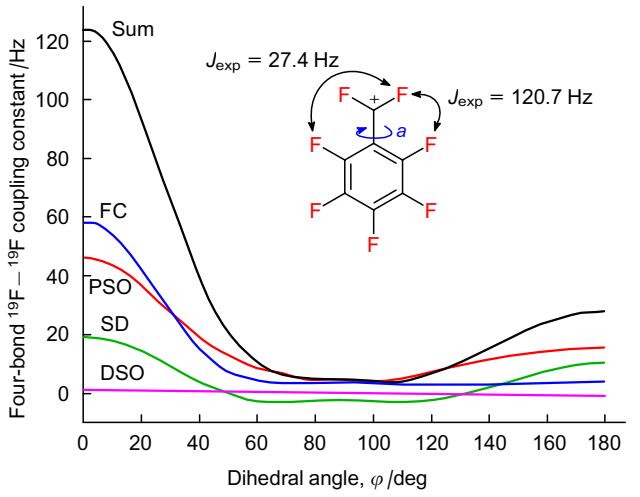


Figure 25. Dihedral angle dependence of $^{4}J_{F,F}$ in the heptafluorobenzyl cation (**154**). Reproduced with minor editing privilege from Fadeev *et al.*[135] with the permission of *Elsevier*.

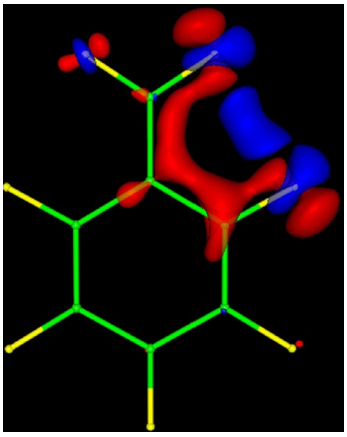


Figure 26. Transmission coupling pathway of $^{4}J_{F,F}$ in the heptafluorobenzyl cation (**154**) calculated as the difference in the electron densities between the states with parallel and antiparallel nuclear spins in terms of the coupling deformation density formalism. Reproduced from Fadeev *et al.*[135] with the permission of *Elsevier*.

$\varphi = 0^{\circ}$ and 180° and one minimum at $\varphi = 90^{\circ}$, which was exemplified for pentafluoroallyl and heptafluorobenzyl cations, **153** and **154**. Those dependences were interpreted in terms of the effective orbital overlap of the fluorine atoms providing the multiple transmission pathways of spin – spin couplings, both through-space and through-bond ones. This is clearly seen in Fig. 26 presenting the transmission coupling pathway of $^{4}J_{F,F}$ in the heptafluorobenzyl cation (**154**) calculated as the difference in the electron densities between the states with parallel and antiparallel nuclear spins in terms of the coupling deformation density formalism.[135]

Some calculations of $^{19}F - ^{19}F$ coupling constants of the fluorinated carbocations reported in those publications[135,136] were performed in the presence of counterions, and geometric parameters of those carbocations were optimized in the Sb_nF_{5n+1} ($n = 1-4$) media. It was found that Sb_2F_{11}, Sb_3F_{16} or Sb_4F_{21} solvents were more preferable than that of the SbF_6 medium. However, the enlargement of the effective size of a counterion required much more computational resources, although almost not improving the accuracy of the performed calculations.

As a result, it was generally concluded that calculation of $^{19}F - ^{19}F$ coupling constants in the most demanding perfluorocarbocations can be performed at the SOPPA(MP2) and SOPPA(CCSD) levels with the accuracy sufficient for the interpretation of the transmission of coupling mechanisms. The reported stereochemical dependences of $^{n}J_{F,F}$ coupling constats in the title carbocations were in a good agreement with the accepted theories of electron resonance delocalization. The performed SOPPA(MP2) and SOPPA(CCSD) calculations of $^{n}J_{F,F}$ provided a more reliable prediction of the ^{19}F NMR spectral parameters of polyfluorinated carbocations and their precursors than those based on empirical correlations.

3.4. Other coupling constants involving ^{19}F nucleus

Very recently, Schnack-Petersen *et al.*[139] performed a systematic study of a number of the through-bond spin – spin coupling constants involving ^{19}F nucleus ($^{1}J_{F,N}$ and related $^{1}J_{F,H}$ and $^{1}J_{F,C}$) together with those across a hydrogen bond ($^{2h}J_{F,N}$ and related $^{1h}J_{F,H}$ and $^{2h}J_{F,F}$) in a number of simple fluorine-containing inorganic molecules: HF, H_2F^+, HF_2^-, F_2H_2, $F_2H_3^+$, CH_3F, NF_3, NH_2F, NH_3F^-. In the cited paper, the RPA(D) and HRPA(D) models for the calculation of linear response functions including spin – spin coupling constants involving ^{19}F nucleus were presented, and the performance of those new models was compared to that of the RPA, HRPA and SOPPA methods in calculations of a number of different couplings involving ^{19}F nucleus. It was essential (in the sense of computational resources) that the RPA(D) model required the CPU times of only 25% of those used for the corresponding SOPPA calculations.

Very little is known about the vibrational corrections to those types of coupling constants. Indeed, vibrational corrections to coupling constants involving fluorine in some of the representative molecules from that series were studied so far only in few cases and were shown to be fairly small.[85,118,140,141]

Two years earlier Faber *et al.*[104] reported the first analytical implementation of the CC3 second derivatives using the so-called 'spin-unrestricted approach', which allowed calculation of all four contributions to spin – spin coupling constants involving fluorine nucleus at the coupled cluster CC3 level, as was exemplified for a series of the simplest fluorine-containing molecules, namely FOH, F_2O, FCN, F–C≡C–H, F–C≡C–F, FNO, FHCO, F_2CO. In that study, a number of fluorine spin – spin coupling constants of different types were calculated at the CC3 level of theory using the aug-ccJ-pVTZ basis sets and compared to those evaluated at the CCSD level.

Previous attempts to calculate spin – spin coupling constants involving fluorine attached to double or triple bonds proved to be a challenging task if the high accuracy was required.[36,103,118,128,142–144] As an example, for the vicinal fluorine – fluorine coupling in difluoroacetylene, it has been shown that the triples correction to the PSO contribution alone was of the same order of magnitude as the total coupling constant itself.[118] However, since there was no analytic implementation that could handle the triplet-type contributions, only the singlet contributions were investigated at the CC3 level at that period of time. It was found that CC3 provided important additional contributions to fluorine spin – spin couplings, not covered by the reference method, CCSD. One-bond coupling constants involving fluorine had a triples correction of a few percent of the corresponding CCSD value. While it was found that in several particular cases, triples effects beyond CC3 appeared to be important, the triples effects in CC3 calculations were in most cases by far more important.

As an illustration of the main results of the study,[104] shown in Fig. 27 are the CC3 and the residual triples corrections to various one-bond, geminal and vicinal spin – spin coupling constants, mostly those involving fluorine. The general finding was that the CC3 triples correction was by far larger than the residual triples correction. However, in a number of cases CC3 strongly overestimated the triples contribution. A large residual triples correction of −4.9 Hz was found for $^{1}J_{F,N}$ in the molecule of F–N=O. For geminal and vicinal couplings between nuclei connected by multiple bonds and shown in Fig. 28, CC3 performed much better taking the largest part of the triples correction with the residual triples corrections being less than 10% of the CC3 value for the FC and SD terms.

Very recently, Faber and Sauer[105] investigated the convergence of several basis sets derived for the calculation of spin – spin coupling constants, namely those of Benedict, ccJ-pVXZ (X = D, T, Q and 5), and Jensen, pcJ-*n* and aug-pcJ-*n* ($n = 1, 2, 3$), benchmarked to Sauer's aug-cc-pVTZ-J in the CCSD calculations of different coupling

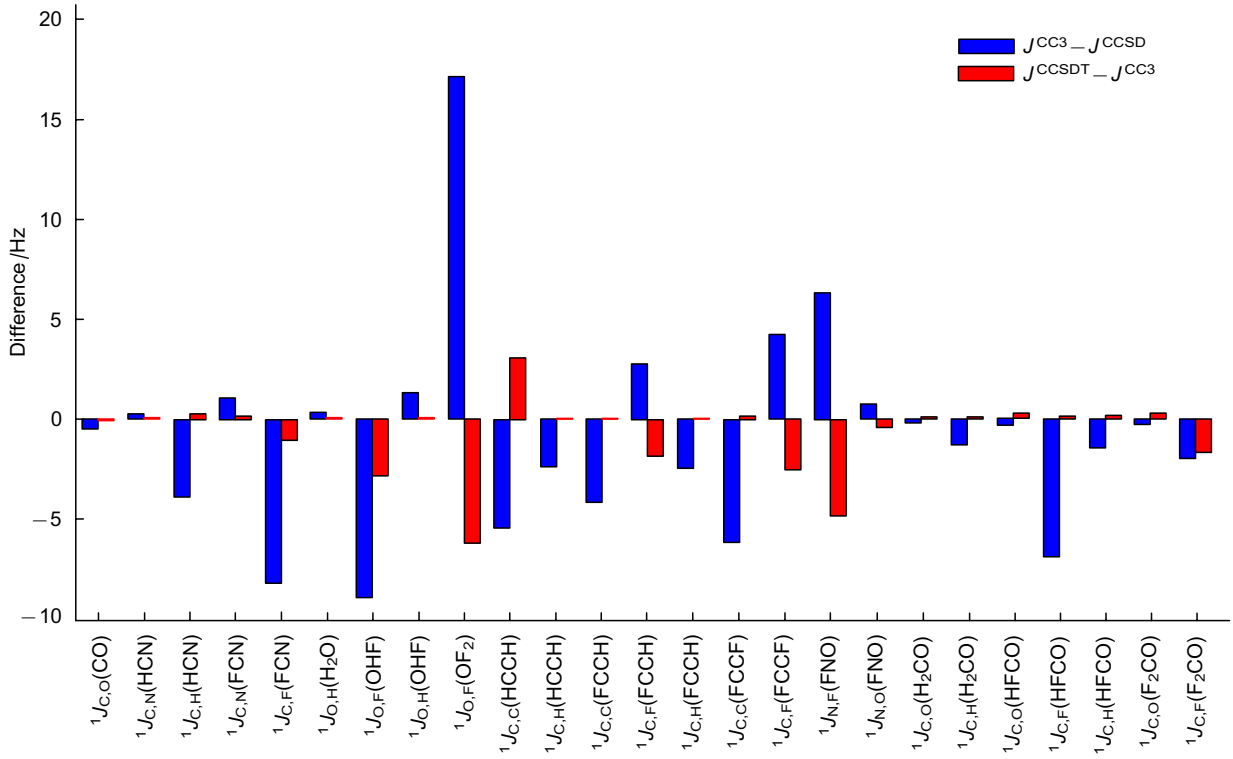


Figure 27. The CC3 triplet corrections (blue bars) and the residual triples corrections (red bars) to the one-bond spin – spin coupling constants of different types (given in Hz) in the series of benchmark molecules. Reproduced from Faber *et al.*[104] with the permission of the *American Chemical Society*.

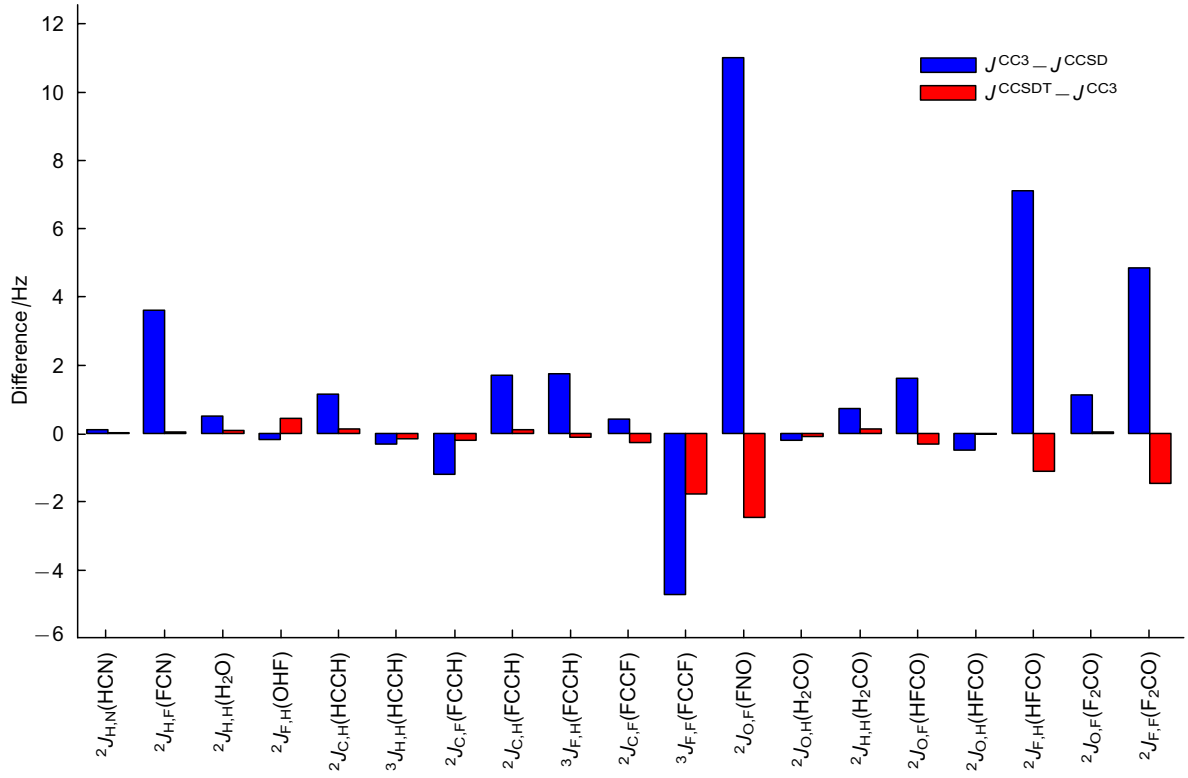


Figure 28. The CC3 triplet corrections (blue bars) and the residual triples corrections (red bars) to geminal and vicinal spin – spin coupling constants of different types (given in Hz) in the series of benchmark molecules. Reproduced from Faber *et al.*[104] with the permission of the *American Chemical Society*.

Table 19. The values of $^{1}J_{F,N}$ and $^{2}J_{F,N}$ (in Hz) obtained in the CCSD calculations using the largest affordable basis set, aug-ccJ-pV5Z-unc, as compared to experiment. Compiled from Faber and Sauer.[105]

Compound	$^{n}J_{F,N}$	DSO	PSO	SD	FC	TO	Experiment
F–N=O	$^{1}J_{F,N}$	–0.27	26.25	–17.22	136.69	145.46	
F–C≡N	$^{2}J_{F,N}$	0.41	17.08	–10.21	42.27	49.55	
cis-F–N=N–F	$^{1}J_{F,N}$	–0.33	–12.13	–19.64	244.42	212.32	211.0
	$^{2}J_{F,N}$	0.17	34.98	–2.13	–47.57	–14.54	–25.4
trans-F–N=N–F	$^{1}J_{F,N}$	–0.30	–21.47	–21.06	220.41	177.58	172.8
	$^{2}J_{F,N}$	0.06	9.67	–6.29	–62.10	–58.66	–62.8

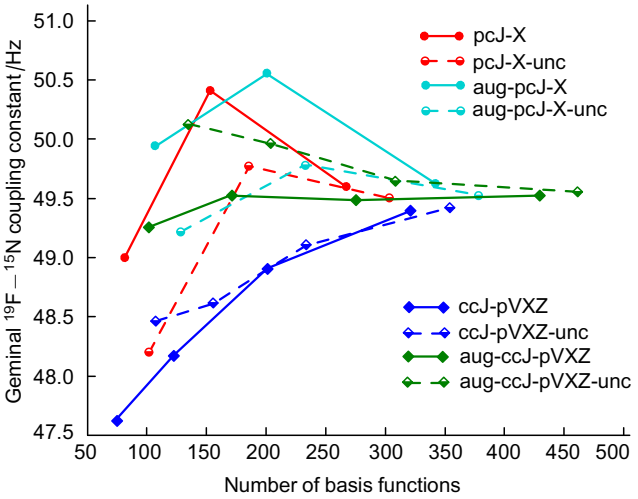


Figure 29. The $^{2}J_{F,N}$ coupling constant of F–C≡N calculated with different basis sets, plotted against the number of basis functions. Reproduced with minor editing privilege from Faber and Sauer [105] with the permission of *Springer Nature*.

constants involving fluorine. In particular, those basis sets were tested in the calculation of $^{1}J_{F,N}$ and $^{2}J_{F,N}$, in a series of 'difficult' small inorganic molecules, F–N=O, F–C≡N, *cis*- and *trans*-F–N=N–F. Performed calculations are exemplified in Table 19. It can be seen that a reasonably good agreement with available experiment was found at that level.

As a result of the performed study, it was found that the contracted pcJ-n basis sets of Jensen exhibited large contraction errors, but in their uncontracted form, they performed noticeably better than the ccJ-pVXZ basis sets. On the other hand, the ccJ-pVXZ basis sets with diffuse functions, aug-ccJ-pVXZ, showed consistent performance, with the triple-zeta (X = T) economic basis set yielding sufficiently good results, as compared to experiment. For geminal couplings, $^{2}J_{F,N}$, the ccJ-pVXZ basis sets converged very slowly. However, upon adding diffuse functions, the convergence was found to be quite fast. The pcJ-n basis sets oscillated randomly with or without diffuse functions, though the removal of the contraction did improve the convergence. In that case, the contracted aug-ccJ-pVTZ

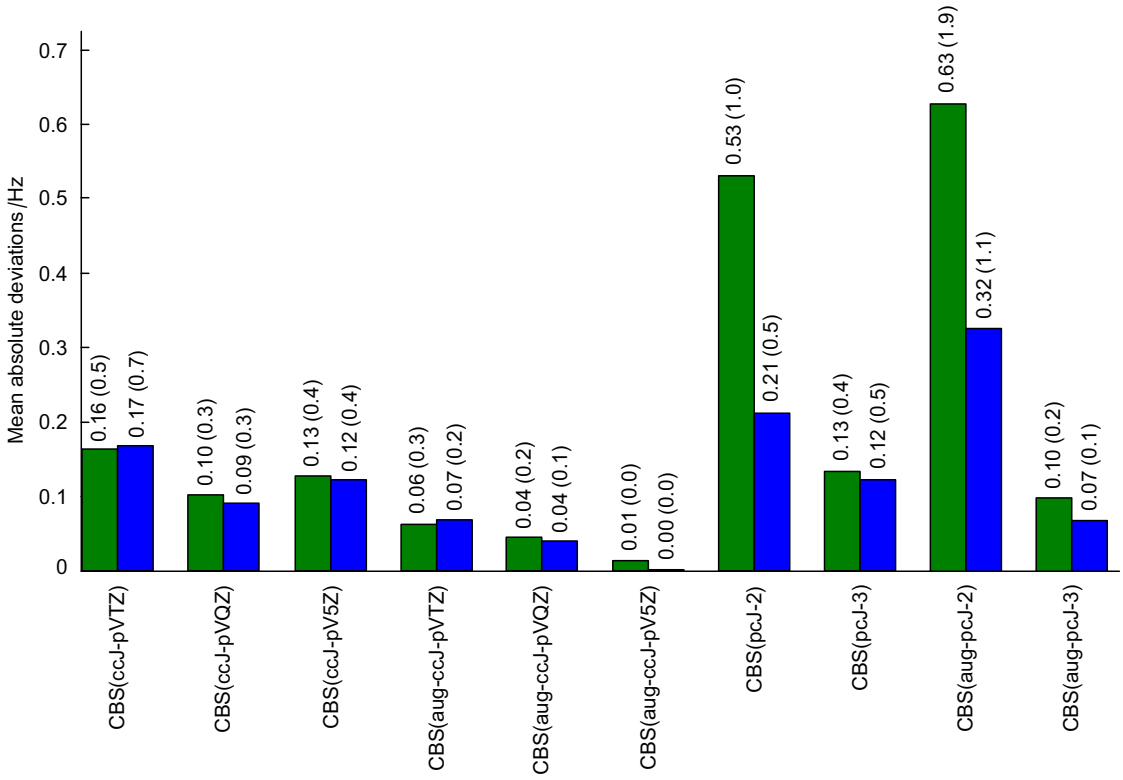


Figure 30. Mean absolute deviations of the extrapolated reduced $^{2}J_{F,N}$ values. Numbers in parentheses are the maximum deviations. Reproduced from Faber and Sauer [105] with the permission of *Springer Nature*.

yielded fully converged results, as demonstrated for $^{2}J_{F,N}$ of F–C≡N in Figs 29 and 30 extracted from the original publication.[105]

As a main result of the performed study,[105] the accuracy of various basis sets for the calculation of indirect nuclear spin–spin coupling constants at the CCSD level was established for a set of the most 'difficult' small molecules. For the one-bond $^{1}J_{F,N}$ and geminal $^{2}J_{F,N}$ couplings, the relatively large contraction errors for both Jensen's pcJ-n and Benedict's ccJ-pVXZ basis sets were found. When not using basis set contraction, the pcJ-2 and pcJ-3 outperformed related ccJ-pVTZ and ccJ-pVQZ; however, on adding computationally demanding diffuse functions, the results were fairly the same. On the other hand, the rather economical triple zeta aug-ccJ-pVTZ basis set gave reasonably good results, and if higher accuracy was needed, the basis set error can be reduced by roughly a factor of two when going to the quadruple zeta basis sets. It was also found that basis set extrapolations can improve the results obtained with the medium-sized basis sets of the ccJ-type, but not those of the pcJ family. However, it was stated by the authors that those extrapolations can be a useful way of improving the results obtained with the medium-sized basis sets, which can eventually replace calculations with very large basis sets when highly accurate results are needed.

In the early paper by Jaszuński,[43] a set of $^{19}F-^{31}P$ spin–spin coupling constants has been calculated in trifluorophosphane, PF_3 and pentafluoro-λ^5-phosphane, PF_5, and compared with the available experiment (Table 20). Those calculations were performed at the CCSD level (which was rather unusual for that period of time) with rather large uncontracted Dunning's basis sets of triple zeta quality augmented with core functions. It is interesting to note that despite the fact of the predominance of the Fermi contact contribution to the one-bond fluorine–phosphorus coupling constants in both molecules, it was not so for the geminal coupling $^{2}J_{F,F}$ in PF_3, where Fermi contact contribution (−5.1 Hz) was essentially smaller in magnitude than paramagnetic spin–orbit (−40.0 Hz) and spin dipolar (+46.3 Hz) terms.

Table 20. $^{19}F-^{31}P$ spin–spin coupling constants (Hz), calculated at the CCSD level, *vs.* experiment. Compiled from Jaszuński.[43]

Compound	Coupling constant	DSO	PSO	SD	FC	TO	Experiment
PF_3	$^{1}J_{F,P}$	0.8	−259.3	32.4	−1070.8	−1296.9	−1400 ± 1
	$^{2}J_{F,P}$	−0.8	−40.0	46.3	−5.1	0.4	
PF_5	$^{1}J_{ax,P}$	1.8	−174.9	17.3	−853.2	−1009.0	−929±1
	$^{1}J_{eq,P}$	1.8	−132.5	18.6	−719.0	−831.0	(averaged)

Passing to organic molecules, let us first recall an essential paper by Favaro *et al.*[145] who performed SOPPA(CCSD)/EPR-III calculations of the long-range $^{n}J_{F,N}$ coupling constants in the series of fluoroximes **156**–**162** demonstrating that the Fermi contact term was the most important contribution to the *through-space* transmission of this type of coupling.

A rather good agreement between $^{n}J_{F,N}$ couplings calculated in that way and experiment was reached at in this series of compounds, as illustrated in Table 21. This agreement suggested that theoretical values of $^{n}J_{F,N}$ should be used with much confidence when experimental data were not available. It was also demonstrated that the Fermi contact term was the most important contribution to those

Structures 156 – 162

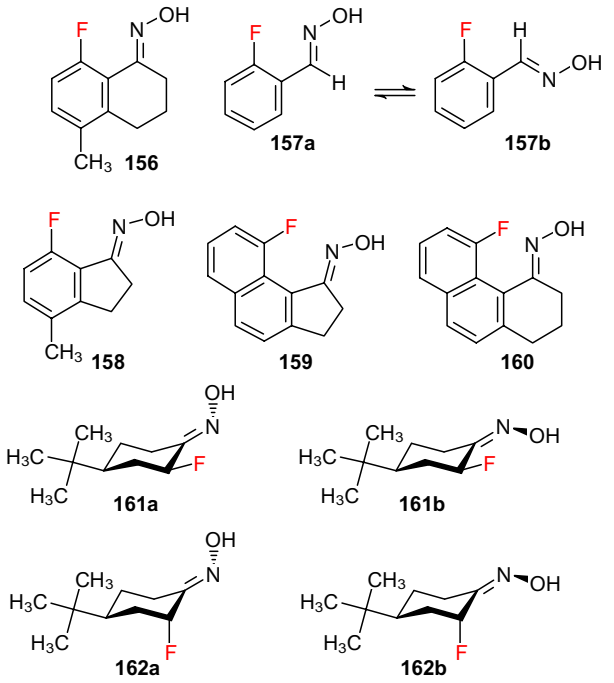


Table 21. The SOPPA(CCSD)/EPR-III calculated $^{n}J_{F,N}$ (n = 3, 4, 5) coupling constants (Hz) in the series of fluoroximes **156**–**162**. Compiled from Favaro *et al.*[145]

Compound	DSO	PSO	SD	FC	TO	Experiment
156	−0.17	−1.25	−0.92	−18.19	−20.53	(−)22.4 [a]
157a	−0.14	−1.30	−2.11	−15.00	−18.25	
157b	0.08	0.52	−1.44	0.24	−0.60	3.2 [b]
158	−0.13	−0.66	−1.68	−6.87	−9.34	(−)8.8
159	−0.21	0.43	0.38	−36.42	−35.82	(−)39.5
160	−0.19	0.97	0.08	−17.79	−16.93	(−)19.4
161a	−0.10	0.81	−0.01	−9.00	−8.31	(−)10.7
162a	0.04	−0.55	0.01	−6.51	−7.01	
162b	0.08	1.85	1.11	−2.62	0.43	0

[a] Supposed signs (not determined experimentally). [b] Conformationally averaged.

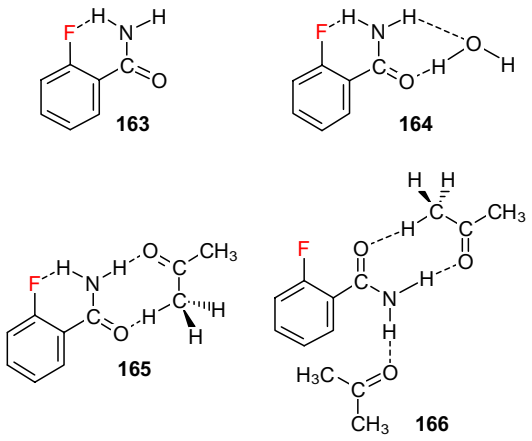
spin–spin coupling constants providing an essential through-space coupling pathway. It is well known that spatial proximity between fluorine and hydrogen atoms can lead to a significant overlap of their electron clouds. In that overlap region, the exchange interactions involving both atoms take place, determining a direct pathway for transmitting the Fermi contact interaction. As a result, the through-space coupling mechanism comes to power involving the transmission of spin–spin coupling between fluorine and nitrogen by the exchange interactions because of their lone pair overlap. The same arguments are applicable to another types of spin–spin couplings, involving those of the long-range fluorine–nitrogen spin–spin coupling constants, $^{n}J_{F,N}$.

The most important aspect of this rationalization suggested by the authors [145] is related to the understanding of the origin and behaviour of some unusual experimental coupling constants involving fluorine between the formally long-range but spatially close coupled nuclei. Indeed, it was explicitly shown that the electronic origin of the through-

space coupling is transmitted through the overlap of the orbitals on coupled nuclei, suggesting that the through-space coupling should be understood as the 'through overlapping orbital coupling' (this term was suggested by the authors).[145]

Alkorta *et al.*[146] calculated, at the B3LYP/6-311++G(d,p) level, intramolecular $^{19}F-^{15}N$ spin–spin coupling constants transmitted mainly across hydrogen bonds, $^{2h}J_{F,N}$, in the isolated 2-fluorobenzamide (**163**) and its intermolecular complexes with water (**164**) and one and two acetone molecules (accordingly, **165** and **166**) together with a series of related compounds. It was found that this coupling dramatically changed when going from **163** (−7.4 Hz), **164** (−8.0 Hz) and **165** (−7.0 Hz) to **166** (+0.2 Hz) which was due to the fact that only in the latter compound, coupled fluorine and amide nitrogen were spatially separated.

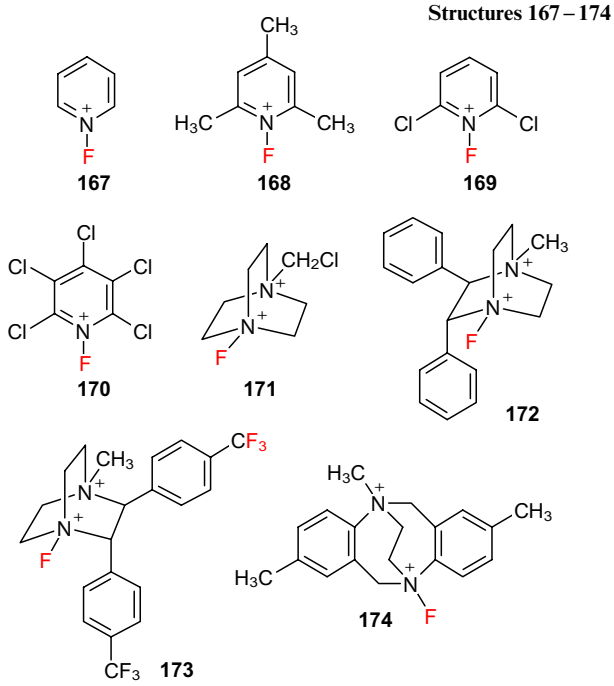
Structures 163 – 166



Very recently, in a special issue of *Magn. Reson. Chem.* (2020) dedicated to quantum chemical calculations and machine learning in the field of NMR, Saielli reported [147] the results of his theoretical study of $^{1}J_{F,N}$ coupling constants calculated by means of several DFT protocols in a series of vitally important cationic fluorinating reagents **167** – **174**. This study was performed in comparison with the available experiment reported earlier by Pereira *et al.*[148] The performance of various levels of theory was evaluated in this submission, and the M06-2X(PCM)/pcJ-2//B3LYP(PCM)/6-311G(d,p) protocol was found to be the most accurate and robust among those performed at reasonable computational costs.

The performance of several accuracy factors affecting the calculation of $^{1}J_{F,N}$, namely, the functional choice, geometry optimization, inclusion of the solvent reaction field, relativistic effects, conformational effects and vibrational corrections were thoroughly investigated. It was found that spin dipolar and paramagnetic spin–orbit terms were quite significant while diamagnetic spin–orbit contribution was negligible. This meant that, together with σ-type orbitals, the fluorine–nitrogen coupling was transmitted also through the p- and π-type orbitals. It was also found that, although the Fermi contact term of $^{1}J_{F,N}$ was positive, the spin dipolar and paramagnetic spin–orbit contributions were opposite in sign and relatively large, accounting for up to 60% of the total coupling constant in some cases.

Structures 167 – 174



Relativistic corrections to $^{1}J_{F,N}$ were evaluated *via* the two-component relativistic ZORA spin–orbit calculations. The results of those calculations showed that such corrections amounted to a systematic shift of −3.5 to −4.0 Hz that slightly improved the agreement between the calculated couplings and experiment. Although the corrections due to relativistic and solvent effects went in a right direction, they did not fully accounted for the relatively large and system-

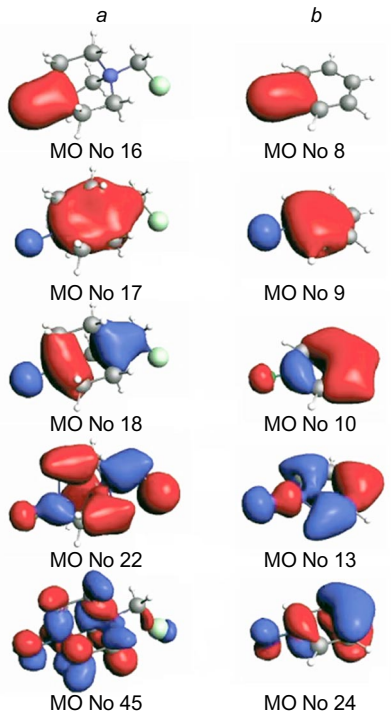


Figure 31. Occupied molecular orbitals providing the largest contributions to $^{1}J_{F,N}$ in compounds **167** (*b*) and **171** (*a*). Reproduced with minor editing privilege from Saielli [147] with the permission of *John Wiley and Sons*.

atic discrepancy between calculated and experimental values.

The paper [147] also repoted the total contributions to $^1J_{F,N}$ due to the occupied molecular orbitals coupled with the virtual ones, as exemplified in Fig. 31 for two representative compounds, **167** and **171**. It was found that the largest positive contribution to $^1J_{F,N}$ was due to the N – F bonding σ-orbital. However, the next contributions in the order of magnitude came from the orbitals having a nodal plane between coupled fluorine and nitrogen. The title molecular orbitals were those having large contributions from the fluorine lone pairs and resulted in a negative term contributing to $^1J_{F,N}$, thereby cancelling the positive term due to the bonding σ-orbitals.

Jaszuński *et al.*[131] calculated a number of $J_{F,N}$, $J_{F,P}$ and $J_{F,Se}$ coupling constants in the series of fluorinated heteroaromatic compounds with a special emphasis on their transmission mechanisms. The set of compounds under study was chosen for the investigation of the through-space transmission of spin – spin coupling constants involving fluorine. Neither vibrational corrections nor solvent effects have been considered in that work, while for the selenium containing molecule, the contribution of relativistic effects in the value of $J_{F,Se}$ was studied at the four-component level. It was generally found that the relativistic correction was as much as 8.5% of its experimental value, indicative of the importance of relativistic effects of selenium for the coupling constants of this type.

Table 22. One-bond $^{19}F-^{77}Se$ spin – spin coupling constants (Hz), calculated at the non-relativisc CCSD level, *vs.* experiment. Compiled from Rusakova *et al.*[149]

Compound	DSO	PSO	SD	FC	TO	Experiment [a]
Me_2SeF_2	0.29	153.90	115.80	125.28	395.27	(+)634.0
SeF_6	0.73	−178.88	55.32	−1237.34	−1360.17	(−)1423.0
F_2SeO	0.31	−124.31	102.75	813.22	−834.47	(−)837.0
F_2SeO_2	0.47	−139.19	64.64	−1311.84	−1385.92	(−)1580.0

[a] Signs are ascribed based on the performed calculations.

The same conclusion (dealing with the importance of relativistic effects) was reached at in the paper by Rusakova *et al.*[149] who performed calculations of the one-bond fluorine – selenium coupling constants, $^1J_{F,Se}$, both at the non-relativistic SOPPA(CCSD) and the four-component relativistic DFT-PBE0 levels in four classical inorganic selenium compounds presented in Tables 22 and 23.

The main finding of the performed study [149] was that taking into account relativistic corrections at both random phase approximation and DFT levels essentially improved the agreement between the theoretical results and experiment, demonstrating the importance of relativistic corrections in $^1J_{F,Se}$ together with other one-bond coupling constants involving selenium. This is illustrated in Fig. 32 showing the importance of relativism in the values of $^1J_{F,Se}$,

Table 23. Relativistic corrections to the one-bond $^{19}F-^{77}Se$ spin – spin coupling constants (Hz), calculated at the four-component relativistic DFT-PBE0 level, *vs.* experiment. Compiled from Rusakova *et al.*[149]

Compound	Scalar correction	Spin – orbit correction	Total relativistic correction	Basic non-relativistic value [a]	Total	Experiment [b]
Me_2SeF_2	122.25	38.85	161.10	395.27	556.37	(+)634.0
SeF_6	−117.91	57.34	−60.57	−1360.17	−1420.74	(−)1423.0
F_2SeO	50.01	34.65	84.66	834.47	−749.81	(−)837.0
F_2SeO_2	−67.89	35.64	−32.25	−1385.92	−1418.17	(−)1580.0

[a] Calculated at the non-relativistic SOPPA(CCSD) level. [b] Signs are ascribed based on the performed calculations.

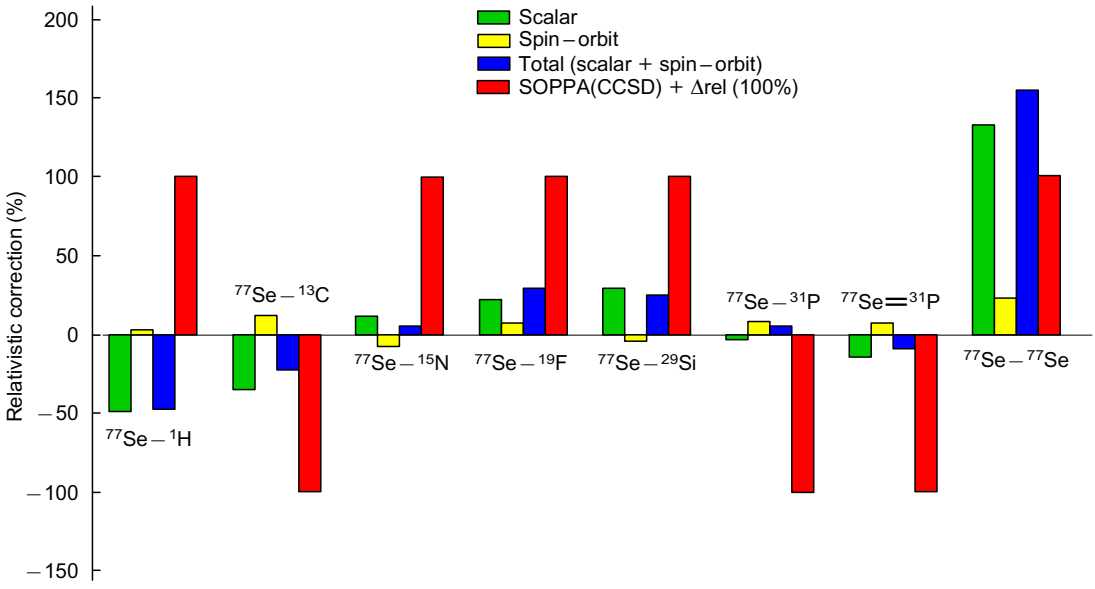


Figure 32. Relative contributions of the scalar, spin – orbit and total relativistic corrections calculated at the DFT-PBE0 level to the total 'relativistically corrected' SOPPA(CCSD) values of $^1J_{Se,X}$ (X = H, C, N, F, Si, P, Se). Reproduced with minor editing privilege from Rusakova *et al.*[149] with the permission of *John Wiley and Sons*.

as compared to some other types of spin – spin coupling constants involving selenium. It was shown that the value of scalar and spin – orbit contributions (considered together) for $^1J_{F,Se}$ was about 25% of the total coupling constant calculated at the SOPPA(CCSD) level taking into account relativistic corrections. The importance of relativistic effects was mostly striking for dimethylselenium difluoride, Me_2SeF_2: the 'non-relativistic' value of $^1J_{F,Se}$ calculated at the CCSD level was 395.27 Hz while 'relativistic' value of $^1J_{F,Se}$ evaluated at the four-component relativistic level was 556.37 Hz, as compared to experimental value of 634.0 Hz.

Another interesting issue raised in the performed study [149] was the sign of $^1J_{F,Se}$. Interesting to note that based on the performed calculations, it was positive for Me_2SeF_2 and negative for the rest of compounds of this series, which, however, had not been yet confirmed experimentally.

4. Conclusion

The main conclusion of the performed survey is that computational ^{19}F NMR is rapidly developing with a general tendency of increasing studies based on more and more sophisticated wavefunction-based methods, involving MP2, CCSD, CCSD(T) and even CCSDT for ^{19}F NMR chemical shifts, and SOPPA(MP2), SOPPA(CC2) and SOPPA(CCSD) for the fluorine-containing spin – spin coupling constants. In view of a rapidly developing organofluorine chemistry,[37] a marked progress in computational ^{19}F NMR is on a cutting edge of the modern chemical science. A thorough analysis of a number of accuracy factors affecting the quality of the performed calculations of ^{19}F NMR parameters (the level of theory and quality of the basis set, solvent, temperature, rovibrational effects and relativistic corrections) is performed, which is substantiated with a number of illustrative examples covering different aspects of this area and claiming for their rigorous consideration.

The author declares no conflict of interest.

References

1. S.P.A.Sauer. *Molecular Electromagnetism. A Computational Chemistry Approach*. (Oxford: University Press, 2012)
2. T.Helgaker, M.Jaszuński, K.Ruud. *Chem. Rev.*, **99**, 293 (1999)
3. T.Helgaker, M.Jaszuński, M.Pecul. *Prog. NMR Spectrosc.*, **53**, 249 (2008)
4. T.Helgaker, S.Coriani, P.Jørgensen, K.Kristensen, J.Olsen, K.Ruud. *Chem. Rev.*, **112**, 543 (2012)
5. D.Cremer, J.Grafenstein. *Phys. Chem. Chem. Phys.*, **9**, 2791 (2007)
6. J.Vaara. *Phys. Chem. Chem. Phys.*, **9**, 5399 (2007)
7. G.A.Aucar, R.H.Romero, A.F.Maldonado. *Int. Rev. Phys. Chem.*, **29**, 1 (2010)
8. M.Bühl, T.van Mourik. *WIREs Comput. Mol. Sci.*, **1**, 634 (2011)
9. *High Resolution NMR Spectroscopy: Understanding Molecules and their Electronic Structures*. (Ed. R.H.Contreras). (The Netherlands: Elsevier, 2013)
10. Y.Y.Rusakov, L.B.Krivdin. *Russ. Chem. Rev.*, **82**, 99 (2013)
11. F.A.A.Mulder, M.Filatov. *Chem. Soc. Rev.*, **39**, 578 (2010)
12. L.B.Krivdin, R.H.Contreras. *Ann. Rep. NMR Spectrosc.*, **61**, 133 (2007)
13. L.B.Krivdin, Y.Y.Rusakov. *Encycl. Magn. Reson.*, **3**, 87 (2014)
14. A.Navarro-Vázquez. *Magn. Reson. Chem.*, **55**, 29 (2017)
15. Y.Xiao, W.Liu, J.Autschbach. In *Handbook of Relativistic Quantum Chemistry*. (Ed. W.Liu). (Berlin: Springer, 2017)
16. J.Autschbach. *Phyl. Trans. Royal Soc. A*, **372**, 1 (2014)
17. M.Repisky, S.Komorovsky, R.Bast, K.Ruud. In *Gas Phase NMR*. (Eds K.Jackowski, M.Jaszunski). (Cambridge: The Royal Society of Chemistry, 2016)
18. I.L.Rusakova, Y.Y.Rusakov, L.B.Krivdin. *Russ. Chem. Rev.*, **85**, 356 (2016)
19. I.L.Rusakova, L.B.Krivdin. *Mendeleev Commun.*, **28**, 1 (2018)
20. L.B.Krivdin. *Magn. Reson. Chem.*, **57**, 897 (2019)
21. L.B.Krivdin. *Magn. Reson. Chem.*, **58**, 5 (2020)
22. L.B.Krivdin. *Magn. Reson. Chem.*, **58**, 15 (2020)
23. L.B.Krivdin. *Prog. NMR Spectrosc.*, **105**, 54 (2018)
24. L.B.Krivdin. *Prog. NMR Spectrosc.*, **108**, 17 (2018)
25. L.B.Krivdin. *Prog. NMR Spectrosc.*, **112 – 113**, 103 (2019)
26. L.B.Krivdin. *Prog. NMR Spectrosc.*, **102 – 103**, 98 (2017)
27. L.B.Krivdin. *Russ. Chem. Rev.*, **89**, 449 (2020)
28. L.B.Krivdin. *Magn. Reson. Chem.*, **58**, 478 (2020)
29. L.B.Krivdin. *Magn. Reson. Chem.*, **58**, 500 (2020)
30. T.E.Field-Theodore, M.Olejniczak, M.Jaszuński, D.J.D.Wilson. *Phys. Chem. Chem. Phys.*, **20**, 23025 (2018)
31. V.G.Malkin, O. L.Malkina, D.R.Salahub. *Chem. Phys. Lett.*, **221**, 91 (1994)
32. R.Dickson, T.Ziegler. *J. Phys. Chem.*, **100**, 5286 (1996)
33. J.E.Peralta, V.Barone, R.H.Contreras. *J. Am. Chem. Soc.*, **123**, 9162 (2001)
34. A.B.Shtarev, E.Pinkhassik, M.D.Levin, I.Stibor, J.Michl. *J. Am. Chem. Soc.*, **123**, 3484 (2001)
35. D.L.Bryce, R.E.Wasylishen. *J. Mol. Struct.*, **602 – 603**, 463 (2002)
36. V.Barone, P.F.Provasi, J.E.Peralta, J.P.Snyder, S.P.A.Sauer, R.H.Contreras. *J. Phys. Chem. A*, **107**, 4748 (2003)
37. L.V.Politanskaya, G.A.Selivanova, E.V.Panteleeva, E.V.Tretyakov, V.E.Platonov, P.V.Nikul'shin, A.S.Vinogradov, Y.V.Zonov, V.M.Karpov, T.V.Mezhenkova, A.V.Vasilyev, A.B.Koldobskii, O. S.Shilova, S.M.Morozova, Y.V.Burgart, E.V.Shchegolkov, V.I.Saloutin, V.B.Sokolov, A.Y.Aksinenko, V.G.Nenajdenko, M.Y.Moskalik, V.V.Astakhova, B.A.Shainyan, A.A.Tabolin, S.L.Ioffe, V.M.Muzalevskiy, E.S.Balenkova, A.V.Shastin, A.A.Tyutyunov, V.E.Boiko, S.M.Igumnov, A.D.Dilman, N.Y.Adonin, V.V.Bardin, S.M.Masoud, D.V.Vorobyeva, S.N.Osipov, E.V.Nosova, G.N.Lipunova, V.N.Charushin, D.O.Prima, A.G.Makarov, A.V.Zibarev, B.A.Trofimov, L.N.Sobenina, K.V.Belyaeva, V.Y.Sosnovskikh, D.L.Obydennov, S.A.Usachev. *Russ. Chem. Rev.*, **88**, 425 (2019)
38. W.Adcock, D.Lunsmann, J.E.Peralta, R.H.Contreras. *Magn. Reson. Chem.*, **37**, 167 (1999)
39. K.B.Wiberg, K.W.Zilm. *J. Org. Chem.*, **66**, 2809 (2001)
40. J.C.C.Chan, H.Eckert. *J. Mol. Struct.: THEOCHEM*, **535**, 1 (2001)
41. D.J.Giesen, N.Zumbulyadis. *Phys. Chem. Chem. Phys.*, **4**, 5498 (2002)
42. H.Fukaya, T.Ono. *J. Comp. Chem.*, **25**, 51 (2003)
43. M.Jaszuński. *Chem. Phys. Lett.*, **385**, 122 (2004)
44. H.Shaghaghi, H.Ebrahimi, M.Tafazzoli, M.Jalali-Heravi. *J. Fluorine Chem.*, **131**, 47 (2010)
45. H.P.Ebrahimi, M.Tafazzoli. *Concepts Magn. Reson. A*, **40**, 192 (2012)
46. H.P.Ebrahimi, M.Tafazzoli. *Concepts Magn. Reson. A*, **42**, 140 (2013)
47. G.Saielli, R.Bini, A.Bagno. *Theor. Chem. Acc.*, **131**, 1140 (2012)
48. G.Saielli, R.Bini, A.Bagno. *Theor. Chem. Acc.*, **131**, 1283 (2012)
49. O.V.Gritsenko, P.R.T.Schipper, E.J.Baerends. *Chem. Phys. Lett.*, **302**, 199 (1999)

50. F.Nozirov, T.Kupka, M.Stachów. *J. Chem. Phys.*, **140**, 144303 (2014)
51. M.Marín-Luna, I.Alkorta, J. Elguero. *Magn. Reson. Chem.*, **56**, 164 (2018)
52. D.García-Pérez, C.López, R.M.Claramunt, I.Alkorta, J.Elguero. *Molecules*, **22**, 2003 (2017)
53. C.I.Nieto, A.Andrade, D.Sanz, R.M.Claramunt, M.C.Torralba, M.R.Torres, I.Alkorta, J. Elguero. *ChemistrySelect*, **2**, 3732 (2017)
54. C.I.Nieto, P.Cabildo, R.M.Claramunt, P.Cornago, D.Sanz, M.C.Torralba, M.R.Torres, M.B.Ferraro, I.Alkorta, M.Marín-Luna, J.Elguero. *Struct. Chem.*, **27**, 705 (2015)
55. O.Martín, M.Pérez-Torralba, M.Á. García, R.M.Claramunt, M.C.Torralba, M.R.Torres, I.Alkorta, J.Elguero. *ChemistrySelect*, **4**, 861 (2016)
56. D.Santa María, R.M.Claramunt, I.Alkorta, J.Elguero, F.J.Zúñiga. *J. Fluor. Chem.*, **192**, 98 (2016)
57. I.Alkorta, J.Elguero, M.Pérez-Torralba, C.López, R.M.Claramunt. *Magn. Reson. Chem.*, **53**, 353 (2015)
58. J.Poater, M.Solà, I.Alkorta, J. Elguero. *Eur. J. Org. Chem.*, 5370 (2014)
59. C.Bonhomme, C.Gervais, F.Babonneau, C.Coelho, F.Pourpoint, T.Azăs, S.E.Ashbrook, J. M.Griffin, J. R.Yates, F.Mauri, C.J. Pickard. *Chem. Rev.*, **112**, 5733 (2012)
60. I.Alkorta, J. Elguero, A.Font, J. Galcera, I.Mata, E.Molins, A.Virgili. *Tetrahedron*, **70**, 2784 (2014)
61. C.I.Nieto, P.Cabildo, M.Á.García, R.M.Claramunt, I.Alkorta, J.Elguero. *Beilstein J. Org. Chem.*, **10**, 1620 (2014)
62. M.M.Quesada-Moreno, J.R.Avilés-Moreno, J.J.López-González, K.Jacob, L.Vendier, M.Etienne, I.Alkorta, J. Elguero, R.M.Claramunt. *Phys. Chem. Chem. Phys.*, **19**, 1632 (2017)
63. F.Blanco, I.Alkorta, J. Elguero. *Magn. Reson. Chem.*, **45**, 797 (2007)
64. N.Fresno, R.Pérez, M.L.Jimeno, I.Alkorta, G.Sánchez-Sanz, J.Elguero, J.E.Del Bene. *J. Heterocycl. Chem.*, **49**, 1257 (2012)
65. A.Llamas-Saiz, C.Foces-Foces, I.Sobrados, J.Elguero, W.Meutermans. *Acta Crystallogr. Sect. C*, **49**, 724 (1993)
66. G.P.A.Yap, R.M.Claramunt, C.López, M.A.García, C.Pérez-Nedina, I.Alkorta, J.Elguero. *J. Mol. Struct.*, **965**, 74 (2010)
67. M.M.Quesada-Moreno, J.R.Avilés-Moreno, J.J.López-González, R.M.Claramunt, C.López, I.Alkorta, J.Elguero. *Tetrahedron Asymmetry*, **25**, 507 (2014)
68. A.L.Webber, L.Emsley, R.M.Claramunt, S.P.Brown. *J. Phys. Chem. A*, **114**, 10435 (2010)
69. A.R.Katritzky, N.G.Akhmedov, J.Doskocz, C.D.Hall, R.G.Akhmedova, S.Majumder. *Magn. Reson. Chem.*, **45**, 5 (2007)
70. R.Mejía-Urueta, K.Mestre-Quintero, R.Vivas-Reyes. *J. Braz. Chem. Soc.*, **22**, 2268 (2011)
71. M.A.Fox, G.Sandford, R.Slater, D.S.Yufit, J. A.K.Howard, A.Vong. *J. Fluorine Chem.*, **143**, 148 (2012)
72. M.A.Fox, G.Pattison, G.Sandford, A.S.Batsanov. *J. Fluorine Chem.*, **55**, 62 (2013)
73. G.Saielli, R.Bini, A.Bagno. *RSC Adv.*, **4**, 41605 (2014)
74. T.Enevoldsen, J.Oddershede, S.P.A.Sauer. *Theor. Chem. Acc.*, **100**, 275 (1998)
75. P.-O.Åstrand, K.Ruud, K.V.Mikkelsen, T.Helgaker. *J. Chem. Phys.*, **110**, 9463 (1999)
76. A.A.Auer, J.Gauss. *J. Chem. Phys.*, **115**, 1619 (2001)
77. P.Bouř, M.Buděšinský. *J. Chem. Phys.*, **110**, 2836 (1999)
78. D.L.Bryce, R.E.Wasylishen. *J. Am. Chem. Soc.*, **122**, 3197 (2000)
79. D.L.Bryce, R.E.Wasylishen. *J. Am. Chem. Soc.*, **122**, 11236 (2000)
80. J.E.Peralta, M.C.Ruiz de Azúa, R.H.Contreras. *Theor. Chem. Acc.*, **105**, 165 (2000)
81. J.San Fabián, J.Casanueva, E.San Fabián, J.Guilleme. *J. Chem. Phys.*, **112**, 4143 (2000)
82. T.Kupka. *Chem. Phys. Lett.*, **461**, 33 (2008)
83. T.Helgaker, M.Jaszuński, K, Ruud, A.Górska. *Theor. Chem. Acc.*, **99**, 175 (1998)
84. T.Helgaker, M.Watson, N.C.Handy. *J. Chem. Phys.*, **113**, 9402 (2000)
85. T.A.Ruden, O.B.Lutnæs, T.Helgaker. *J. Chem. Phys.*, **118**, 9572 (2003)
86. P.Lantto, J.Vaara. *J. Chem. Phys.*, **114**, 5482 (2001)
87. A.Soncini, P.Lazzeretti. *J. Chem. Phys.*, **118**, 7165 (2003)
88. V.Sychrovský, J. Gräfenstein, D.Cremer. *J. Chem. Phys.*, **113**, 3530 (2000)
89. T.W.Keal, T.Helgaker, P.Sałek, D.J.Tozer. *Chem. Phys. Lett.*, **425**, 163 (2006)
90. A.Gryff-Keller, P.Szczeciński. *RSC Adv.*, **6**, 82783 (2016)
91. I.Alkorta, F.Blanco, J.Elguero. *J. Mol. Struct.*, **964**, 119 (2010)
92. I.Alkorta, F.Blanco, J.E.Del Bene, J.Elguero, L.Hernández-Folgado, M.-L.Jimeno. *Magn. Reson. Chem.*, **48**, 68 (2010)
93. R.V.Viesser, L.C.Ducati, J.Autschbach, C.F.Tormena. *Phys. Chem. Chem. Phys.*, **18**, 24119 (2016)
94. F.B.Mallory, C.W.Mallory, K.E.Butler, M.B.Lewis, A.Q.Xia, E.D.Luzik, Jr., L.E.Fredenburgh, M.M.Ramanjulu, Q.N.Van, M.M.Francl, D.A.Freed, C.C.Wray, C.Hann, M.Nerz-Stormes, P.J.Carroll, L.E.Chirlian. *J. Am. Chem. Soc.*, **122**, 4108 (2000)
95. R.H.Contreras, L.C.Ducati, C.F.Tormena. *Int. J. Quant. Chem.*, **112**, 3158 (2012)
96. J. San Fabián, J.Guilleme, E.Díez. *J. Magn. Reson.*, **133**, 255 (1998)
97. J. San Fabián, J.Guilleme. *Chem. Phys.*, **206**, 325 (1996)
98. T.M.Barbosa, R.V.Viesser, L.G.Martins, R.Rittner, C.F.Tormena. *ChemPhysChem*, **19**, 1 (2018)
99. M.Hennig, M.L.Munzarová, W.Bermel, L.G.Scott, V.Sklenĭ, J.R.Williamson. *J. Am. Chem. Soc.*, **128**, 5851 (2006)
100. R.A.Cormanich, M.A.Moreira, M.P.Freitas, T.C.Ramalho, C.P.A.Anconi, R.Rittner, R.H.Contreras, C.F.Tormena. *Magn. Reson. Chem.*, **49**, 763 (2011)
101. L.A.F.Andrade, J.M.Silla, C.J.Duarte, R.Rittner, M.P.Freitas. *Org. Biomol. Chem.*, **11**, 6766 (2013)
102. D.C.Favaro, R.H.Contreras, C.F.Tormena. *J. Phys. Chem. A*, **117**, 7939 (2013)
103. P.F.Provasi, G.A.Aucar, S.P.A.Sauer. *J. Phys. Chem. A* **108**, 5393 (2004)
104. R.Faber, S.P.A.Sauer, J.Gauss. *J. Chem. Theory Comput.*, **13**, 696 (2017)
105. R.Faber, S.P.A.Sauer. *Theor. Chem. Acc.*, **137**, 35 (2018)
106. M.C.Caputo, I.Alkorta, P.F.Provasi, S.P.A.Sauer. *Mol. Phys.*, **116**, 2396 (2018)
107. H.Bürger, S.Sommer. *J. Chem. Soc. Chem. Commun.*, **42**, 456 (1991)
108. J.D.Vilcachagua, L.C.Ducati, R.Rittner, R.H.Contreras, C.F.Tormena. *J. Phys. Chem. A*, **115**, 1272 (2011)
109. A.Koch, B.Stamboliyska, B.Mikhova, P.Breznica-Selmani, K.Mladenovska, E.Popovski. *Magn. Reson. Chem.*, **57**, S75 (2019)
110. P.Breznica-Selmani, K.Mladenovska, G.Dräger, B.Mikhova, N.Panovski, A.Kaftandzieva, Z.Kavrakovski, A.Hoxha, N.Sheqerxhiu, M.J.Pavlova, E.Popovski. *Maced. J. Chem. Chem. Eng.*, **35**, 179 (2016)
111. A.Gryff-Keller, P.Szczeciński. *RSC Adv.*, **4**, 27290 (2014)
112. A.Gryff-Keller, P.Szczeciński. *J. Mol. Struct.*, **1091**, 222 (2015)
113. M.P.Freitas, M.Bühl, D.O'Hagan. *Chem. Commun.*, **48**, 2433 (2012)
114. M.P.Freitas, M.Bühl, D.O'Hagan, R.A.Cormanich, C.F.Tormena. *J. Phys. Chem. A*, **116**, 1677 (2012)
115. J.M.Silla, M.P.Freitas. *J. Fluor. Chem.*, **172**, 1 (2015)
116. J.Silla, M.P.Freitas, R.A.Cormanich, R.Rittner. *J. Org. Chem.*, **79**, 6385 (2014)
117. P.R.Anizelli, D.C.Favaro, R.H.Contreras, C.F.Tormena. *J. Phys. Chem. A*, **115**, 5684 (2011)

118. R.Faber, S.P.A.Sauer. *Phys. Chem. Chem. Phys.*, **14**, 16440 (2012)
119. L.C.Ducati, R.H.Contreras, C.F.Tormena. *J. Phys. Chem. A*, **116**, 4930 (2012)
120. G.A.Aucar, A.F.Maldonado, M.D.A.Montero, T.Santa Cruz. *Int. J. Quant. Chem.*, **119**, e25722 (2019)
121. P.F.Provasi, S.P.A.Sauer. *J. Chem. Theory Comput.*, **2**, 1019 (2006)
122. J.M.García de la Vega, J.San Fabían. *Mol. Phys.*, **113**, 1924 (2015)
123. J.E.Peralta, R.H.Contreras, J.P.Snyder. *Chem. Commun.*, 2025 (2000)
124. M.Sanchez, P.F.Provasi, G.A.Aucar, S.P.A.Sauer. *Adv. Quant. Chem.*, **48**, 161 (2005)
125. R.H.Contreras, T.Llorente, L.C.Ducati, C.F.Tormena. *J. Phys. Chem. A*, **118**, 5068 (2014)
126. J.E.Del Bene, I.Alkorta, J.Elguero. *J. Chem. Theor. Comput.*, **4**, 967 (2008)
127. J.E.Del Bene, J.Elguero. *Solid State Nucl. Magn. Reson.*, **34**, 86 (2008)
128. J.E.Del Bene, P.Provasi, I.Alkorta, J.Elguero. *Magn. Reson. Chem.*, **46**, 1003 (2008)
129. J.E.Del Bene, I.Alkorta, J.Elguero. *J. Chem. Theor. Comput.*, **5**, 208 (2009)
130. J.E.Del Bene, I.Alkorta, J.Elguero. *J. Phys. Chem. A*, **114**, 2637 (2010)
131. M.Jaszuński, P.Świder, S.P.A.Sauer. *Mol. Phys.*, **117**, 1469 (2019)
132. I.Ghiviriga, L.Zhang, H.Martinez, R.H.Contreras, C.F.Tormena, L.Nodin, W.R.Dolbier. *Magn. Reson. Chem.*, **49**, 93 (2011)
133. L.H.Zhang, K.Ogawa, I.Ghiviriga, W.R.Dolbier. *J. Org. Chem.*, **74**, 6831 (2009)
134. I.Ghiviriga, F.Dulong, W.R.Dolbier. *Magn. Reson. Chem.*, **47**, 313 (2009)
135. D.S.Fadeev, I.P.Chuikov, V.I.Mamatyuk. *J. Fluorine Chem.*, **182**, 53 (2016)
136. D.S.Fadeev, I.P.Chuikov, V.M.Karpov, V.I.Mamatyuk. *J. Fluorine Chem.*, **197**, 1 (2017)
137. I.P.Chuikov, D.S.Fadeev, V.I.Mamatyuk, T.A.Vaganova, E.V.Malykhin. *J. Fluorine Chem.*, **132**, 512 (2011)
138. D.S.Fadeev, I.P.Chuikov, V.I.Mamatyuk. *Russ. J. Struct. Chem.*, **54**, S180 (2013)
139. A.K.Schnack-Petersen, P.A.B.Haase, R.Faber, P.F.Provasi, S.P.A.Sauer. *J. Comp. Chem.*, **39**, 2647 (2018)
140. S.Hirata, K.Yagi, S.A.Perera, S.Yamazaki, K.Hirao. *J. Chem. Phys.*, **128**, 214305 (2008)
141. K.Jackowski, W.Makulski, A.Szyprowska, A.Antusek, M.Jaszuński. *Magn. Reson. Chem.*, **47**, 857 (2009)
142. P.Lantto, J.Vaara, T.Helgaker. *J. Chem. Phys.*, **117**, 5998 (2002)
143. P.F.Provasi, S.P.A.Sauer. *J. Chem. Phys.*, **133**, 54308 (2010)
144. P.F.Provasi, M.C.Caputo, S.P.A.Sauer, I.Alkorta, J.Elguero. *J. Comp. Theor. Chem.*, **998**, 98 (2012)
145. D.C.Favaro, R.H.Contreras, C.F.Tormena. *Magn. Reson. Chem.*, **51**, 334 (2013)
146. I.Alkorta, J. Elguero, H.-H.Limbach, I.G.Shenderovich, T.Winkler. *Magn. Reson. Chem.*, **47**, 585 (2009)
147. G.Saielli. *Magn. Reson. Chem.*, **58**, 548 (2020)
148. R.Pereira, J.Wolstenhulme, G.Sandford, T.D.W.Claridge, V.Gouverneur, J.Cvengroš. *Chem. Commun.*, **52**, 1606 (2016)
149. I.L.Rusakova, Y.Y.Rusakov, L.B.Krivdin. *Magn. Reson. Chem.*, **52**, 500 (2014)